Addis Ababa Institute of Technology (AAiT)

School of Multidisciplinary

Center for Renewable Energy

Parabolic Trough Solar Collector Design, Modeling and Simulation for the Application of Industrial Parks: A Case Study of Bole Lemi Industrial Park

A Thesis Submitted to the School of Graduate Studies of Addis Ababa University in Partial Fulfillment of the Requirements for the Degree of Master of Science in Energy Technology

By

Mengesha Abreha

Advisor: Tilahun Nigussie (PhD)

Addis Ababa, Ethiopia

July 2022

Addis Ababa University

Addis Ababa Institute of Technology (AAiT)

School of Multidisciplinary

Center for Renewable Energy

Parabolic Trough Solar Collector Design, Modeling and Simulation for the Application of Industrial Parks: A Case Study of Bole Lemi Industrial Park

Submitted by Mengesha Abreha

Approved by Board of Examiners

Dr. Tilahun Nigussie	_____	_____
Advisor	Signature	Date
Mr.Mesfin Belayneh	_____	_____
Internal Examiner	Signature	Date
Dr.Abudlkadir Aman	_____	_____
External Examiner	Signature	Date
_____	_____	_____
Chair Person	Signature	Date
_____	_____	_____
Director of Post Graduate Program	Signature	Date

Declaration

I declare that I wrote this thesis from start to finish and that it has never before, in whole or in part, been submitted as part of an application for a degree. Except when otherwise indicated by citation or acknowledgment, the work presented is entirely mine. I confirm that the thesis submitted in partial fulfillment of the requirements for the Master of Science in Energy Technology, has

i) Been composed the entire pieces by myself.

ii) Been only as a result of my efforts.

iii) Not been submitted for any other degree or professional qualification.

Name of student Mengesha Abreha Berihe Signature _____

Date of submission _____

This thesis has been submitted for examination with my approval as the University advisor

Advisor name _____

Advisor's Signature _____

Certification

The undersigned, certify that I read and here by the recommend for the acceptance by Addis Ababa University, Addis Ababa Institute of Technology, Center for Renewable Energy a thesis entitled “Parabolic Trough Solar Collector Design, Modeling and Simulation for the Application of Industrial Parks: A Case Study of Bole Lemi Industrial Park”. This certificate is used a partial fulfillment of the requirement for the degree of Masters of Science in Energy Technology.

Mengesha Abreha Berihe

Signature _____ Date _____

Acknowledgement

First and foremost, I want to thank God Almighty for His tremendous gifts during my research. As this thesis has been completed, I would like to thank my adviser, Dr. Tilahun Nigussie, for his perseverance, excitement, cooperation, and suggestions to deliver in the current shape.

I can't seem to go on without expressing my sincere gratitude to Dr. Solomon T/Mariam for his diligent oversight throughout the study time.

I would like to express my gratitude to the Addis Ababa Institute of Technology (AAiT) for providing me with the financing necessary to pursue my studies at the forefront of energy technology.

Further, yet importantly, sense of respect goes to my father Mr.Abreha Berihe, mother Mrs. Ta'emo Alemayehu, my brothers Sabawi Abreha and Getachew Abreha for their strong support as well as regular encouragement in every step to make me in present stage. Similarly other relatives are also subjects to special thanks for their inspiration and cooperation in my study.

My special thanks also go to my sister and all time best friends Asqual Abrha, her unwavering and constant support of all kind.Asquye, this work is done because of your central role.

Finally, my warm and sincere thanks goes to my friends Danite Negash,Hermela Estifanos,Selamawit G/giorgis and Rahel Welday for their colossal back and hope they had given to me. Without that hope, this thesis would not have been conceivable.

Thank you all for the strength you gave me.

Abstract

Despite the need for additional research to bring concentrator solar plants up to a competitive economic level, molten salt integrated parabolic trough solar collector plants produce essentially lower levels of carbon dioxide than conventional power systems. Priority study areas in the thermal engineering applications for the textile industry include the optimal design, mathematical modeling, performance simulation, and cost investigation of parabolic trough solar power plants. This thesis is concentrated on the dynamic modeling of 50 MWe parabolic solar trough collector up-scaled versions for power supplies in Bole Lemi Industrial Park. Prior evaluations was carried out to choose the finest collector and receiver geometry, heat transfer fluid ,solar field design points and energy storage systems based on diverse determination criteria. In addition to satellite driven solar resource data collected from NASA, direct normal irradiance (DNI) on daily and monthly basis were measured using Payranometer.The solar field components then coordinated into power generating module and the systems performance was simulated to create genuine working environment. The input parameters such as declination angle, azimuth angle, hour angle and equation of time were analyzed using empirical equations. Assessment of daily global solar radiation and sun shine duration at the case study area was conducted using Meteonorm8 .Taking all the collected primary and secondary data, comprehensive numerical simulation of parabolic trough solar power plant employing System Advisor Model (SAM) was developed. The average monthly DNI as function of thermal power produced on the field, monthly energy generation, thermal cycle efficiency and levelized cost of energy with solar multiple were plotted in order to investigate their correlation pattern. The simulated time series yield showed that maximum annual power cycle efficiency of the system to be 25.5% and the maximum average thermal power output occurred in the months of January through April and November through December. The findings were further cross checked with similar previous scientific works using common parameters and fair agreement has been achieved, illustrating the proposed technology is applicable for any industrial application.

Key words: *Parabolic Trough Solar Collector, Direct Normal Irradiance, Receiver Geometry, Heat Transfer Fluid, Molten Salt, System Advisor Model (SAM), Simulation, Levelized Cost of Energy (LCOE)*

Table of Contents

List of Tables

List of Figures

Nomenclatures

$h_{c,ca}$ … … … … … ….Heat transfer coefficient between cover & the surrounding

C_p … … … … … … … …. Specific heat capacity

C_{pr} ……..... Molten salt specific heat

K_a … … … … … … …. ….Thermal air conductivity

$S_{\dot{u}}$ … … … … … … … …. Thermal power

$T_{r,i}$ ……..Temperatures inlet to the receiver

$m_{\dot{r}}$ … … … … … … … … Receiver mass flow rate

d……..Discount rate

Do ……..….Mean earth-sun distance

E^c ……...Energy storage cost

E^m …….Specific mass energy density

E_T ……..….Equation of Time

E^v ……..….Specific volumetric energy density

f……..Friction factor

G_{sc}…….Solar constant

H_o ……....Daily average extra terrestrial irradiation on a horizontal surface

h_{tank}: ……...Tank height

I ……..extraterrestrial solar radiation

I_H…….....Hourly Global Solar Radiation on Horizontal Surfaces

I_o…….....Hourly Extraterrestrial Radiation

k ... ... Thermal conductivity

Kt ……..Clearness index

L_L…….. Longitude of the location

Ls …….Standard meridian for a local zone

LS3……. LUZ solar collector, third generation

L_T ……..Local standard time

MWe …….....….Megawatt electric

MWt……Megawatt thermal

n……..Years of analysis

N_{Ua}……. ….Nussle number

Pr…….…….Prandtl Number

Q_n .....Energy output or saving in years

R .....…...Earth distance correction factor

r ……Tracking angle

R_e……..Reynolds's Number

R_H…….Relative Humidity

r_t ……Hourly / daily average irradiance ratio

T_{amb}…….....Ambient temperature

T_{dec} …….Decomposition temperature

T_{fus} ……..Fusion temperature

A_{ap}……..collector aperture area

A_r……...Receiver aperture area

Dc …….Outlet diameter of the cover

D_r…….....Outlet diameter receiver

F_1…….Collector efficiency factor

F_R …….Factor of the heat removal

Lc…….Collector length and, and the

T_C …… …Average temperatures of cover.

U_L ……Collector coefficient of overall heat loss

U_O ……Coefficient of collector overall heat transfer

Wc ……...Collector width

k_θ ……. Incidence angle modifier

Acronyms

AC ……....Alternating Current

BLIP……..…Bole Lemi Industrial Park

CSP ……...Concentrated Solar Power

DC……....Direct Current

DHI…….....Diffused Horizontal Irradiance

DNI……..……Direct normal Irradiance

DSG……....Direct Steam Generation

EU……...European Union

GHG…….Green House Gas

GHI…….....Global Horizontal Irradiance

GSF …….Gossamer Space Frames

GWh……Gig watt hour

HCE…….....Heat Collector Portion

HTF …….....Heat Transfer Fluid

KPI…….....Key performance Indicator

LAT...…… ……..Large Aperture Trough

LAT…….Local Apparent Time

LCOE…….……Levelized Cost of Energy

MBE…….Mean Bias Error

NASA……...National Aeronautics and Space Administration

NREL……...National Renewable Energy Laboratory

NSRDB …….....National Solar Radiation Database

O&M……..Operation and Maintenance

PCM …….....Phase Change Material

PSP …….....Parabolic Solar Power plant

PTC ……Parabolic Trough Collector

RMSE…….……Root Mean Square Error

RMY……....……Representative Metrological years

RSIs ……..…Rotating Shadow band Irradiometers

RSY……..Representative Solar Years

SAM……..System Advisor Model

SCA…….....Solar Collector Assembly

SEGS…….. Solar Electric Generating System

SHIP ……..…Solar Heating Industrial Process

Sm……..….Solar multiple

SODA……..…European Commission's solar data

SSE …….....Surface Meteorology & Solar Energy

TCS…….Transient Component Simulation

TES …….....Thermal Energy Storage

TLCC……..Total Life Cycle Cost

TMY…….....Typical Metrological Year

WMO…….....World Metrological Organization

Greek Letters

ε_{cv}..... Cover emittance

∅……Intercept factor

a .....Solar altitude Angle

m…… Fluid viscosity

γ…….Solar Azimuth Angle

δ …….Declination angle

θ_i……....Incidence angle

θz …….Zenith angle

ρ……..…Fluid density

τ ……Glass cover transmittance

ϕ…….Latitude angle

ω ……....Hour angle

α_r …….. Receiver absorption

σ ……Stefan Boltzmann constant

ϱ_c …….. Mirror reflection coefficient

Chapter One

Introduction to Parabolic Trough Solar Collector Technology

1.1 Introduction

This chapter introduces the solar energy research problems, as well as the accompanying specific research topics and objectives to be achieved. The topics to be discussed are: Background of the research area, objectives, the study's scope, the problem statement of the study, as well as the thesis' structural arrangement is the core discussions of this chapter.

1.2 Background

Basically, the sun is the ultimate source of energy for every life on earth and even fossil fuels including oil, coal and natural gas in a manner stores solar energy formed from the bodies of organisms that lived millions of years ago [1]. But direct utilization of solar energy got prime importance as it is the most abundantly available source of sustainable energy with no bad impacts on the environment. Solar energy has been used in a variety of applications which can be classified into two major categories: solar thermal applications and solar electrical power applications[2]. Many technologies have been developed for utilization of solar energy. This thesis research focuses on Parabolic Trough Collector technology which is amongst the most successful thermal energy utilization technologies in a wide range of industrial applications.

Parabolic Trough Collector (PTC) is actually a type of solar concentrator, used to produce high temperature thermal energy.

A solar concentrator captures sunlight over a large aperture area and concentrates this energy onto a much small receiver area, multiplying intensity of the solar radiation by a concentration ratio in the range of 10–80 (for parabolic trough collectors)[3].However, to achieve such concentration, a trough tracks the sun continually throughout the day. Parabolic trough collectors are made by bending a sheet of reflective material into a parabolic shape. A metallic tube, covered with a glass tube to reduce heat losses, is placed along the focal line of the collector .The concentrated radiation reaching the receiver tube heats the fluid that circulates through it, thus transforming the solar radiation into useful heat[4].This high temperature heat energy produced in receiver can further be used to produce steam in the bleaching and drying applications of

garment and textile industries. The main objective of this research work is to develop a simplified design and modeling procedure of a parabolic trough solar field for a specific garment industry in Bole Lemi industrial zone thermal load. Thermal output patterns of designed solar field, under local environmental conditions, will be obtained through simulation using System Advisor Model and Metronome software. These patterns will then be used for parametric optimization of designed parabolic trough solar field. These results can further be used as baseline for feasibility study of local industrial applications.

1.2.1 Components of PTC

Mirrors, a supporting structure, a receiver, working fluid, and a monitoring device are the key components of a PTC. Each component is created to serve a specific purpose and is made from materials that are appropriate for its functions and desired properties. These components are explained as follows.

1.2.2 Mirrors

The principal function of mirrors is to reflect solar radiation and concentrate it onto the receiver. Mirrors are made of high-reflective material layers (aluminum or silver) with substrates and superstreets that protect the reflective layer against corrosion or abrasion so that longer life is achieved[5].

1.2.3 Supporting structure

The primary function of the supporting structure is to secure the collector's components, providing rigidity and stability to the entire device. Generally, structural materials such as steel or aluminum are used to build the frame. From a structural standpoint, the PTC supporting structure is made up of three parts: the main support (columns, piles, and box), the frame, and the receiver brackets.

1) The key support acts as a collector's structural anchor and keeps it in place. Since the aperture of the collector is exposed to the wind, the main support would be able to withstand wind loads structurally [6]

2) The mirrors' rigidity is provided by the frame, which allows them to maintain their parabolic shape at all times. It also transmits the tracking system's torque.

3) The brackets are connected to the mirrors' supports, and the receiver is fixed to the parabola's focal line. To minimize heat losses from the receiver to the bracket,an insulating material is typically mounted between the two components.

To avoid misalignments that result in output losses, the parabolic shape of the mirrors and the position of the receiver at the parabola's focal line should always be retained. As a result, proper structural system design is critical[6].

1.2.4 Receiver

The receiver's main job is to absorb as much radiation as possible and effectively transfer that energy to the heat transfer fluid (HTF). Depending on the use, the receiver may be made of metal (heating) or glass (solar disinfection).The pipe receiver, cover glass, and selective coating are the three main components of the receiver for heating applications. The cover glass reduces heat loss and protects the pipe from deterioration. The selective coating is applied to the pipe's external surface to maximize the absorption of solar heat flux.

To mitigate heat losses, a vacuum is applied in the annular region between the glass and the tube and the receiver is sealed to avoid vacuum losses. These receivers are known as evacuated receiv ers. The bellows are the receiver's airtightportion, as well as the pipe and glass cover's thermal ex pansion.It is well understood that during the entire process, the pipe and the glass cover do not expand at the same time. Because of the large temperature difference with the atmosphere, bellows allow thermal expansion without losing vacuum in the annulus. The primary purpose of the hydrogen getters is to absorb any residual hydrogen that may form as a result of the HTF's thermal degradation. The glass-to-metal seal connects the pipe and the glass cover, and its primary purpose is to minimize mechanical stresses caused by thermal expansion differences.

1.2.5 The heat transfer fluid (HTF)

The working fluid, also known as the HTF, is a material that can absorb heat from the receiver and use it as process energy. This fluid should have a high thermal power and thermal conductivity, as well as low thermal expansion, low viscosity, low corrosive behavior, low toxicity, and thermal and chemical stability over its entire operating temperature range. Liquids are commonly used as HTFs. Thermal oils (such as Syltherm or Therminol) are used in solar

power generation along with a heat exchanger to produce steam for use in a Rankin cycle, while water is mainly used in low enthalpy and direct steam generation (SG) applications. In industrial applications, the most commonly used HTFs are water and thermal oils[7].

For typical process industries such as the garment industry in Bole Lemi industrial zone 45 to 65% of its thermal energy consumption can be replaced by solar energy. We will discuss about heat transfer selection criteria in chapter 5 in detail.

1.3 Statement of the problem

One of the most crucial components in any industrial operation is energy. Its availability is limited, nevertheless. Due to a shortage of energy and high fuel prices in Ethiopia, increased efforts were made to maximize energy conservation. The garment sector, one of the largest energy consumers, holds the record for the lowest efficiency in energy use.

Some of the energy gap issues were discovered during the site inspection at Bole Lemi Industrial Park includes,

1) To wash and dry the clothes, enormous heat is required. The wet method employed in dying, which results in a massive amount of water being heated, has a significant energy requirement.

2) A significant proportion of thermal energy is lost in steam generating boilers as a result of poor fuel and water use.

3) As a result of continued use of the devices under inefficient working conditions, electricity consumption and power costs are on the rise.

4) The textile sector consumes a lot of fuel and power. Spinning uses about 34% of the energy used, weaving uses 23%, chemical processing uses 38%, and other uses take up the remaining 5%.The wet processing section of the Bole Lemi industrial park requires significant amounts of thermal energy in the form of steam as a source of heating in addition to electrical energy. For instance, the Bole Lemi industrial park needs between 4500 and 5500 Kcal of thermal energy, and each meter of cloth requires between 0.45 and 0.55 KWh of electrical energy. This translates into massive amounts of fossil fuels being used to generate the direct energy required to run the mill, generate heat and steam, and run air conditioners.

5) The amount of water consumed is almost immediately inversely correlated with fuel consumption. Additionally, increased fuel use raises the cost of energy overall.

6) In addition, the massive fuel consumption results in the emission of greenhouse gases like carbon dioxide, which has an adverse effect on the environment.

Bole Lemi Industrial Park needs a new strategy that is effective and emission-free alternative source of energy in order to deliver clean energy at a low cost. Solar energy has the potential to develop an environmentally friendly electrical system and can be used as a clean alternative energy to minimize electrical output. Numerous in-depth studies have so far been conducted on the solar energy system, which has become a well-known use in residential, commercial, and industrial settings. Utilizing solar thermal energy systems is uncommon in Ethiopia, and the textile industry is notably lagging. Therefore, it's crucial to research thermal solar energy collecting systems as a substitute energy supplying method in order to lessen the environmental and energy expense limits.

1.4 Objectives

1.4.1 General Objective

The main goal of this thesis is to use analytical and simulation software to design, model, and simulate parabolic trough solar collector for an energy application in the Bole Lemi Industrial Park.

1.4.2 Specific objectives

- To access and analyze solar resources for parabolic trough solar collector at Bole Lemi Industrial Park.
- To select and specify solar thermal heat transfer fluid based on key parameters.
- To model and configure receiver and collector components of parabolic trough collector.
- To specify design parameters of solar thermal storage.
- To simulate and optimize solar multiple, solar thermal energy storage capacity and other relevant design parameters using System Advisor Modeling (SAM) and METEONORM 8 software.

1.5. Scope of the Thesis

The main decision variables of parabolic trough solar thermal collector highly vary geographically. Design parameters such as, direct normal irradiance, slope of surface, azimuth of surface, ground reflectance, overall heat loss coefficient, and the overall efficiency of solar thermal collector systems are bounded within the Bole Lemi industrial zone. Relevant data for the analysis will be incorporated using empirical calculations, NASA Surface meteorology and Solar Energy (SSE) and System Advisor Modeling (SAM). Since this thesis is a partial fulfillment for the masters of Science (MSc) in energy technology, its completion is expected within one year time frame.

1.6 Limitation of the Thesis

There were a few more drawbacks to this study, which are listed below. Meeting potential interviewers was difficult. Design and renewable technology experts were critical stakeholders in the example firm because the research focuses on solar thermal energy. However, because it plays such an important role in the company, it has had to postpone or cancel interviews on several occasions due to other pressing matters. Furthermore, the Corona virus put additional strain on daily activities, making already-busy potential candidates less available; as a result, the researcher had to customize the number of participants to the circumstances and goals. Despite the fact that the study's population is the Bole Lemi Industrial Park in Addis Ababa, the sample was drawn using a specific criterion, and so does not reflect the total population.

The respondents were at ease responding to the interview question because they were potential customers for this technology. The research questions will thus be resolved. Despite the fact that homogeneous sampling was the intention, the sample for this study ended up being varied in nature. However, by including a wider diversity of perspectives in the interviews; it raised the study's caliber. English, which was neither the researchers' nor the interviewees' native tongue, was used for the interviews. This was a problem because it was challenging to explain the study's expectations effectively. As a result, certain details might have been interpreted incorrectly, which would undermine their legitimacy. Because there were so few participants in the case studies, it was impossible to generalize the results. However, the results can operate as a guide for other global businesses wishing to include solar thermal systems into their production

methods. The chosen case industry is in the textile sector, which has a different potential for success than other sectors and businesses outside of Ethiopia. Generally,

- Due to time constraint, material selection and solar power generation analysis will not cover on the thesis.
- Since this thesis is a case study, metrological resources such as temperature, radiation duration, also geometric data such latitude, azimuth angle, and other parameters are geographically restricted to Bole Lemi Industrial Park (BLIP).
- The detailed sensitivity analysis is extensive, and is not included in the thesis.

1.7 Significance of the Study

- Impact on the Environment: Solar energy has the least negative impact on the environment compared to any other energy source. It does not produce greenhouse gases and does not pollute the water.
- Reduce Energy Bill: Generating solar energy means that using less energy from the utility supplier. This will immediately translate to savings energy bill. Plus, the generating company can also make money by selling the unused electricity, to the grid.
- Applicable everywhere: As long as there is sunshine, solar energy can be deployed anywhere. This is particularly useful for remote regions with no access to any other source of electricity.
- Less electricity lost during long-distance: Some of the energy, around 3-5%, is lost during transportation and distribution. The longer the distances between the production and the supply points, the more energy is lost. Those losses might not seem significant but they can influence the performance of the installation in regions with high population density.
- Improves grid security**:** The grid is less vulnerable to blackouts if there are many power plants which are spread out. A grid with high penetration of solar energy has thousands of energy production centers which are widely spread out. This improves the security of the grid in case of overload, natural or human-caused disasters.

1.8 Ethical Considerations

Ethical questions will come up as the researcher plans and organizes this activity, collects, evaluates, retains, and submits data for access to organizations and people. In science, ethics

refers to a system of rules that determine how a researcher should act in light of the needs of those whose lives are affected or influenced by their research [8]. Three ethical questions are the main focus of this study:

(1) Anonymity,

(2) Confidentiality, and

(3) Informant consent.

During the compilation, interpretation, and recording stages of the research, participants' identities and confidentiality were kept a secret. The researcher obtained informed consent from the interview subjects before disclosing the goals of the study.

1.9 Organization of the Thesis

This thesis research is structured into seven chapters .**Chapter One** discusses general introduction about Parabolic Trough Solar Collector Technology. Based on scientific journal assessments and recorded data from Bole Lemi Industrial Park, problems of the thesis statement, general and specific objective of the thesis research will be explained. It also highlights significance of the research and frames its scope and limitations.

Chapter Two presents reviewed Literatures and scientific journals related to parabolic trough solar collector in the industrial application with more focus on the textile sector. Some of the steps to be followed in the literature survey process include,

- **a)** Examine the major concepts/theory that led to research problems.
- **b)** Highlight knowledge gaps cited in the proposed study.
- **c)** Summarize findings of previous studies on the same subject.

Chapter Three, deals about Research Methodology to be applied on the mathematical modeling design and simulation of parabolic trough solar collector for Bole Lemi Industrial Park. It includes the research approach and design methods, collection of relevant data using payranometer measurement. In addition to the measured data, NASA-SSE and EU solar data grids are collected at Bole Lemi Industrial zone using latitudinal and longitudinal inputs. Then numerical analyses of the collected data are presented.

Chapter Four investigates Solar Radiation and Geometric Analysis of Parabolic Trough Collector. On this segment, solar geometry and models of solar geometry and single axis solar tracking will be discussed.

Chapter Five introduces Heat Transfer Fluid Selection and Storage System Design **.**In this chapter molten salt is selected as heat transfer fluid for the mathematical modeling designing of parabolic Trough Collector in Bole Lemi Industrial Park. The technical and economic decision factors of molten salt will also be explored.

Chapter Six This chapter explores Simulation of Parabolic Trough Solar Power Plant. Under this section, mathematical modeling of parabolic trough solar collector, design parameters and system performance analysis will be centre of the topic. Simulations using Solar Advisor Modeling (SAM) based on satellite and Payranometer measurement driven data will be compared and validated against previous scientific works. Finally, simulation and optimization results proposed at Bole Lemi Industrial Park will be discussed.

Finally, in **Chapter Seven** based on previous chapter's discussions and analysis results, conclusions and recommendations of the thesis will be presented.

Chapter Two

Literature Review

2.1 Introduction

This chapter introduces reviewed literatures and scientific journals related to parabolic trough solar collector in the industrial applications with more focus on the textile sector. This section mainly examines the major concepts/theories that led to research problems, summarize findings of previous studies on related subjects and identify the research gaps from the literatures.

2.2 General Literature Survey

Recent trends of energy production and consumption in manufacturing industries are notably unsustainable due to rapidly increasing greenhouse gas emissions. Developing countries throughout the world are trying to industrialize their own economy to create new opportunities for the young generation to address their own country as a developed one. As a response to this situation, many researchers are concentrating on improving new energy efficiency measures, developing environmentally friendly devices and components and finding effective energy production methods[3]. As the non-renewable energy sources are going to be finished in future and considering all the drawbacks like GHG emissions, demand for renewable energy sources is imminent. The demand for energy is significantly increasing with increases in population and the rapid development of world's economy[8]. As a result, the price of energy from conventional sources such as fossil fuels and nuclear power, are escalating through time. Nowadays, about 80 percent of the global primary energy demand is comes from fossil fuels, which are limited and thus become too expensive to exploit in the future[8] .If the regional and seasonal variation is not significant, then a supplementary energy storage system may not be necessary depending on the type of application. Where seasonal variation is quite dominant where reduced radiation available in winter for a few months, energy storage systems may improve the overall performance of the system.

Different studies show that the potential in the field of solar industrial process heat integrated with suitable industrial processes is feasible. In another work, Lauterbach et al. methodically analyzed an installed solar process heating system based on simulation and compared it with a validated model [9]. Weiss et al. reviewed the solar industrial process heating potential among

countries for medium temperature collectors and sought a solution for SHIP integration problem [10] . Schnitzer et al. applied a newly developed investigation tool to investigate industrial energy systems and heat integration feasibilities through an Austrian dairy industry case study [11]. IEA SHC task 33 and Solar Paces Task IV: Solar Heat for Industrial Processes identifies and discusses potential industrial sectors for SHIP integration [12]. Mekhilef et al. reviewed solar energy utilization by industrial applications thus identified potential industries [13] . Norton illustrated the industrial applications of solar heat such as solar water heating system, solar drying system, solar furnaces, green houses, heating and ventilation systems, solar cooking, solar desalination and solar refrigeration [14], [15]. Vajen et al. outlined solar heat integration potential at supply level and process level in Europe, Germany and worldwide [16] . Taibi et al. reviewed and discussed renewable energy potential in industrial sectors such as biomass and low temperature solar process heat [17]. Schmitt performed several comprehensive studies to show the utilized process installations in food and beverage industries. He also developed a classification mechanism for SHIP integration [18]. Modi et al. reviewed solar driven heat and power generation systems [19]. Pietruschka et al. reported on the fundamental design, process system layout, operating conditions and industrial processes of three large scale solar process heat installations [20]. Calderoni et al. studied the feasibility analysis of integration of solar process heating systems in industrial processes in Tunisia followed by an economic analysis [21]. Montes et al. presented the parabolic trough solar collector based process heating system and their design results[22] . Frein et al. studies and presents the design procedure and analysis basics required for integrating a solar thermal plant into an industrial system [23]. Schramm et al. presents a new concept of solar process heat integration system based on solar tanks through solar tank volume simulation results [24]. Larcher et al. experimentally investigated the parabolic trough solar collector based integrated solar process heating system [25]. Kalogirou presented simulated results of the parabolic trough collector based solar process heating system performance located on Cyprus [26] . Esen experimentally investigated and presented the thermal performance of vacuum tube collector based solar cooker under varied refrigerant conditions [27]. Silva et al. developed an optimization method for parabolic trough solar collector based solar industrial process heating systems. In another research work Silva et al. also conducted uncertainly and sensitivity analysis for parabolic trough collector based steam generation plant [28]. Coccia et al. designed and experimentally tested a prototype model of a

parabolic trough solar collector for process heating application[29] .Naik et al. reviewed all kinds of medium temperature application areas of concentrated solar thermal technologies in India [30].

Celuppi et al. studied and analyzed the performance of vacuum solar collectors for boiler water preheating [31]. Esen et al. investigated the performance of heat pump integrated solar space heating system [32].

2.3 Application of Solar Thermal Energy in the Textile Industry

The textile industry, like most other industrial sectors, requires a constant supply of water, mostly for the dying process. The temperature of the water must be maintained not only at a normal level, but also at a higher level, such as 80°C, which necessitates a significant quantity of heat energy. As a result of the increased usage of traditional energy sources for water heating, environmental consequences will also increase. Solar water heating using solar process heat has the potential to significantly improve the textile industry's environmental impact by replacing traditional fossil fuel sources. Greece, China, and India are the leading countries with solar process heating systems in their textile sectors. Water heating is a common process operation that uses solar collector to achieve a maximum temperature of 100°C. Table 2.2 summarizes the other process procedures, which include solar preheating, painting, and textile manufacture.

Table 2.1 Literature Review for SHIP in Textile Industries

Year	Global Analysis/country specific	Existing SHIP Analysis	Reference
2006	Pakistan	Alternating solution to solar heating	[33]
2008	Turkey	Experimental investigation of solar water heating	[34]
2013	Global	Small and medium scale industry	[35]
2015	Global	A medium scale industry	[36]

2.4 Summaries of Literature Survey

Table 2.2 Comparisons among the previews of related works

Literature work	**Potential industrial sector**	**Feasibility analysis**	**Modeling &simulation**	**Experimental investigation**	**Solar collector type & temperature requirement**
Weiss et.al [10]	3 key sectors	Solution to integration problems	No	No	N/A
Kalogirous[5]	No	No	TRNSYS simulation	No	Parabolic trough collector
Esen [30]	No	No	No	Yes, based on different refrigerants	Vacuum tube collector
Schnitzer et.Al[9]	5 key sector,8 key process	System integration feasibilities	No	No	N/A
IEA SHC TASK [37]	10 key sectors	No	N/A	N/A	N/A
Mekhlif et.Al[11]	11 key sector,6 key process	No	No	No	N/A

Lauterbach et.Al [14]	7 key sector,3 key process	Feasibility and cost analysis	TRNSYS simulation	No	No
Lauterbacha et.Al [14]	No	No	Yes	Yes	N/A
Pietrustchka et.Al[18]	No	No	Simulation for control and optimization	No	3 different collectors
Vajen et .Al [14]	4 key sectors	System integration feasibilities	No	No	No
Montes et. Al[20]	No	No	No	Yes	Parabolic trough collectors
Frein et. Al [21]	No	No	No	Yes	N/A
Schramm et. Al [22]	No	Storage system	Yes	Yes	4 systems
Silva et.Al [26]	No	Economic analysis &optimization	No	No	Parabolic trough collectors

Silva et.Al [27]	No	Uncertainty and sensitivity analysis	No	No	Parabolic trough collectors
Larcher et.Al [23]	No	No	No	Yes	Parabolic trough collectors
Schmitt et.Al [16]	No	System integration by load profile	No	No	No
This Thesis	Textile Sector,2 process	No	Yes	No	Yes

2.5 Research Gap

Table 2.2 displays recent research on the integration of solar industrial process heat applications at the supply or process level, the viability of process heat integration based on modeling, and cost analysis. However, no such work offers a thorough analysis of every industry based on its operations and processes where a solar process heating system is currently in use, available thermal energy generation capabilities, including solar collector types, and the highest process heating temperature that can be achieved through solar heat in Ethiopia. The design and modeling of solar collectors for general industrial applications has also been the subject of numerous studies. Researchers have looked into the effects of different variables on the effectiveness and production of solar energy, including latitude, sun intensity and irradiance, temperature elevation, and relative humidity. However, there hasn't been much attention paid to potential methods and uses of parabolic trough solar thermal collector for Ethiopian Industrial Parks. The design, modeling, and analysis of a parabolic trough solar thermal collector for a particular textile and apparel factory application at the Bole Lemi Industrial Park, which is located in the Eastern part of Addis Ababa, is the objectives of this work.

Chapter Three
Research Methodology

3.1 Introduction

As it is indicated in the title, this chapter includes the research methodology of the thesis. In more details, in this part the researcher outlines the study area, strategies applied to the research, methods used, techniques to the research approach, methods of data collection, and types of data analysis mechanisms.

3.2 Description of the Study Area

Bole Lemi Industrial Park, located in the south eastern part of Ethiopia's capital city, Addis Ababa, with GPS coordinates of 8° 58' 17.2200" N and 38° 51' 24.5088" E. According to the Ethiopian Investment Commission, the industrial park started with 20 sheds (10 sheds of 5500 m^2 each and the remaining 10 sheds of 11,000 m^2), and the park houses enterprises that export garments, apparel and textiles, and leather and leather products (shoes).Bole Lemi Phase 1 (156 hectares) has started operations in 2014, with all pre-erected factories already rented-out to 11 foreign private factories. In the future, a residential and recreational area adjacent to the site will also be developed[38].

Figure 3.1 *Bole Lemi Industrial Park*

The garment industry requires a continuous supply of water like most of other industrial sectors, mainly for the dying process. The temperature requirement for the water is not only at a normal level but also at a higher level like 80°C, which requires a considerable amount of heat energy. If conventional energy sources are used consequently for water heating, environmental impacts will also increase as a consequence. Solar thermal energy using solar process heat is a potential candidate to replace conventional fossil fuel sources in the textile industry to substantially reduce

the environmental impact. Bole Lemi Industrial Park has installed power capacity of 50 megawatt.

Shortages and unpredictable power supplies are cited as a challenge for effective operations by investments operating both inside and outside of the industrial parks. Ethiopia now generates 4,064MW of hydropower capacity, 324MW of wind power, and 25MW of waste-to-energy capacity. However, the electrical system has a loss of more than 21% of its power, and over 60% of the population is without power[39].

This thesis is motivated to propose production of solar thermal energy by parabolic trough collector for process heating. Hence, designing, mathematical modeling and simulation of parabolic trough collector system for Bole Lemi industrial park is the center of the thesis research.

3.3 Research Design

The study that was done in relation to this thesis was not original, but it was applied. Instead, a great deal of prior academic study has been done on the use of parabolic solar collectors in buildings and industries, not just for the textile industry in particular but also for other industries in other parts of the world. As a result, the proposed research was a fresh study that focused on an already studied topic. The several data sources utilized to arrange the research inquiries are shown in Figure 3.2 below.

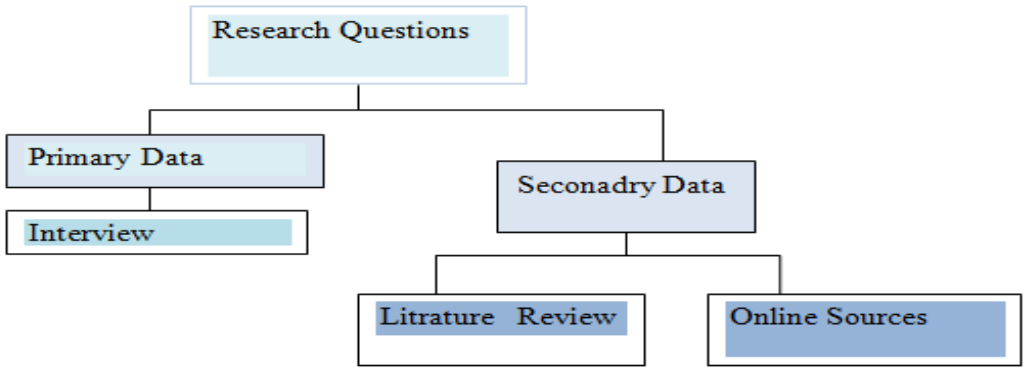

Figure 3.2 Data collection

3.4 Research Approach/Strategy

An inductive research strategy was applied to achieve the goals of this study. This approach to research begins with specific observations, which are then used to produce generalized concepts and study findings. The inductive method was chosen since it takes into account the context of the research as well as the fact that small samples with quantitative data work best with it. The underlying aspect of the inductive approach, however, is that it develops wide hypotheses and conclusions based on a sparse set of data, raising questions about the reliability of study results [41]. A literature survey was conducted at the start of the study to better understand solar thermal systems.

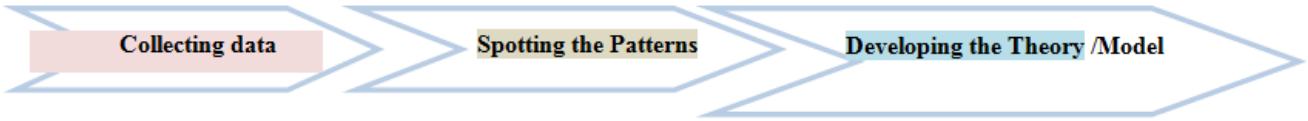

Figure 3.3 Inductive approach [40]

3.5 Data collection

The data for the study was gathered using both primary and secondary sources. Secondary data was gathered through a literature study, government data that was publicly available and scientific articles that had been published. Semi-structured interviews with employees at Bole Lemi Industrial Park us to gather preliminary data. The Current and power consumption were collected for different installed electrical loads.

3.5.1 Literature survey

To map existing solar thermal systems research features in the textile industrial sector and identify research needs, a literature review was conducted. It provides a summary of prior research on the utilization of solar thermal energy in the textile industrial sector. As the research intends to evaluate existing drivers and barriers of solar thermal systems in the industrial sector, the aspects will be compared to the findings of the case studies. The comparison of the literature review with the case findings aids in determining which components of the research are well-known and which bring fresh insights and knowledge for future research. Bothe old and new publications were chosen because they contributed significantly to the material for the literature review. In addition, updated information on these topics was obtained from a range of web sources (reports, blog entries, and newspaper articles). Despite this, the literature review does not adopt a systematic approach, instead attempting to provide a broad overview of current topics.

3.5.2 Interview

The study discovered that interviews were the best method for gathering the essential primary data since they provided in-depth information on the many drivers and barriers to solar thermal energy technology adoption in the industrial process. To be specific to the case study setting while sticking to the research purpose and research question, the researcher chose to conduct semi-structured interviews. Conversations were held in English to ensure that both participants felt at ease while developing inquiries and responses.The study did not collect any further relevant data from the respondents after these interviews. The interviews with the respondents lasted 30 to 45 minutes, depending on the length and depth of the responses received. Because of the COVID-19 epidemic, all meetings are conducted over online channels such as Skype and phone making face-to-face interviews difficult for the study. Each responder was given an outline of the subject before to the interview so that they may plan and arrange their thoughts. The conversations were videotaped and transcribed for data analysis once the respondents gave their permission. Finally, in the outcome section, the interview findings were analyzed and listed.

3.5.3 Sampling Method

Various sampling strategies are employed in the research to select a suitable population sample, depending on the requirement and situation. Purposive sampling was employed to find the case industry in the study at first. Purposive sampling's major goal is to collect cases and individuals that are relevant to the research topics [41] . The case industry was chosen based on the following criteria.

1. The sector needs to follow the UN's Affordable and Renewable Energy as the seventh sustainable development target.
2. The sector must have a plan for future emission reductions or a zero-CO_2 goal (as set out in the Paris Climate Change Agreement).
3. Ethiopia must host solar energy production plant for the industry.

Following these parameters, a number of industries were evaluated, and an email invitation for an interview outlining the purpose of the study was sent to each of them.

Only a few industries, including Bole Lemi Industrial Park, Ethiopian Industry Corporation, and Ethiopian Meteorology Agency, however, replied to the researcher's offer because of unforeseen circumstances and a global pandemic issue. With a greater acceptance rate of respondents for the interview, the study's convenience sampling method was employed to select interview subjects

from the case industries and agencies. Additionally, the study employed a snowball sampling technique to track down more suitable individuals with pertinent experience following each interview in order to get a more in-depth and technical understanding.

3.5.4 Interview guide

Before conducting interviews, an interview guide was prepared; it is found in Appendix A. The interview guide's questions are based on what readers learned in the literature review and theory chapters as well as from prior interviewing experience. To give the interviewee an overview, it opens with a brief explanation of the topic and the greater context of the research. Following this, a series of introductory questions about the interviewee's background and knowledge of solar thermal systems in the industrial sector are asked before the actual interview starts. A series of introductory questions about the interviewee's background and knowledge of solar energy systems in the industrial sector are then asked before the main interview starts.

3.5.5 Interview participants

For this investigation, the researcher spoke with four experts in industrial issues and multinational governments. The many parties involved in this study are listed in Table 3.1. For reasons of confidentiality, the identities of those who were interviewed are not disclosed. On the other hand, subject specialists are published to increase the legitimacy and openness of the research.

Table 3.1 Details of Interview Participants

Respondents	Company /Industry	Job Title	Exprience
Topic Expert 1	Ethiopian Metrological Agency	Climatology Expert	7 years
Topic expert 2	Ethiopian Industry Parks Corporation	Industry Parks Technical Expert	12 years
Topic Expert 3	Bole Lemi Industrial Park	Electromechanical Engineer	6 years
Topic Expert 4	Bole Lemi Industrial Park	Control engineer	8 years

3.6 Data Collection Method and Instruments

For the purposes of this research, previous research papers, journals conference papers and other secondary data sources are investigated in depth. In addition, primary data sources such as site measured data using Ethiopian Meteorology Agency payranometer; satellite data from NASA SSE and Metronome 8 data grid were used. In depth interviews has been held with Ethiopian

industry parks development corporation officials, technical coordinators and plant managers and site supervisors. The rated current and power of selected loads is depicted in Appendix A'.

3.6.1 Data Collection Instruments

3.6.1.1 Modeled Data Sets

As mentioned earlier, long-term computed data sets are rare, have varied record lengths, and are not necessarily simple to obtain. Although there are many different types of solar radiation data with widely varying quality accessible, measuring networks or stations that provide high-accuracy, real-time measured data are rare. These forms of data need to be carefully analyzed and contrasted with data from other sources, such as anticipated or modeled data, to establish whether their usage is suitable. The European Solar Radiation Atlas (ESRA), the Swiss Methodist METEONORM data set, the National Aeronautics and Space Administration (NASA) Surface Meteorology and Solar Energy (SSE), and the European Commission's solar data (SODA) data sets are a few examples. Another typical modeled data set is the Typical Metrological Year (TMY) for a particular area. To make calculating the heating and cooling load for buildings simpler, TMY data sets were developed. TMY is used to describe the weather at a specific location and is based on years' worth of meteorological data. Different algorithms and TMY data sets can be used to generate TMYs. The RMYs (Representative Meteorological Years), RSYs (Representative Solar Years), and TRYs (Representative Temporal Years) all employ comparable methods and data sets (test reference years). These data sets are not appropriate for performance optimization and are primarily used to estimate the relative performance of different conversion device types in relation to a standard data set. Although this was not the intended purpose of the TMY manufacturing, several software programs use TMY data to forecast typical solar conversion system outcomes.

3.6.1.2 Measuring Solar Radiation

It's crucial to take accurate measurements of the incoming irradiance when designing solar power plant projects. Because irradiance measurements are more complex and expensive than other meteorological measurements, they are only available for a small number of locations. For DNI, this is especially true. Irradiance measurements are frequently used to create and test models for estimating irradiance and other solar irradiance components using readily available surface meteorological observations or satellite remote sensing techniques. Irradiance measurements will

play a significant role in the advancement of forecasting methods for solar resource availability. The graph below displays the average normal irradiance as measured by a payranometer for particular months and dates at the Bole Lemi industrial park. The measured DNI for two years in a row (from mid-2019 to mid-2021) is shown in Appendix C.

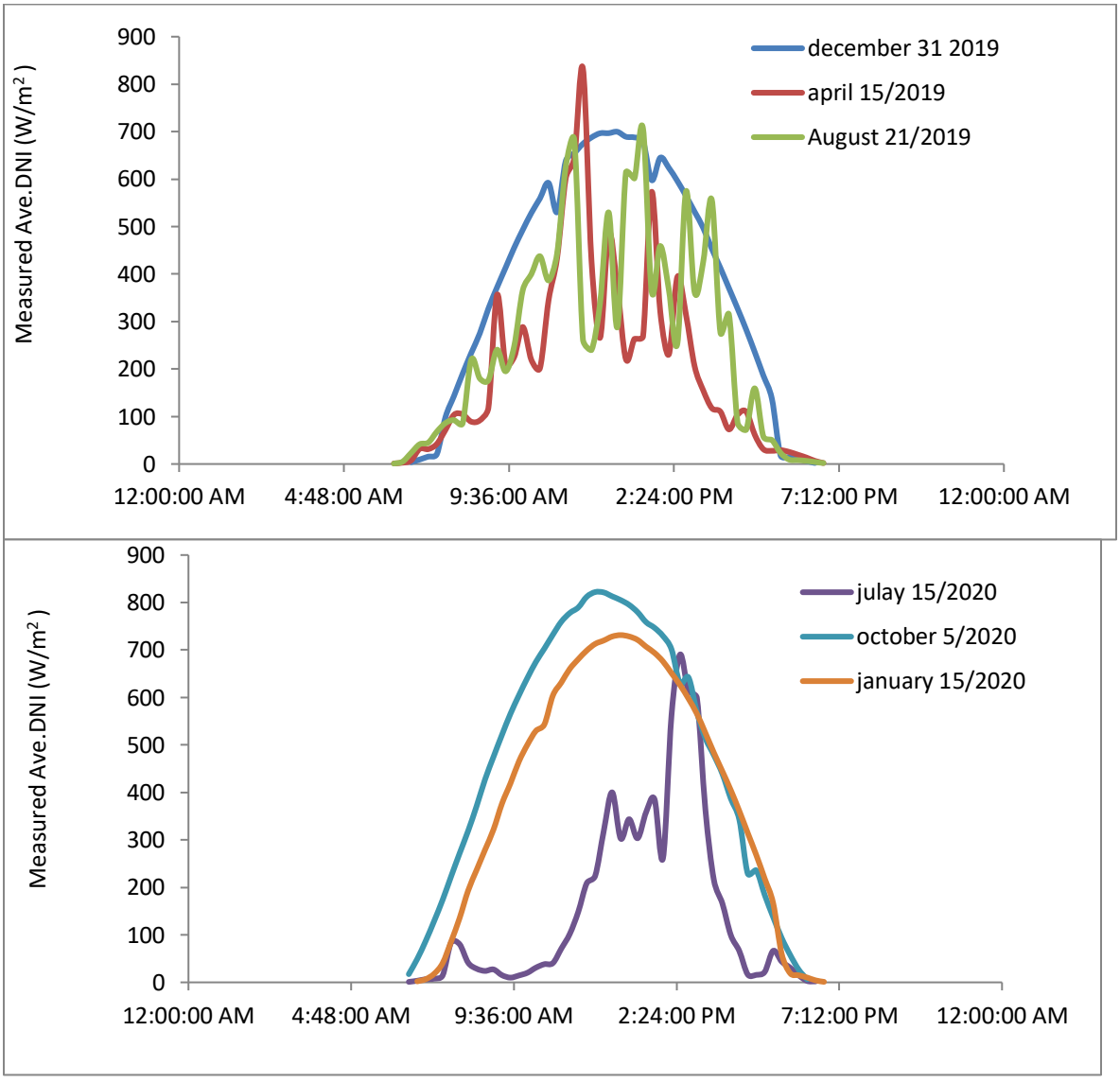

Figure 3.4 Measured solar irradiance at Bole Lemi industrial park using pyranometer CMP3

i) Instrumentation Selection

Before weighing instrumentation options and costs, the consumer must first assess the data quality or uncertainty levels that will satisfy the final analyses based on radiometric

measurements. This ensures that the best value is obtained after considering all of the available measurement and instrumentation choices. Specifically, the most precise instrumentation (ISO 9060 first class; WMO "high quality" or ISO 9060 secondary standard) should not be purchased if project resources cannot sustain the necessary maintenance to ensure measurement quality compatible with radiometer design requirements and manufacturer recommendations. Alternative instrumentation with lower maintenance needs, such as pyranometers with diffuser disks or rotating shadow band irradiometers (RSIs), should be preferred in this situation. Another critical factor for ensuring data quality trust is redundant instrumentation. Regardless of the primary measurement need, having several radiometers on site and/or measuring all three solar irradiance components (GHI, DHI, and DNI) will significantly improve opportunities for post-measurement data quality evaluation.

ii) Instrument Used

Radiometers are instruments that are used to measure some form of radiation. The types of radiometers most used to measure solar radiation resources for this thesis is CMP3 Payranometer.A device for measuring sun irradiance. The solar energy collected from the entire solar spectral range and the entire hemisphere is measured using the thermopile sensor architecture (180 degrees field of view). Watts per square meter are used to describe the output. The CMP3 pyranometer is made for continuous usage both inside and outside. The ISO 9060 spectrally flat Class C CMP3 pyranometer is designed to detect shortwave global sun radiation in the spectral region from 300 to 2800 nm. The thermopile detector has a response time of 20 seconds, a sensitivity range of -10 ^{o}C to +40 ^{o}C, and can measure irradiance up to 2000 W/m^{2}. Operating temperatures range from -40 ^{o}C to +80 ^{o}C, with better than 1 percent annual stability [44]. The CMP3 pyranometer comes pre-wired with 10 meters of signal cable for easy installation and has a snap-on white sun screen, integrated leveling, and a weather proof connector. Longer cable lengths and an optional mounting rod are both available. It is simple to mount two CMP3 back-to-back to create a cheap albedometer.In proportion to the amount of incoming radiation; the Pyranometer produces a low voltage of 0 to 20 mV and does not require any power [45].

Figure 3.5 CMP3 Payranometer [42]

3.6.1.3 Measurement Station and Design Considerations

The efficient design and installation of a solar resource measurement station or network of stations is to collect useful DNI resource data necessitates careful consideration of the elements summarized in this subsection.

a) Location

A solar resource measurement station is primarily set up to collect information that will allow an analyst to precisely define solar irradiance and other associated meteorological characteristics at a specific site. Over larger spatial scales, lesser topography and climate variability often results in lower solar resource variability. These impacts need to be properly understood before deciding on the final location of a measuring station. Operational factors including fuel, communications, and maintenance access must be weighed against the target area's closeness. Assume about how nearby sources of dust or pollution, like the traffic on a dirt road, might affect the measurements. The apparent sun path fluctuations throughout a year at Bole Lemi Industrial Park are shown in Figure 3.6.

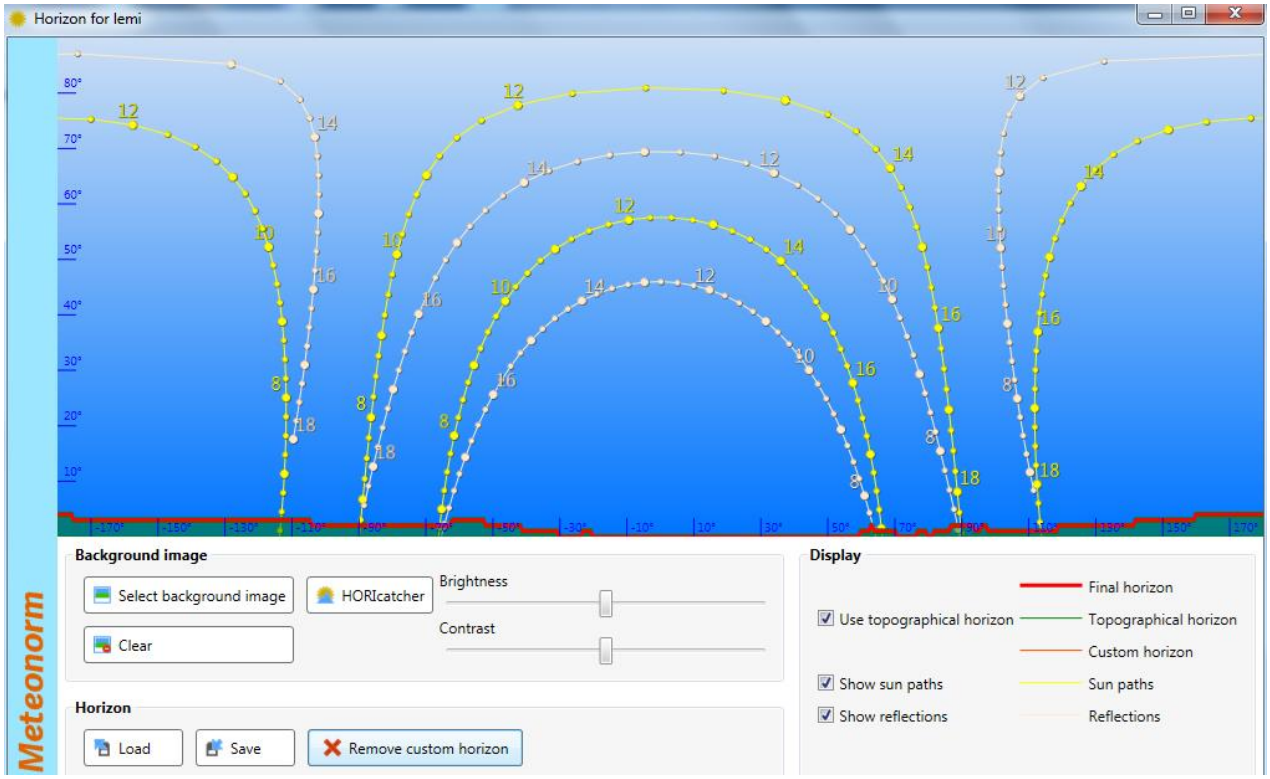

Figure 3.6 Apparent sun path variations during a year at Bole Lemi Industrial Park Generated by METEONORM 8

When measuring stations are built in urban areas, industrial areas, or even electrical substations, potential sources of radio frequency signals that could cause excessive noise in sensors or cables should be considered. For example, the same tall structure that would provide an appealing, unobstructed site for solar measurements may also be an ideal location for radio or television transmission towers or other communication equipment. The effects of electromagnetic radiation

on the health of station maintenance personnel should also be studied at such locations. Instrument selection is important because more accurate measurements would better represent the actual resource; however, instrument placement is also important. If nearby objects shade the instruments for a period of time during the day, such as trees or houses, the resulting calculation may not accurately represent the available solar resource. Distant objects, especially mountains, can be valid obstructions because the shadows they cast are likely to have an effect beyond the instruments' immediate vicinity. A nearby wall, window, or other highly reflective object may be one of these instances. Instruments should be placed away from any items that would be visible to the instrument detector. For radiation and all other measure, the WMO (2008) guidelines apply. Scanning the horizon for a complete 360 degrees of azimuth and noting the height of any objects protruding into the sky above the local horizon is the simplest way to calculate the quality of solar access. Buildings, trees, antennae, power poles, and even power lines can all be found. Most places will have certain obstructions, but it must be decided if they will be important in the sense of the necessary measurements. Within around 5 degrees elevation above the horizon, pyranometers are generally insensitive to sky blockage. Pyrheliometers, on the other hand, are more sensitive because, depending on the regular direction of the sun throughout the year, objects will fully block the DNI. The length of each day's blockage will be determined by the object's width and height above the horizon. The number of blockage days each year will be determined by where the object is located on the horizon. The item must be in the region of the sun near sunrise or sunset, which varies in time and azimuth throughout the year. Since the sun rises in a limited range in the east and falls in a limited range in the west during sunset (e.g., at 40° N latitude, sunrise near the summer solstice happens at approximately 60° from true North), objects blocking the sky may not be a consideration for much of the horizon. The greater the range of these sunrise and sunset areas of interest, the further north in latitude the site is located. [43].A solar horizon diagram, or even a sketch of obstructions by elevation and azimuth, will aid in determining the areas where horizon artifacts would have an effect on the measurement (see Figure 3.6). Environmental issues, such as wildlife habitat, migratory routes, drainage, and antiquities or archeological areas, should all be taken into account when deciding where to build a station.

b) Power Requirements

To avoid system downtime due to power outages, ongoing measurements require a consistent source of electrical power. Energy from the electric grid is reliable in some regions, with downtime measured in minutes per year. Multiple regular power outages are common in other areas. Depending on the appropriate study tolerance for missing data, steps should be taken to ensure that gaps in the data stream caused by power outages do not have a significant impact on the results. An uninterruptible power supply is the most common and cost-effective bridge for power outages. Unwanted or dangerous line voltage variations can occur for a number of reasons and an uninterruptible power supply can filter them out. Internal storage batteries serve as a backup power source in the event of an alternating current (AC) power outage. Internal circuitry makes an almost smooth transition from grid-connected AC power to AC provided by an inverter connected to the battery bank when the AC power is interrupted. When power is restored, the uninterruptible power supply uses AC line power to recharge the internal battery. Power loss, as well as switching to battery, is detected easily and calculated in milliseconds or partial line cycles. Some equipment may be especially vulnerable to even millisecond power interruptions during switching, and this should be determined by trial and error to avoid unplanned downtime despite the use of an uninterruptible power supply. The uninterruptible power supply is sized according to:

- Operating capacity—amount of power in watts; it can continuously supply either on or off grid-connected AC power
- Longevity of battery power—how long the battery can last under anticipated maximum load.

Users can calculate the length of the longest potential power loss and size the uninterruptible power supply to handle the full load of connected devices and the maximum battery life duration. Batteries should be checked on a regular basis to ensure that the battery continues to function as intended. Internal battery test functions sometimes report errors only when batteries are on the verge of failure, rather than when performance has deteriorated. Periodically perform a timed full-power-off test to ensure that the uninterruptible power supply can provide backup power for the time required to prevent measurement system failure. Local power generation can be devised in remote areas where utility power is unavailable. PV or small wind turbine systems (or both) and gasoline or diesel-fueled generators with battery storage are both viable options for on-site electrical power generation. Renewable energy systems should be sized to provide enough

energy to meet the full continuous load and power for many days of cloudy weather when solar production is low. This will involve places where there is a lot of ground fog. The sizing is based on the solar climate's extremes and should take into account the longest gap during reduced generation, the shortest recharge time available after discharge, and the generation capacity and storage required providing continuous power to the target place. In the event of a power failure, equipment should be defined and checked for self-power-on capability. When power is restored, the equipment can resume measurements and recording without the need for operator interference. The critical concern for remote areas where there could be significant downtime before staff can be deployed to restart a device.

3.7 Data Analysis

One of the fundamental tenets of quantitative research is the concurrent gathering and analysis of data. It enables researchers to narrow the emphasis of their observations and interviews over time and determine how to test their results. To provide a more thorough explanation, quantitative research methodologies are broken down into three groups: memos and displays, linking techniques including narrative analysis and case studies, and coding and thematic analysis. Because the researchers are flexible, this study evaluates the gathered data transcripts using a case study methodology. Engineering case studies are common since engineering is fundamentally an investigation of the present situation. This thesis illustrates how to structure case studies using a fundamental engineering problem-solving method, but the framework can be used for other engineering reports as well (including undergraduate thesis). This thesis focuses on designing mathematical modeling and system simulation for a specific textile business known as Bole Lemi Industrial Park, using all accessible solar resources on the site.

Having established the annual, monthly and daily levels of direct (beam) solar irradiation, its impact on the power yield of the parabolic solar power plant (PSP) can be analyzed. The analysis includes the following activities.

- January 1st where measurement of relevant solar data took place is considered for the analysis of thermal energy in parabolic collectors. 6:00 a.m. is taken into account.
- The direct sun irradiance and the interactions of the factors that will be taken into account from the location will be predicted using a regression model.
- Using the achievable region optimization technique, the optimal process temperature and direct normal irradiance (DNI) will be determined on an hourly basis.

- Microsoft Excel, Metenonorm 8, and SAM will be used to examine and look into the measured data at the site and solar resource from NASA solar surface energy (SSE). The general design, modeling, and simulation process for a parabolic trough collector is illustrated here.

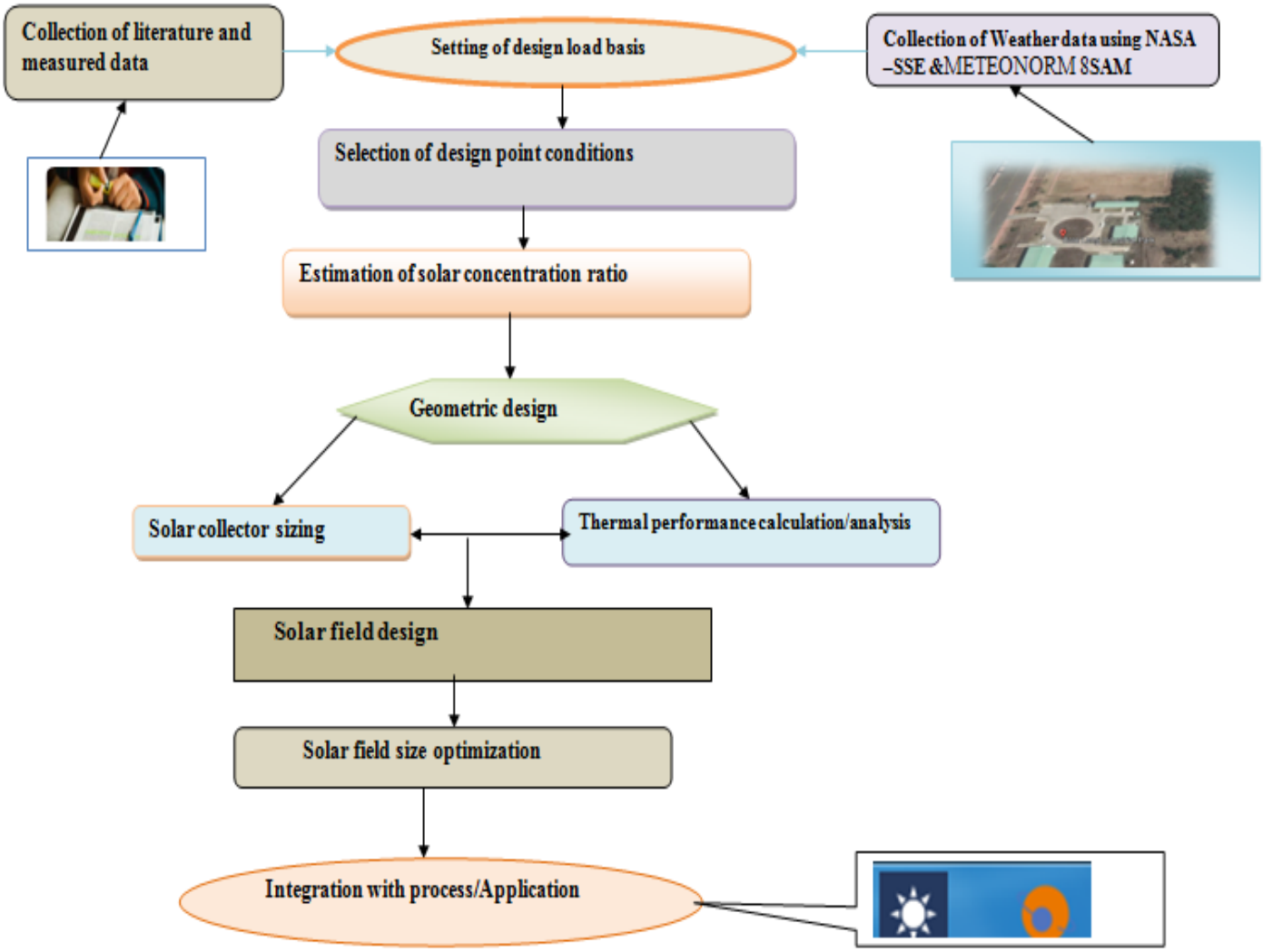

Figure 3.7 Design steps of Parabolic Trough Collector

Chapter Four

Solar Radiation and Geometric Analysis of Parabolic Trough Collector

4.1 Introduction

This chapter investigates solar radiation, basic solar components, and geometric analysis of parabolic trough collector. Furthermore, hourly extraterrestrial radiation, hourly global solar radiation on horizontal surfaces, models of solar geometry and single axis solar tracking will be explained.

4.2 Solar Radiation

Designing and assessing the economic viability of parabolic trough solar power facilities requires comprehensive knowledge on the availability of solar radiation at any given site. For several areas in Ethiopia and other regions of the world, long-term measured data on sun radiation are available. Different physics and satellite models can be used to estimate the solar energy availability for those regions where long-term observed data are not available. Solar energy is electromagnetic radiation with wavelengths between 0 and 3 mm (10-6 m), which correspond to ultraviolet, visible, and infrared light. The majority of this energy is focused in the visible and near-infrared wavelength range. The energy per unit time per unit area (kW/m^2), also known as irradiance, is used to measure incident sun radiation, also known as isolation. The solar constant, Gsc, is the average quantity of solar radiation, extraterrestrial insulation, that falls on a surface normal to the sun's rays outside of the earth's atmosphere at mean earth-sun distance Do. Recent research has revealed that the solar constant is currently 1366.1 W/m^2 [14].

"Extraterrestrial radiation" refers to solar radiation that enters the planet's atmosphere from a distance. The surface of the earth won't receive all of this radiation. In the course of its ascent through the atmosphere: a portion is re-radiated

- A portion is absorbed
- A Portion Is scattered (Diffuse)
- The Remainder is transmitted to the earth’s surface (Direct)

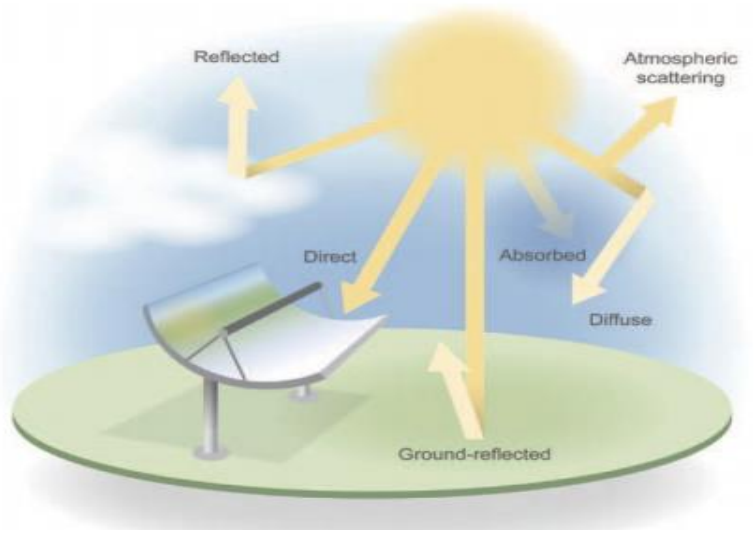

Figure 4.1 Solar radiation components resulting from interactions with the atmosphere. Image by Al Hicks, NREL

The availability of solar radiation at any site is crucial for the design and economic analysis of parabolic trough power facilities. Numerous factors affect the quantity and quality of solar radiation that a place or body of water receives.

Latitude, season, time of day, cloud cover, and altitude are a few of the variables that must be considered. In wavelengths, the frequency of solar radiation is expressed. The distance between a wave's peaks is known as a wavelength, and it is measured in nanometers (nm). Although many locations in Ethiopia and around the world have long-term monitored sun radiation data, the Bole Lemi Industrial Park does not. Solar radiation availability is employed when there are no long-term computed data available at the study location.

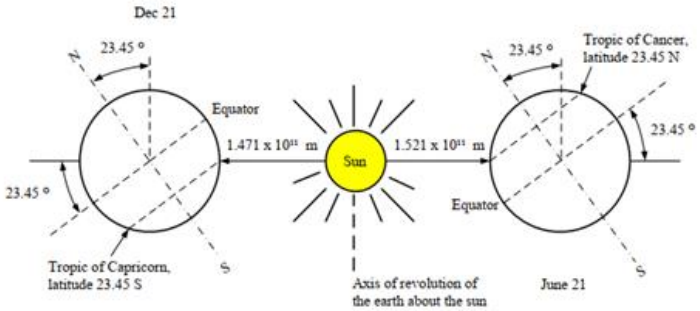

Figure 4.2 Motion of the earth about the sun, adopted from [44]

4.3 Solar geometry

An understanding of solar geometry is important for better preparedness when designing solar power systems. The Earth's daily rotation around its axis, which passes through its two celestial poles (north and south),is perpendicular to the equator but not to the plane of its orbit. In reality, the Earth's axis is currently tilted or obliquity to a line perpendicular to the plane of its orbit is around 23.45[45].

4.3.1 Basic Solar Components

a) Declination angle δ

The declination is the angle between the sun's north or South Pole and the equator of the planet. Seasonal fluctuations are caused by the maximum and lowest declination angles, as schematically shown in Figure 4.3. Between 23.45 degrees north and 23.45 degrees south is the declination. Around December 21, which is the winter solstice for the northern hemisphere and the summer solstice for the southern hemisphere, the northern hemisphere is tilted 23.45 degrees away from the sun.

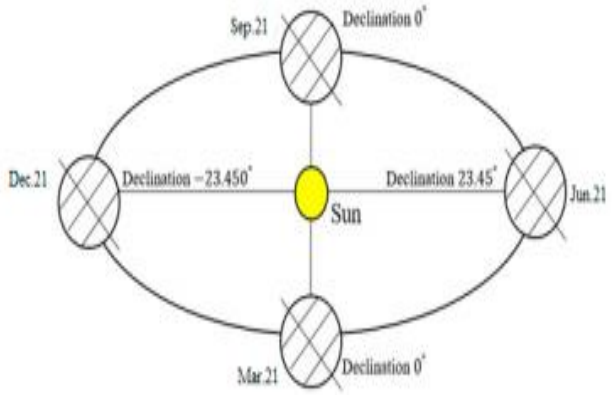

Figure 4. 3Maximum and minimum value of declination angle [46]

The earth's regular rotation axis is at a 23.45-degree angle to the axis of its ecliptic orbital plane around the sun. This tilt is the primary cause of seasonal variations in the amount of solar radiation available at any given place on earth. The solar declination angle is the angle formed by the earth-sun line (which passes through their center) and the plane passing through the equator

.During its yearly period, the declination angle varies from – 23.5° to + 23.5°. The angle of solar declination is measured as follows:

$$\delta = 23.45^{o} \sin\left[\frac{360(284+n)}{365}\right] \quad \text{.....4.1}$$

Where *n* is the number of days with January 1 being *n* = 1. In general, the declination angle is assumed to remain constant during a specific day.

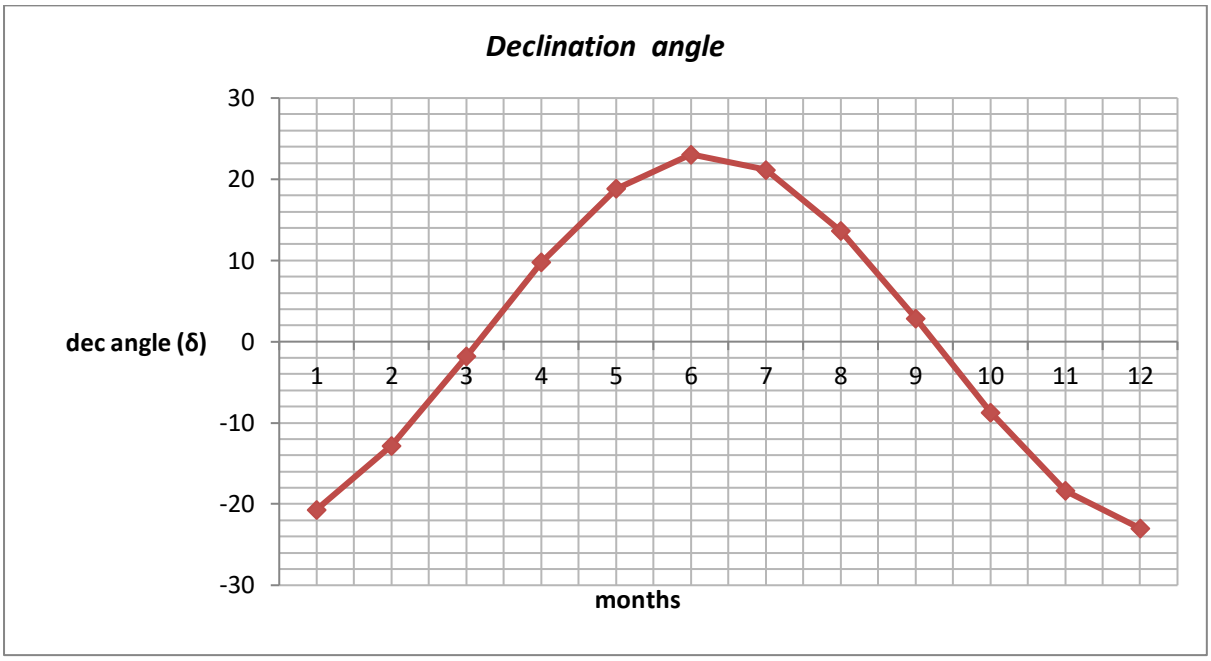

Figure 4.4 Variation of declination angle, δ, thought the year

b) Hour angle

The concept of hour angle is used for describing the rotation of the earth around its polar axis which is equivalent to +15◦ per hour during the morning and −15◦ in the afternoon. It is the angular distance between the observer's meridian and the meridian whose plane contains the sun (Figure 4.5).

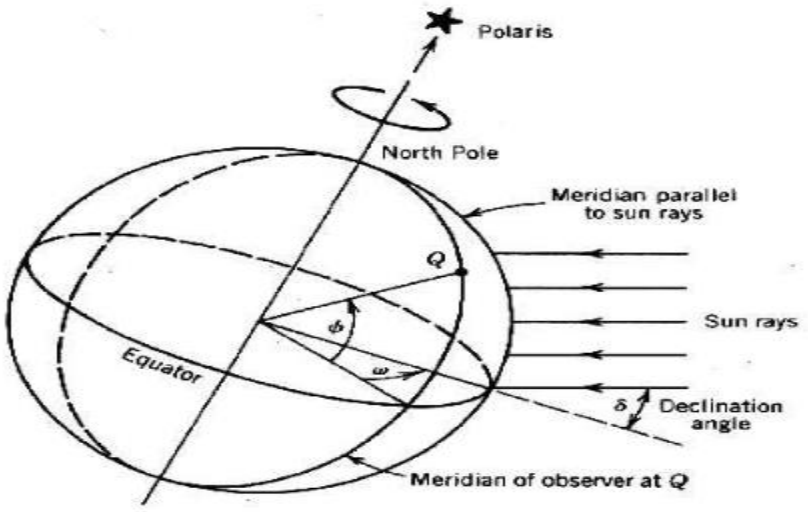

Figure 4.5 hour angle, ω,for a point [47]

The following equation can be used to calculate the hour angle in degrees. It should be noted that at noon the hour angle ω is zero [48]

$$\omega = 15(12 - S_T) \quad \text{.....4.2}$$

Where S_T is the local solar time $S_T = L_T + \frac{E_T}{60} + \frac{4}{60}[L_s - L_L]$

Where L_T is the local standard time, Ls is the standard meridian for a local zone, L_L is the longitude of the location under study in degrees and E_T is the equation of time given by Tasdemiroglu [49] as:

$$E_T = 1.000110 + 0.034221 \cos \Gamma + 0.001280 \sin \Gamma + 0.000719 \cos 2\Gamma + 0.000077 \sin 2\Gamma \quad \text{.....4.3}$$

Where $\Gamma = 360\ (n\text{-}1)/365^{\circ}$.Table 4.1 shows monthly average solar declination angle, δ, and sun-earth distance correction factor, and equation of time (E_T-minutes) adapted from [44]

Table 4.1 solar declination angle and sun-earth correction factor

Month	**Dec angle (δ)**	R	E_T
1	**-20.71**	1.032	-9.97
2	**-12.81**	1.025	-14.54
3	**-1.8**	1.011	-9.36
4	**9.77**	0.994	-0.22
5	**18.83**	0.978	3.75
6	**23.07**	0.969	0.57
7	**21.16**	0.967	-5.80
8	**13.65**	0.975	-3.88
9	**2.89**	0.99	5.68
10	**-8.72**	1.007	14.97
11	**-18.37**	1.002	14.95
12	**-22.99**	1.031	10.25

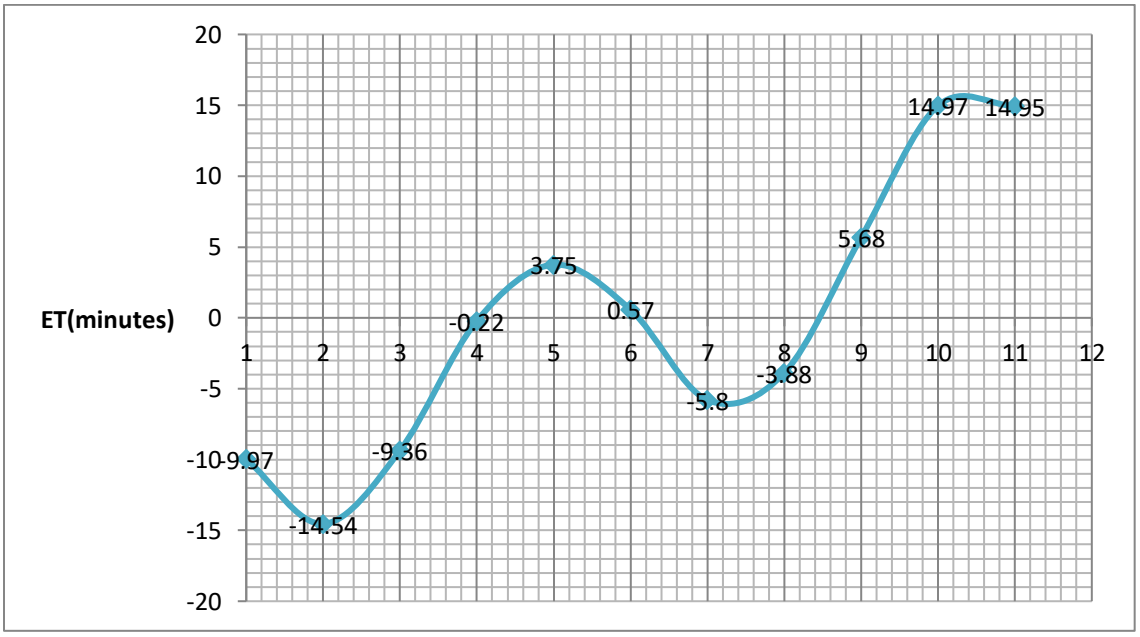

Figure4.6 Equation of time thought a year

c) Solar Azimuth Angle (γ)

The angular displacement from the south of the beam radiation projection on the horizontal plane is defined as the solar azimuth angle. This is schematically illustrated in Figure 4. 7

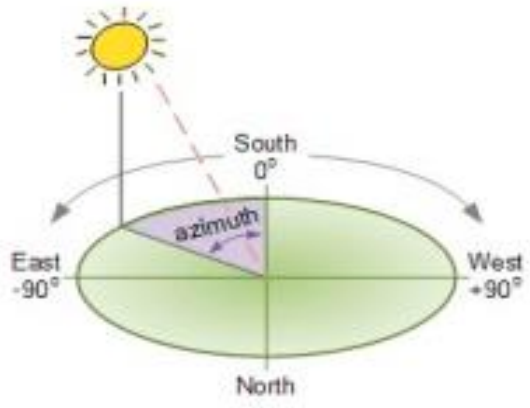

Figure 4.7 solar azimuth **[50]**

d) Latitude (φ)

The position north or south of the Equator that is relevant for a given area is its latitude. Latitude varies from ˚0 to 90º (positive for the northern hemisphere and negative for the southern), with ˚0 at the equator and 90º at the poles.

4.3.2 Hourly Extraterrestrial Radiation

Extraterrestrial radiation is defined as the incidence of solar radiation outside the earth's atmosphere and is computed with the following equation:

$$Io = \frac{43.2}{\pi} GscE_T \left((sin\phi \cos\delta)(sin\omega_2 - sin\omega_1) + \frac{\pi(\omega_2 - \omega_1)}{180} (sin\phi \sin\delta) \right) \quad \text{.....4.4}$$

Where Gsc is a solar constant (1367 W/m^2); E_T is the eccentricity correction factor[47] δ is the declination angle; ϕ is the latitude of location; ω_1 and ω_2 are the hour angle at the beginning and end of the time interval, where all angles are given in degrees. The eccentricity correction factor E_T(equation of time)can be calculated [51]. The equation for time is calculated using equation 4.3.For most engineering and technological applications, however, a very simple expression used by Beckman may be employed [47]:

$E_T = 1+0.0033\cos\left(\frac{2\pi n}{365}\right)$……..4.5

4.3.3 Hourly Global Solar Radiation on Horizontal Surfaces (IH)

A pyranometer, a device that detects global solar radiation from all angles, can be used to measure global solar radiation on horizontal surfaces. In order to determine monthly average worldwide solar radiation, a model based on latitude and altitude of a location has been created Chandel et al. [55]. Following Gueymard [51]'s daily integration approach, the values of solar radiation obtained using this model are utilized to estimate hourly solar radiation. The hourly solar radiation is also approximated using the measured daily solar radiation data for Bole Lemi Industrial Park in order to confirm the accuracy of the results. This method is first used to predict hourly global solar radiation for Addis Ababa [Latitude 9˚N, Longitude 38.8˚E, altitude 2324 m] for which 10-15 years measured data are available.

The daily average extraterrestrial irradiation on a horizontal surface H_o is given as

$H_o = k\omega_0 R G_{Sc} \sinh_0$ ..... (4.6)

Whre $k = 24/\pi$, ω_0 is the sunrise hour angle (in radians) ,R is the inverse square of the sun–earth radius factor (from Table 4.1) and h_0 is the daily-average solar elevation outside of the atmosphere [48], such that

$\sinh_0 = qA(\omega_0)/\omega_0$ …… (4.7)

Where $q=\cos\emptyset\cos\delta$ and $A(\omega_0) = \sin\omega 0 - \omega_0\cos\omega_0$

Caution needs to be exerted during the polar day and night, which occur in the absence of sunrise and sunset. The practical solution used here is to fix $\omega_0 = 0$ for polar nights (i.e when $-\tan\emptyset\tan\delta>1$) and $\omega_0=\pi$ for polar days (i.e., when $-\tan\emptyset\tan\delta<1$).

The day length (in hours) is simply obtained as

$S_0 = k\omega_0$ …… (4.8)

Solar elevation is calculated hourly from

$\sin h = q(\cos\omega - \cos\omega_0)$ ……(4.9)

Where $\omega = \pi$ (1-t /12) and t is the Local Apparent Time (LAT) of the middle point of each hourly period. For an hourly period evaluated at the middle of the hourly interval. Accordingly, the present procedure, the extraterrestrial hourly / daily ratio can be obtained [52] simply as,

$r_0 = (\cos\omega - \cos\omega_0) / k\,A(\omega_0)$ ……(4.10)

Following Gueymard [48] the daily irradiation H is given by

$H = kqRGsc[a1\,A(\omega_0) + qa_2\,B(\omega_0)]$ ……(4.11)

Where $B(\omega_0) = \omega_0(0.5+\cos^2\omega_0) - 0.75\sin 2\omega_0$.

The hourly average irradiance / daily average irradiance ratio, r_t , E/H, is obtained

$r_t = E/H$ ……4.12

Where $E = RG_{sc}(a_1 \sin h + a_2 \sin^2 h)$

$r_t = r_0[1+q(a_2/a_1)kA(\omega_0)r_0] / [1 + q(a_2/a_1)B(\omega_0) / A(\omega_0)]$ ……(4.13)

Where

$a_1 = 0.41341\,K_t + 0.61197K_t^2 - .0.01886Kt\,S\,0 + 0.00759S_0$

$a_2 = Max(0.054, 0.28116+2.2475K_t - 1.76118K_t^2 - .1.84535\sinh_0 + 1.6811\,\sin^3 h_0$

The solar constant, Gsc, is the average amount of solar radiation falling on a surface normal to the sun's rays beyond the earth's atmosphere (extraterrestrial) at a mean earth-sun radius. Gueymard [48] determined that the solar constant in this simulation is 1366.1 W/m^2.Figure 4.6 represents the extraterrestrial solar radiation spectrum, with the solar constant of 1366.1 W/m^2, the corresponding black body (normalized) curve, and the attenuated spectrum for air mass of 1.5. The seasonal variation of extraterrestrial solar radiation at the earth's surface is well understood thanks to the earth's rotation around the sun.

Extraterrestrial radiation is proportional to the inverse square of the distance between the earth an d the sun, as follows:

$I = Gsc\,(Do/D)^2$ ……4.14

Where D is the distance between the sun and the earth, and Do is the yearly mean earth-sun distance (1.496×10^{11}m). The factor $(Do/D)^2$is calculated as [49]:

$$(Do/D)^2 = 1.00011+0.034221 \cos(x)+0.00128 \sin(x) +0.000719 \cos (2x)+0.000077 \sin(2x) \quad ...4.15$$

where $x = 360\ (n\text{-}1)/365^{\circ}$

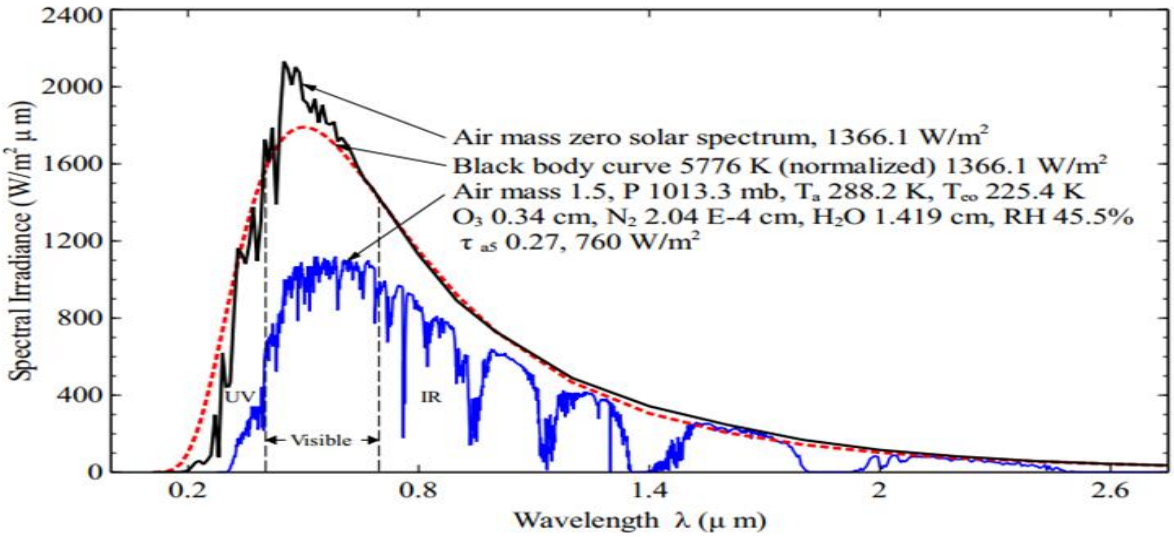

Figure 4.7 Extraterrestrial solar radiation spectrum (in vacuum below 280 nm, in air above 280 nm); also shown are equivalent black body and atmosphere-attenuated spectra (SMARTS2, U.S. Standard Atmosphere USSA, rural aerosol model, Z=48.19° (Air mass 1.5)). Adapted from [53]

Figure 4.9 shows the variation of the factor $(Do/D)^2$ throughout the year. As extraterrestrial solar radiation, I , passes through the atmosphere, a part of it is reflected back into

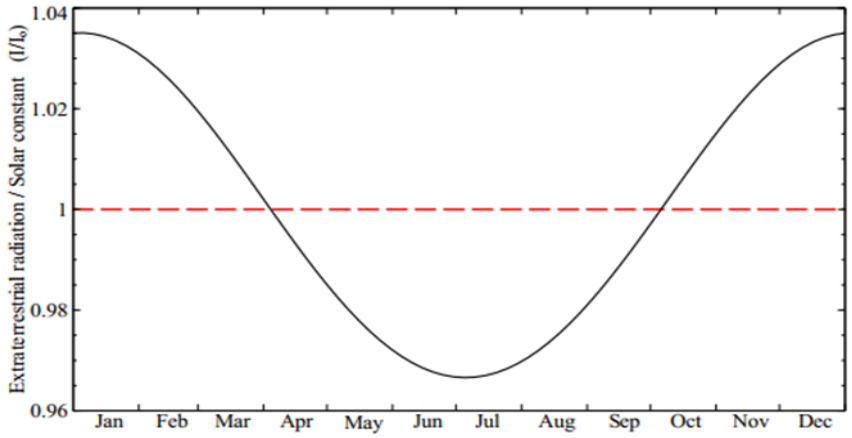

Figure 4.8 Variation of $(\mathrm{Do/D})^2$ *throughout the year*

the space, a part is absorbed by the air and water vapor, and some gets scattered by the molecules of air, water vapor, aerosols and dust particles (Figure 4.10) [44].

The amount of solar radiation that enters the earth's surface with little to no change in direction is referred to as direct or beam radiation. The diffused radiation from the sky that disperses and reaches the surface is known as sky diffuse radiation.

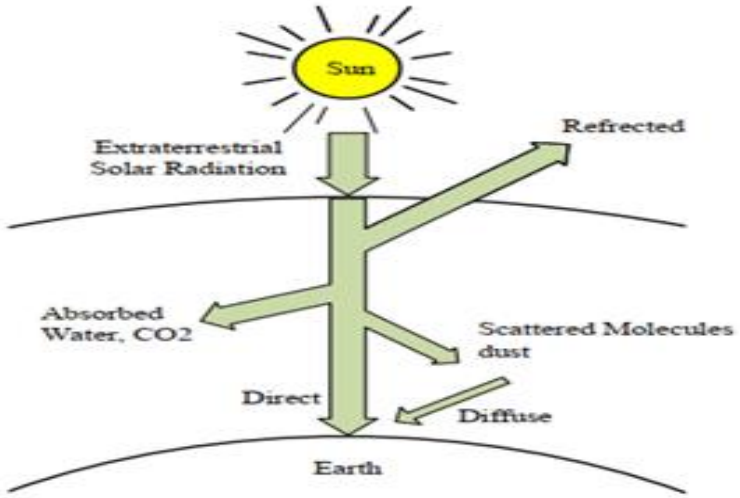

Figure 4.9 Attenuation of solar radiation as it passes through the atmosphere. Adaptedfrom[14]

Gueymard [54] used a wide data collection of 135 stations with a variety of geographic locations (82.58 N to 67.68 S) and climates to establish the daily integration method for predicting monthy average hourly global irradiation.

Gueymard compared his proposed model with previous hourly radiation models, the Collares-Pereira and Rabl Model CP&R[55] and the Collares-Pereira and Rabl Model updated by Gueymard [56], and found that the regular integration model is the most reliable.

4.3.4 Hourly Diffuse Radiation on Horizontal Surface (DHI)

The portion of sunlight known as diffuse solar radiation is absorbed, scattered, or reflected by water vapor, dust, or other pollutants as it travels through the atmosphere. Because it cannot cast precise shadows, this sort of radiation cannot be concentrated [61].

The received global irradiation on horizontal surfaces is typically measured by a large number of meteorological/radiometric stations. Obtaining these measurements is challenging due to the

high expense of the measuring apparatus. As a result, a large number of mathematical models have been created to estimate diffuse radiation on horizontal surfaces. There are two types of models that can predict diffuse radiation on horizontal surfaces: parametric and decomposition models.

4.3.4a) Parametric Models: Specific information of environmental conditions such as atmospheric turbidity, fractional sunshine, cloud cover, and perceptible water content are necessitates of parametric models [57]

$$I_H = I_{bN}\cos\theta_z + I_d \quad \text{.....4.16}$$

$$I_{bN} = A\exp[-B/\cos\theta_z] \quad \text{.....4.17}$$

$$D_{HI} = C_{IN} \quad \text{.....4.18}$$

Where I_{bN} is normal solar beam radiation on horizontal surfaces, θz is the zenith angle and can be calculated from following equation:

$$\theta_z = \cos{-1}\ (\sin\delta \sin\phi + \cos\delta \cos\phi \cos\omega) \quad \text{.....4.19}$$

A, B, C are values of constants and are given for each model in Table 4. 2.

i) **ASHRAE Model: The** ASHRAE algorithm offers a simpler method, which is widely utilized by the engineering and architectural communities [58]

ii)Machler and Iqbal'sModel: Machler and Iqbal [59]studied estimating hourly diffuse irradiation from hourly global solar radiation measured on horizontal surfaces. They recommended investigating solar altitude ranges above 40°. They improved the invariables A, B and C (of the ASHRAE model), which considers the improvements in solar radiation research over the previous decades

iii)Parishwad's Model: Parishwad et al. assessed the constants of the ASHRAE model (A, B, and C) using statistical indicator analysis of measured solar radiation data of six cities from different locations in India[60].

iv)Nijegorodov's Model : Nijegorodov revised the constants of ASHRAE's model, using a computer program to predict hourly and daily global solar radiation in Botswana based on recorded solar radiation components in Botswana, Namibia, and Zimbabwe[61].

Table 4.2 Estimated values of A,B,C for different models [47]

	January	February	March	April	May	June	July	August	September	October	November	December
						ASHARE						
A	1230	1215	1186	1136	1104	1088	1085	1107	1152	1193	1221	1234
B	0.142	0.144	0.156	0.180	0.196	0.205	0.207	0.201	0.177	0.160	0.149	0.142
C	0.058	0.060	0.071	0.097	0.121	0.134	0.136	0.122	0.092	0.073	0.063	0.057
						Machler and Iqbal						
A	1202	1187	1164	1130	1106	1092	1093	1107	1136	1166	1190	1204
B	0.141	0.142	0.149	0.164	0.177	0.185	0.186	0.182	0.165	0.152	0.144	0.141
C	0.103	0.104	0.109	0.120	0.130	0.137	0.138	0.134	0.121	0.111	0.106	0.103
						Parishwad et al.						
A	610.00	652.20	667.86	613.35	558.39	340.71	232.87	240.80	426.21	584.73	616.60	622.52
B	0.000	0.010	0.036	0.121	0.200	0.428	0.171	0.148	0.074	0.020	0.008	0.000
C	0.242	0.249	0.299	0.395	0.495	1.058	1.611	1.624	0.688	0.366	0.253	0.243
						Nijegorodov						
A	1163	1151	1142	1146	1152	1157	1158	1152	1150	1156	1167	1169
B	0.177	0.174	0.170	0.165	0.162	0.160	0.159	0.164	0.167	0.172	0.174	0.177
C	0.114	0.112	0.110	0.105	0.101	0.098	0.100	0.103	0.107	0.111	0.113	0.115

4.3.4b) Decomposition Models: When estimating diffuse radiation from data on global solar radiation, decomposition models normally only employ data pertaining to global radiation. On a correlation between the diffuse and total radiation on a horizontal surface (Kt = clearness index), decomposition models are constructed. The atmosphere's clarity can be measured using the clearness index [67]. It is the portion of solar energy that is converted into the hourly extraterrestrial radiation (Io) that strikes the planet by passing through the atmosphere. It is calculated as the surface radiation divided by extraterrestrial radiation, resulting in a dimensionless number between 0 and 1. Under clear, sunny conditions, the clearness index has a high value, and under gloomy circumstances, a low value. It is a random parameter that changes according on the season, time of year, weather, and geographic location of a location [68].

$$Kt = \frac{I_H}{I_O} \quad \text{.....4.20}$$

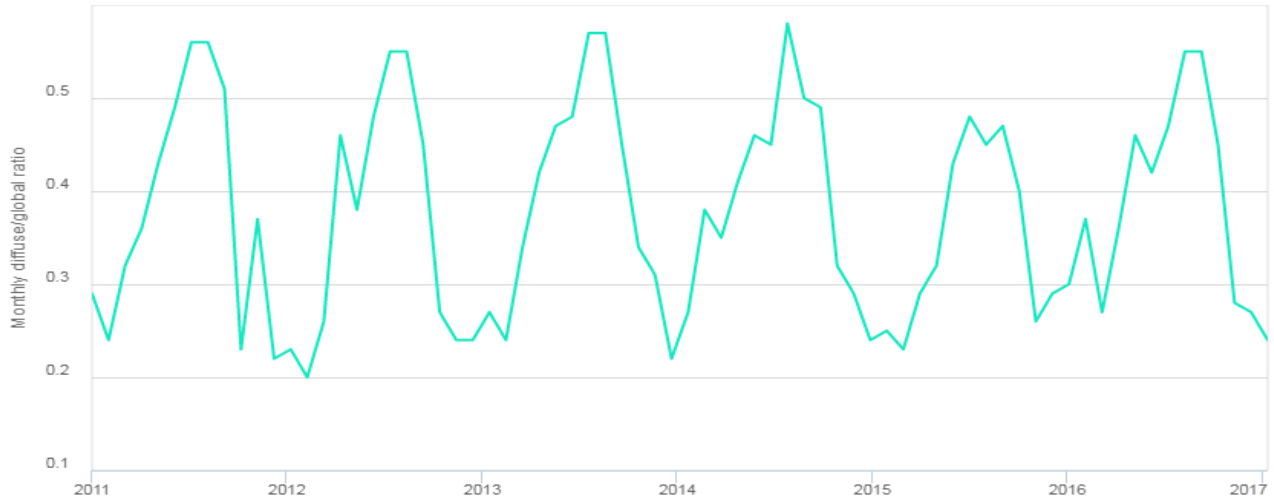

Figure 4.10 Monthly averages diffuse to global ratio at Bole Lemi Industrial Park (generated using PVGIS-5 geo- temporal irradiation database)

4.4 Solar tracking system

Solar tracking systems are required since PTCs use direct beam radiation. As was already mentioned, a solar tracking device lines up the collector with the sun to maximize output from the one-axis rotating collector (see Figure 4.11). There are two categories of solar trackers: passive and active. While active trackers employ electrical signal conversion to orient the collector, passive trackers use the thermo siphon effect. Passive trackers aren't frequently utilized in PTCs, though, due to the fact that wind forces cause misalignment when in use.

The two types of active trackers used in concentrating solar systems are closed-loop and open-loop trackers. The primary distinction between these two varieties of active trackers is the signal conversion mechanism used. Closed-loop trackers use electronic signal conversion and feedback control.

Both closed-loop and open-loop active trackers are employed in concentrating solar systems. The method utilized for signal conversion is the primary distinction between these two categories of active trackers. Electronic signal conversion and feedback control are used in closed-loop trackers[69]. Open loop truckers use a computer, timing controls, pre-recorded data, and algorithms to track the sun. Figure 4.12 shows the activity of each type of active solar trucking.

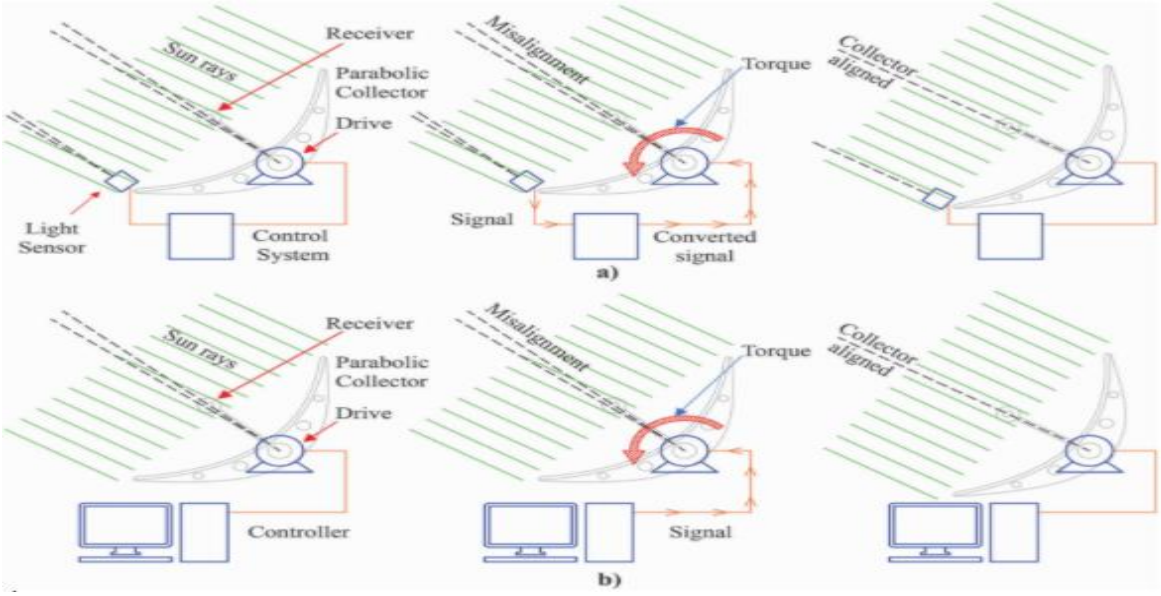

Figure4.11 Solar tracker types: (a) active closed-loop, (b) active open-loop[62].

Active closed-loop trackers consist of a light sensor, a control system, and a driving system (Figure 4.12 a). The sensor, which detects a high light intensity when it is aligned and is engaged when the collector is out of alignment with the sun, sends a signal to the control device as a result of the misalignment. The control system converts this signal, causing the driver to shift and apply torque to the structure before the collector is correctly aligned. A pair of light-receiving diodes or photovoltaic cells is the most typical closed-loop tracking sensor. The key advantage of this tracking system is its excellent tracking accuracy; however it is vulnerable to shadowing. The key drawback is the control system's inability to recover or find the sun's path during long cloudy periods.

Active open-loop trackers consist of a drive and a controller (Figure 4.12b). The controller's algorithm orders the drive to pass the collectors while it is running. Open-loop trackers come in two varieties: timed trackers and altitude/azimuth trackers. Timed trackers use time-based algorithms to gradually track the collector. Algorithms used by altitude/azimuth trackers are based on astronomical data and are modified for position and time. These methods have a flaw in that the consistency of the equations utilized in the algorithms might lead to significant misalignments. A PTC employs direct sun light as its heat source. The sun's relative position changes every second, necessitating the deployment of a solar tracking device to increase efficiency. According to Figure 4.13, there are two types of solar tracking employed in PTCs: east-west and north-south. The names of the tracking methods are derived from the direction of

rotation of the aperture plane of the collector. North-south tracking causes the aperture plane of the collector to spin from north to south and vice versa because the receiver, which is parallel to the tracking axis, is oriented to the east-west direction. The polar opposite is the east-west tracking approach, in which the aperture plane moves from east to west while the receiver is oriented north-south. The advantage of the north-south tracking approach is that it uses fewer tracking resources while producing a stronger result. Similarly, east-west monitoring systems have a lower end impact and use more energy [69].

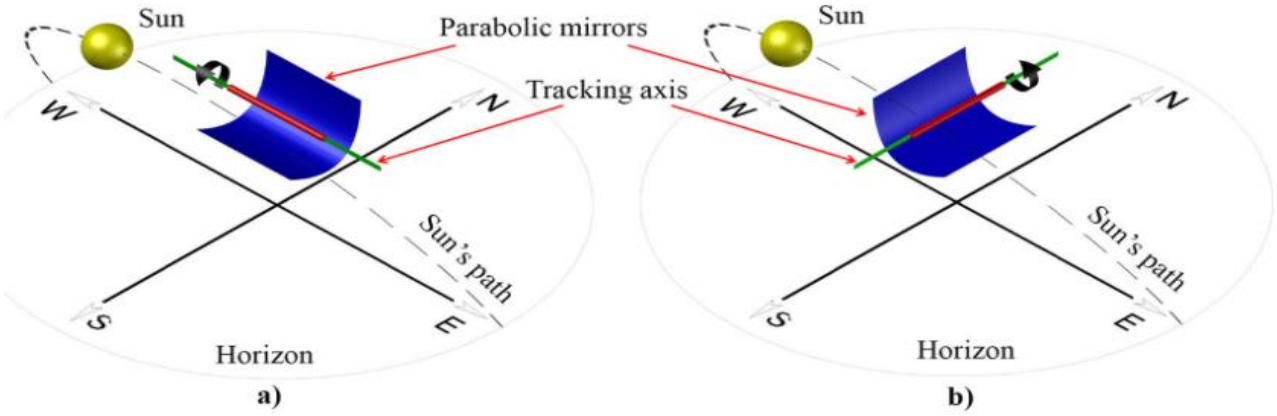

Figure 4.12 Common tracking methods : (a) north-south, (b) east-west [62].

4 .4 .1 Single Axis Tracking

The sun's position at any particular time can be determined using the altitude and azimuth angles (Figure 4.14). The solar altitude angle [70] is the angle between a line parallel to the sun's beams and the horizontal plane. The solar azimuth angle is the angle formed by a due south line and the horizontal projection of the line linking the site to the sun[70]. Positive and negative signs for azimuth angles are used west of south and east of south, respectively. The angle produced by the site to the sun line and the vertical at the site location is known as the solar zenith angle (abbreviated as z):

θ_z =90- *solar altitude angle (a)* ……..*4.21*

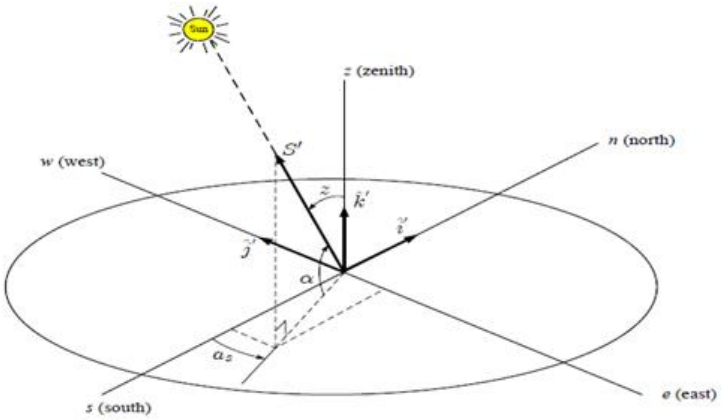

Figure 4. 13 Earth surface coordinate system for observer at Q showing the solar azimuth angle (as), the solar altitude angle (a) and the solar zenith angle (z) for a central sun ray along direction vector S'. Also shown unit vectors i^', j^', k^' along their respective axes. Adapted from [63]

The solar altitude and azimuth angles must be compared to the fundamental angles of the hour, latitude, and declination because they are not fundamental. PTCs, as was already said, are made to operate with just one monitoring axis. A tracking drive mechanism rotates the collector around an axis of rotation until the aperture normal region and the sun's central beam are coplanar. Figure 2.13 shows the rotation of a collection aperture around a tracking axis r. The tracking angle, r, and aperture normal, which form the plane and tracking axis, respectively, create the central ray unit vector S.

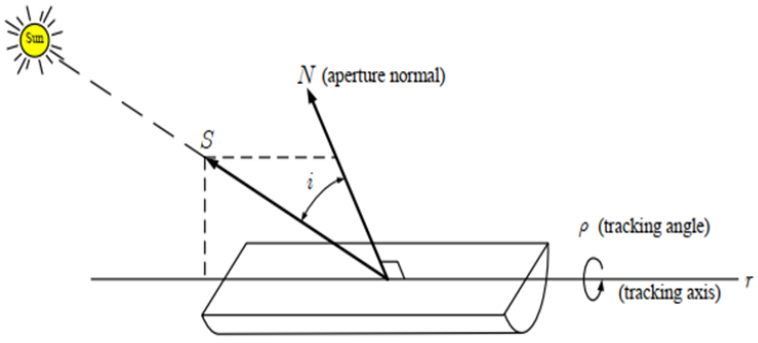

.

Figure 4.14 single axis aperture, adopted from [63]

In order to formulate formulae for i and r in terms of collector orientation and solar angles, it is crucial to convert the original coordinates, x0; y0; z0 (Figure 4.14) to a new coordinate system

with the tracking axis as one of its three orthogonal axes. One of the other two axes is turned such that it is parallel to the surface of the earth. With r as the tracking axis, b as the axis that is always parallel to the earth's surface, and u as the third orthogonal axis, the new coordinate system is depicted in Figure 4.16.

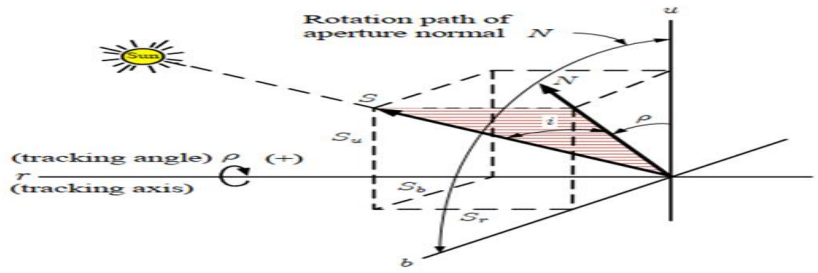

Figure 4.15 Single Axis Tracking system coordinates .Adopted [63]

The same orientation is used for the other two axes. It is important to keep in mind that the aperture normal N rotates in the u-b plane. Both i and r can be described by the direction cosines of the central ray unit vector S along the u, b, and r axes. The following formula is used to calculate the tracking angle:

$$\tan r = -\frac{S_u}{S_b} \quad \text{.....4.22}$$

And the cosine of incidence angle θ_i is given by:

$$\cos\theta_i = \sqrt{(S_u^2 + (S_b^2} \quad \text{.....4.23}$$

Or, $\cos\theta_i = \sqrt{1 - (s_r^2)}$ 4.24

4.4.2 Horizontal Tracking Axis

To characterize this group, the z, w, and n coordinates that were previously used to create the sun ray unit vector must be rotated by an angle of g to become the u, b, and r coordinates. In Figure 4.16 As seen in Figure 4.17, the rotation revolves around the z axis since the axis monitoring remains perpendicular to the surface of the earth. Path cosines in the S (new coordinate system) is calculated as

$$\begin{vmatrix} S_r \\ S_b \\ S_u \end{vmatrix} = \begin{vmatrix} cos\gamma & -sin\gamma & 0 \\ sin\gamma & cos\gamma & 0 \\ 0 & 0 & 1 \end{vmatrix} . \begin{vmatrix} S_i' \\ S_j' \\ S_k' \end{vmatrix} \quad \text{.....4.25}$$

Substituting into Equation (4.22), it is obtained that the tracking angle is:

$$\tan r = \frac{\sin(\gamma - \alpha_s)}{tan\alpha} \quad \text{.....4.26}$$

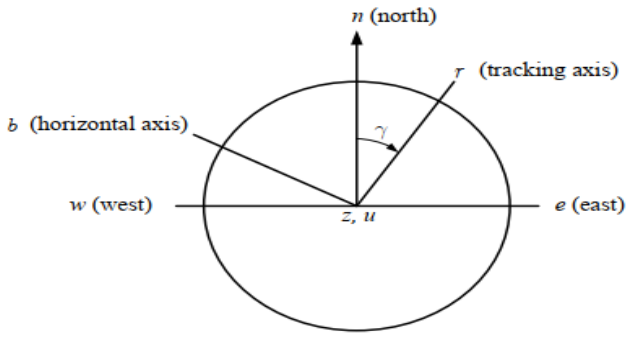

Figure 4.16 Rotation of u, b, and r from z, w, and n coordinates about the *z axis. Adapted* [63]

The angle of incidence for a single axis, horizontal trucking collector is

$$\cos\theta_i = \sqrt{1 - \cos^2\alpha\cos^2(\gamma - \alpha_s)} \quad \text{.....4.27}$$

When the trucking axis is oriented in the north –south direction ($\gamma = 0$) the above equation reduces to:

$$\tan r = -\frac{sin\alpha_s}{tan\alpha} \quad \text{.....4.28}$$

$$\cos\theta_i = \sqrt{1 - \cos^2\alpha\cos^2\alpha_s} \quad \text{.....4.29}$$

When the trucking axis is oriented in the east-west direction ($\gamma = 90$) and combining equation (4.26) and (4.27) the above equation reduces to:

$$\tan r = \frac{cos\alpha_s}{tan\alpha} \quad \text{.....4.30}$$

$$\cos\theta_i = \sqrt{1 - \cos^2\alpha\sin^2\alpha_s} \quad \text{.....4.31}$$

Chapter Five

Heat Transfer Fluid Selection and Storage System Design

5.1 Introduction

This chapter introduces heat transfer fluid and thermal energy storage systems design. The chapter mainly explores how heat transfer is selected and based on major selection standards molten salt is used as working fluid for the proposed modeling and designing of parabolic trough solar collector at Bole Lemi Industrial Park. In addition, molten salts system design considerations and modeling of thermal energy storage tank will be discussed. Based on several journal references, energy and cost analysis of thermal energy storage materials and the impact of heat transfer fluid on system performance will be presented.

5.2 Introduction to Heat Transfer Fluid and Molten Salt

Recently the use of molten salts, which consist of eutectic mixtures of nitrate and nitrite-salts as heat transfer fluid in parabolic trough receivers, has been discussed and initial testing with these fluids have proven their feasibility. Besides a high temperature stability of up to 600 °C, higher densities and higher heat conductivities with nontoxic and nonflammable liquid salts are also broadly available at lower prices than thermal oil [64] . This is why molten salts are already used in solar receiver systems and as sensible heat storage media in parabolic trough power plants where they have proven their effectiveness [65].The main advantage of molten salts is their higher achievable operating temperature of the heat transfer fluid in the solar field (Table 5.1). Since, with these higher temperatures, the conversion from thermal to electrical power in the connected steam cycle can yield higher efficiencies.

Table 5.1 HTF operating temperatures in parabolic trough power plant (data from [66][67]***)***

	Therminol –VP1	**Solar salt**	**HITEC**
HTF operating temperatures	20°C-390°C	290°C-550°C	200°C-450°C

Furthermore, the combination of higher densities and higher heat conductivities of molten salts lead to higher heat capacities per transported volume unit of heat transfer fluid (as shown in Table 5.2), so storage costs can be reduced due to smaller tanks and heat exchangers[68] .The main drawbacks of these fluids are the required fail-safe freeze protection caused by the high

melting point of the molten salts and the higher heat losses mainly through radiation in the solar field caused by higher operating temperatures. Whether these drawbacks compensate the given advantages and whether there are optimization parameters that can increase energy yields for molten salts will be discussed in this section.

Table 5.2 Relations of mean fluid property values in respective of HTF temperature ranges (data from [66][67]***)***

Parameters	Solar/therminol VP-1	HITEC/therminol VP-1
Heat capacity	0.62	0.67
Density	2.36	2.4
Heat capacity per volume	1.47	1.61
Kinematic viscosity	3.71	5.72
Thermal conductivity	5.93	4.16
Thermal expansion coefficient	0.22	0.23

5.3 Selection of Molten Salts over Thermal Oil

Selecting the appropriate heat transfer fluid for a thermal fluid heating system can be difficult. There are several decision factors to consider .These factors would almost certainly play a significant role in determining the best heat transfer fluid for a given situation.

a. Thermal efficiency

For solar thermal power plants with parabolic trough collectors, the most common concept is to use molten salt as heat transfer medium in the solar field circuit. Due to the maximum operating temperature of the molten salt of about 565°C, the live steam temperature of thermal oil is limited to about 377°C and generates an efficiency of up to 40% at a steam pressure of 5 bar.

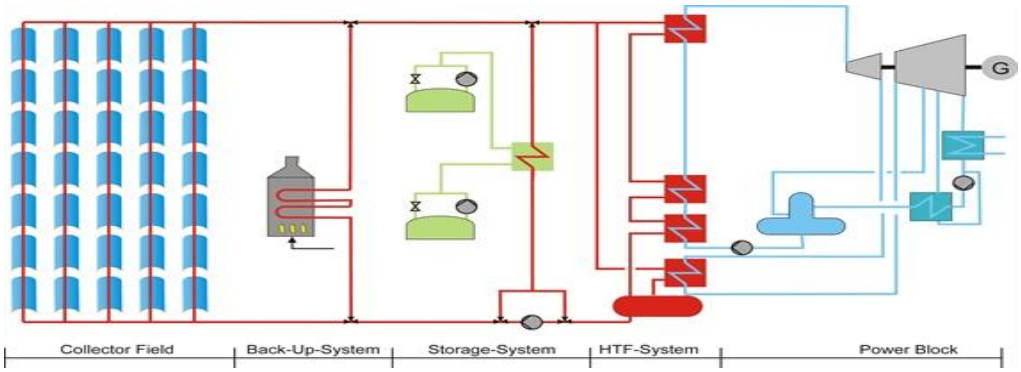

Figure 5.1 Solar thermal power plants with thermal oil as heat transfer medium and molten salt as storage medium (red: thermal oil, blue: water/steam, green: molten salt). (Source: https://www.dlr.de/sf/en/desktopdefault.aspx/tabid-10647/18795_read-44147/)

Thermal energy storage integration is a key benefit of solar thermal power systems. It enables the separation of the production of electricity from solar energy. According to daytime and nighttime demand, electricity can be fed into the system. Molten salt, a more affordable heat transmission medium than thermal oil, is utilized in thermal storages. The use of molten salt in the solar field as a heat transfer fluid in addition to a storage medium would have various technical and practical benefits. Below is an explanation of some benefits solar salt has over thermal oil.

b. **Working temperature**

The useful temperature level is raised to at least 565°C when salt is used as the heat transfer and storage medium instead of thermal oil, pushing the power block efficiencies over 45 percent. Additionally, the higher temperatures cause the energy density in thermal storage to rise, resulting in a smaller and more economical storage.

c. **Strict separation of the gained solar energy and the electricity generation**

The molten salt that circulates in the solar field as a heat transfer medium is employed both as a direct storage medium and as a heat transfer medium to the power block. Due to the lack of direct thermal oil circulation between the solar field and the power block, the solar field completely decouples from the power block, or the separation of solar irradiation from electricity generation (compare illustrations above and below). Storage tanks keep the two systems securely apart, preventing any impact on energy generation in the event of significant short-term fluctuations in the irradiation caused by, for example, passing clouds.

d. **Cost**

Studies conducted by several institutions over the past ten years have shed light on the financial benefits of employing molten salt in parabolic troughs. According to all findings, molten salt systems can save levelized power prices by up to 25% as compared to thermal oil-based reactors now in operation. The picture below depicts the design of a plant that might greatly reduce the levelized cost of electricity.

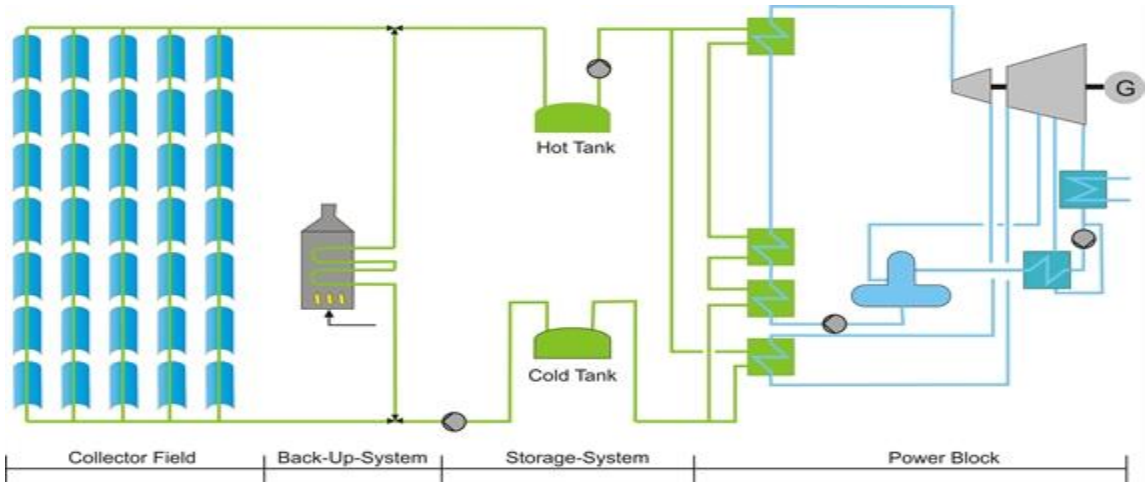

Figure 5.2 Solar thermal power plant with molten salt as heat transfer as well as storage medium (blue: water/steam, green: molten salt)
Picture:(Source:https://www.dlr.de/sf/en/desktopdefault.aspx/tabid-10647/18795_read-44147/)

5.4 General Description of Molten Salts

At ambient pressures between 220 ºC and 600 ºC, molten salt becomes liquid, which is ideal for superheated steam power cycles used today. In this temperature range, the medium has a strong volumetric heat capacity, and its specific cost is also reasonably low. However, the highest temperature poses a restriction for modern, high efficiency supercritical steam or Brayton cycles. The TESS's pipelines and valves must be protected against freeze blockage due to the high melting temperature; however storage tank insulation has been shown to be effective against thermal losses and mechanical stresses. It is possible to keep tank system corrosion and pipe corrosion under control.

High volumetric heat capacities, low viscosity, low vapor pressure, and high boiling temperatures are all characteristics of molten salts [77]. A smaller storage tank volume equates to a larger heat capacity. To optimize the temperature range for the molten salt, it is beneficial to choose a chemical mixture with a low melting point and a high boiling point. Additional heating may be necessary to prevent freezing if the melting point is too high[77]. The melting points and volumetric heat capacities of salts used for storage, such as sodium nitrate NaNO3 and potassium nitrate KNO3, range from 300 to 500 °C and 1670 to 3770 kJ/m3 °C, respectively[77]. Although it can be utilized up to 800°C and has a 320°C melting point, sodium hydroxide (NaOH) is extremely corrosive[78]. A commercially available "HITEC" salt with a liquid temperature range

of 149 - 538°C is used in solar plants. It is composed of potassium nitrate (53 percent by weight), sodium nitrite NaNO2 (40 percent by weight), and sodium nitrate (7% by weight)[79].

The salt is fed into a steam generator when energy is required, which boils water, turns a turbine, and produces electricity. Rankine, Brayton, and Air-Brayton cycles[77] are a few examples of different cycles that can be used to convert thermal energy to electricity. Other uses include utilising the heat that has been stored directly for high temperature processes (such producing H2 and turning coal into liquid), which eliminates the thermodynamic expense of converting to electricity [77]. Pumped back into the storage tank to be heated and reused is the cooled salt.

In conclusion, molten salt is a versatile storage option. The highest temperature restriction, which prevents higher power cycle efficiency, is the major downside. Freeze protection is important due to the relatively high melting temperature, which mostly affects its use as HTF. The medium's cost is low but, due to the large amounts of storage medium necessary, plays a big role in CSP plants' total cost.

5.4.1Heat transfer fluid differences

Molten salts provide superior heat transfer characteristics, are thermally stable, and can be employed at higher temperatures than synthetic oils or silicone solutions (Table 5.1). *Table 5.3 Comparison of molten nitrate salts Vs Synthetic HTF*

Property	Synthetic heat transfer fluid	Molten nitrate salt
Melting/freezing point	<25°C	130 to 220°C
Operating temperature	25 to 390°C	150 to 565°C
Volumetric heat capacity	2000 KJ/m^3	300KJ/m^3
Thermal conductivity	0.2W/mk	0.6W/mk
Viscosity	<1cp	<0.2cP
System pressure	Moderate to high	Low
Cost	$8 to 15/lb	$1/lb
toxicity	moderate	low

Source:https://www.process-heating.com/articles/91918-using-molten-salts-as-a-heat-transfer-fluid-and-thermal-storage-medium

The disadvantage of molten salts is that they freeze at 120 to 220°C, which is much higher than ambient temperature.

This could be extremely dangerous for systems that weren't designed with this in mind. To keep the salt from freezing, heat tracing is required in all pipelines and machinery used in molten salt applications. Salts frequently expand as they re-melt. If the salt is not heated uniformly while being re-melted, it may damage pipelines, valves, and other machinery. As a result, it's crucial to take the necessary precautions to stop the molten salt from freezing while it's being used.

5.4.2 Design Considerations of Molten Salt Systems

Weighing the benefits and drawbacks of employing synthetic oil or molten salt is crucial when building a high-temperature system that requires a heat transfer medium. Because synthetic oils can be charged and circulated fast, they are typically more practical to utilize. Molten salts have good heat transfer characteristics, are thermally stable, and can be employed at higher temperatures than synthetic oils or silicone solutions. If the system is designed with the right heat trace, molten salts can offer efficient heat transfer and little degradation over the course of its lifespan. Molten salts are employed in many different applications, such as phase-change systems, thermal storage systems, and high-temperature circulating systems. Because they can store solar heat for a long time, molten salts are frequently utilized in concentrated solar power plants (CSP). In some CSP systems, salt is pumped straight into the receiver tubing, where it is concentrated by a parabolic mirror when sunlight strikes it. Other technologies combine salt storage with a high-temperature synthetic fluid. The synthetic fluid flowing through the receiver tubing conducts the heat to the storage tanks for molten salt. This lessens the likelihood of freezing and makes use of the salt's outstanding heat transfer capabilities.

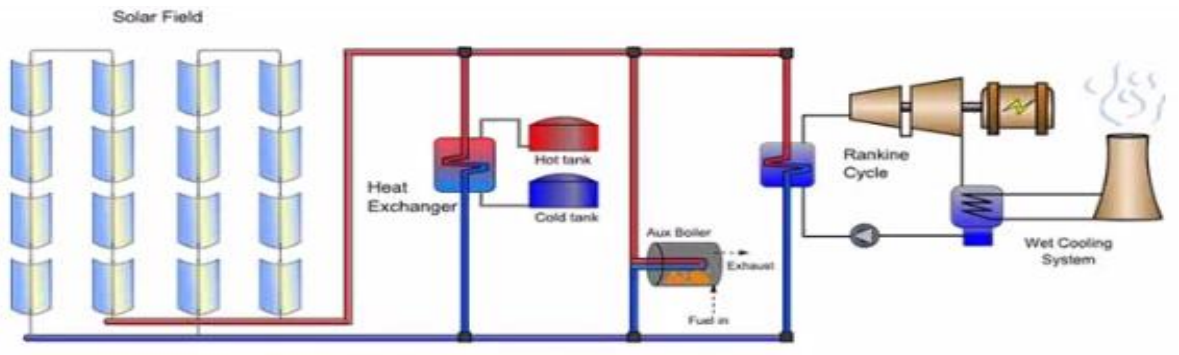

Figure 5.3 Schematic of a parabolic trough plant [75]

5.4.2.1 Mechanical design considerations

Numerous manufacturing processes consume a large amount of energy and physical space. The placement of collectors could provide a challenge if solar power is to be considered for certain purposes. Since collector arrays may be mounted on neighboring buildings or grounds, lengthy lines of pipe or duct may be necessary. The roof area and facility orientation may put a cap on the collector area. Collector array support structures must occasionally be added to existing structures because they are frequently not built or oriented to fit collector arrays [76]. It is simple and inexpensive to include collector mounting and entry into new constructions. It is necessary to interface with conventional energy sources in a process-friendly manner.

5.5 Introduction to Thermal Energy Storage Systems

Thermal energy storage systems (TESS) have several uses in CSP facilities. They enable stable turbine conditions and more full-load hours by balancing the plant during transient times, such as during cloudy weather. The ability to provide dispatchable or base-load power to the plant, and even to stabilize it on demand, is the primary rationale for the installation of massive TESS. Additionally, this boosts the power block's capacity factor and lessens mirror defocusing. This section gives an overview of the available types of TES for CSP applications and their characteristics. The major requirements on TES for parabolic trough solar collector are:

- Volumetric energy capacity
- Charge and discharge heat rates
- Maximum and minimum temperatures, sensible or latent heat storage
- Safety and environmental impact
- Thermal and chemical stability for thousands of cycles in contact with different materials
- Heat losses
- Quality of the thermocline after charging
- Degradation of the thermocline during idle mode
- Power requirements for charge and discharge
- Costs (for the whole storage system)

5.5.1 Active storage direct system: The active storage systems are characterized by forced heat exchange into the storage media which circulates by itself through a heat exchanger. A direct system means that the HTF is the same as the storage material and it is usually store in two different tanks which store the hot and cold media separately.

5.5.2 Active storage indirect system: The HTF in this instance differs from the storage media. Additionally, the storage can be done in one tank or two tanks. The single solar tank has the benefit of being less expensive, while dual solar tank systems allow for the safe separation of hot and cold storage materials. Finally, it's crucial to be aware that the single tank is frequently referred to as a thermocline. Due to the difference in densities, the hot fluid in this system is kept at the top of the tank and the cold at the bottom. The filler materials stored inside the tank are what cause the stratification throughout its length. Typically, silica sand and quartzite rock are used as filler materials. Furthermore, it is necessary to consider the filler material as the primary thermal storage medium.

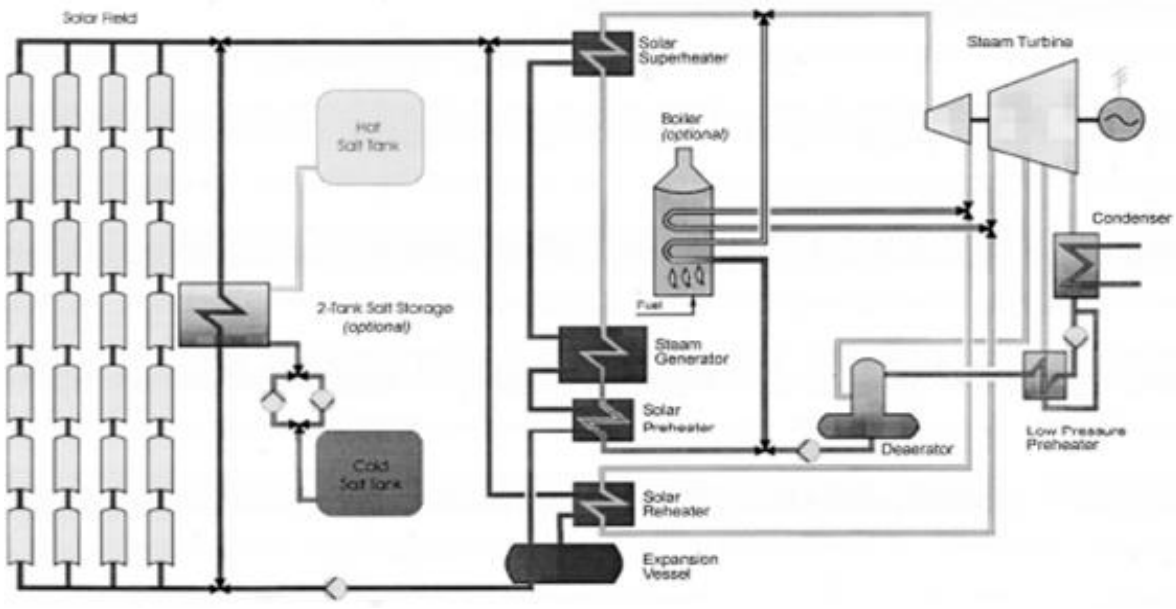

Figure5.4 Process Scheme for SEGS plant with 2 Tank TES [69]

5.5.3 Passive storage system: The storage media is not circulated in passive storage systems. The only time the HTF circulates through the storage media is when the tank is being charged or discharged. Typically referred to as regenerators, the technology functions as a dual medium storage system. In addition to this, solid storage systems—which often use castable ceramics or

concrete as the storage medium—are the most popular for passive storage. Additionally, it is feasible to use PCM as a kind of material storage, but the necessary technology has not yet been created. Thermal energy can be stored in three different forms: as a temperature rise (sensible heat), a phase change (latent heat) or chemical potential[70]. Chemical and phase change material (PCM) storage systems promise great opportunities but are still subject to research whereas all existing TESS of CSP plants store sensible heat.

Another crucial quality is the molten salt mixture's thermal stability. The highest upper temperatures (thermal stability) of several modern nitrate and nitrite salt combinations range between 500°C and 600°C. The thermal stability of combinations under study is estimated to be at least 500°C, while more research is needed to prove it. Another crucial characteristic is viscosity, especially close to the salt freeze point. The Arrhenius plot of the viscosity data for the candidate mixture, a commercial molten nitrate salt mixture, and Hitec XL (solar salt) is shown in Figure 5.6. As of now, the candidate combinations have revealed viscosities of fewer than 100 cP close to the freezing point. Viscosities are equivalent to binary solar salt over the range of operational temperatures. Finally, it will be crucial to ascertain the commercial cost of these salts. It is possible to optimize the potential combinations such that fewer of the more expensive ingredients are used. Even if there is more work to be done, the cost targets for this new HTF formulation should be attainable and lower than those for organic HTF.

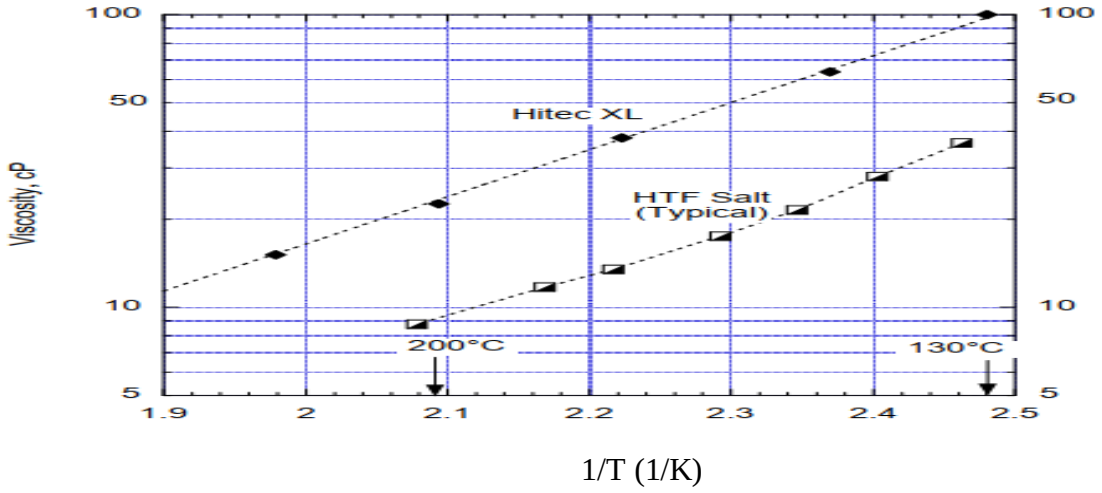

Figure 5.5 Viscosity of molten nitrate salt HTF[71]

5.6 Modeling of TESS

The basic modeling of a CSP plant consisting of collector, TESS, boiler and control system [72].

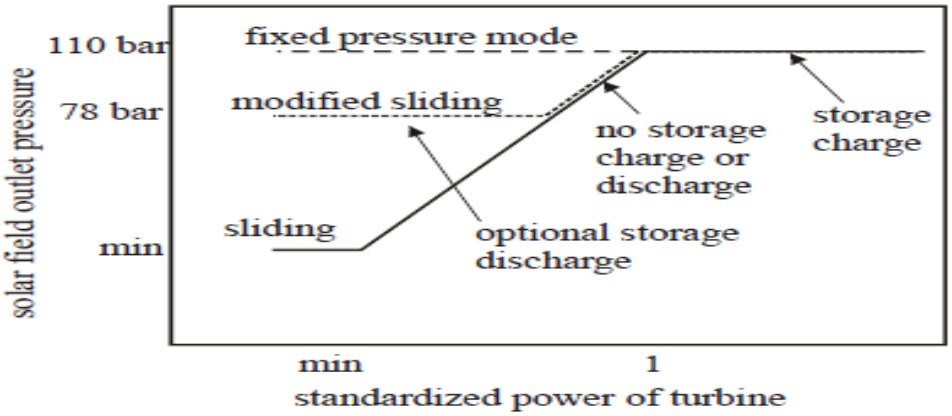

Figure 5.6 Pressure characteristics of DSG cycle at part-load [73]

The thermal properties of molten salt (binary) for this modeling are fluid density (ρ, kg/m3), viscosity (μ, Pa s), thermal conductivity (k, W/m-K) and specific heat (Cp, J/kg-K) in the form temperature –dependent function [66]:

$$\rho(T) = 2090 - (0.63)T \quad \ldots\ldots 5.1$$

$$\mu(T) = 10^{-3}[(22.714) - (0.12)T + (2.281 * 10^{-4})T^2 - (1.474 * 10^{-7})T^3] \quad \ldots\ldots 5.2$$

$$k(T) = 0.443 + (1.9 * 10^{-4})T \quad \ldots\ldots 5.3$$

$$C_p(T) = 1443 + (0.172)T \quad \ldots\ldots 5.4$$

Where T: temperature in ^{o}C

The thermal storage capacity for TES, E_{stored} in MJ ht, and the thermal storage mechanism is primarily based upon the utilization of sensible heat in various kinds of liquid material; sensible heat is brought to a material definitely via heating it up. Usually, all energies that are concerned in heat conversion of a fluid are known as sensible heat. In addition, it amounts simply to produce the specific heat and the temperature changes. So, it is given by the following equation:

$$V_{TES} = \frac{E_{stored}}{\rho_{hmss} c_{ph}(T) * (T_{hot} - T_{cold})} \quad \ldots\ldots 5.5$$

Where:

V_{TES}: $the\ storage\ volume\ in, m^3$

T: fluid temperature $\left[\left(\frac{T_{hot+T_{cold}}}{2}\right)\right]$,°C

Thermal capacity for TES is:

$$E_{stored} = \frac{Gross\ power}{desired\ efficeincy} * t_{full\ load} \ldots\ldots\ldots\ldots\ldots\ldots\ldots\ldots\ldots\ldots\ldots\ldots\ldots\ldots\ldots\ldots\ldots\ldots\ldots\ldots\ldots\ldots\ldots\ldots 5.6$$

Where, $t_{full\ load}$: $tolal\ full\ load\ hours\ of\ thermal\ storage.hrs$

Diameter of the tank, D_{tank} can be estimated as:

$$D_{tank} = 2 * \sqrt{\frac{V_{TES}}{h_{tank} * \pi * N_{pairs}}} \ldots\ldots\ldots\ldots\ldots\ldots\ldots\ldots\ldots\ldots\ldots\ldots\ldots\ldots\ldots\ldots\ldots\ldots\ldots\ldots\ldots\ldots\ldots\ldots 5.7$$

Where: h_{tank}: The height of the tank less than 10.0 m

$Npairs$: Number of tank pairs

Estimation of heat loss, q_{loss}, is:

$$q_{loss} = \left(h_{tank} * \pi * D_{tank} + \pi \left(\frac{D_{tank}}{2}\right)^2\right) * N_{pairs} * (T - 20) * C_{ph} \ldots\ldots\ldots\ldots\ldots\ldots\ldots\ldots\ldots\ldots\ldots 5.8$$

The minimum fluid volume, $V_{TES.min,}$ is:

$$V_{TES,min} = V_{TES} * \frac{h_{min}}{h_{tank}} \ldots\ldots\ldots\ldots\ldots\ldots\ldots\ldots\ldots\ldots\ldots\ldots\ldots\ldots\ldots\ldots\ldots\ldots\ldots\ldots\ldots\ldots\ldots\ldots 5.9$$

The thermal storage capacity may be changed to fulfill completely various load necessities, and different choices based on the storage capacity involved in:

i)Electricity is only produced from a tiny store while the sun is out.

ii) A delayed moderate load configuration, in which solar energy is gathered during the daytime but with increased electrical generation.

iii) A completely constant mode, which includes power generation between sunrise and sundown by utilizing the large storage capacity.

5.7. Energy and Cost Analysis of TES Materials

Numerous economic evaluations of CSP plants and TES systems have been conducted elsewhere [71,72, 73,74,75-76], and it has been shown that a CSP plant is more cost-effective if it has a TES system [77,78]. The techno-economic analysis of TES materials can be performed using a variety of key parameter indicators (KPIs), and the following were employed in this study:

- The amount of energy that the TES material can store in its working temperature range is measured by its specific mass energy density E^m (in MJ/kg), which is provided in Equation (5.10).

- The same energy as the previous KPI is quantified by the specific volumetric energy density E^v (in MJ/m3), which has a definition in Equation (5.11). This is significant for assessing the flow rate and whether it was going to be used as HTF, as well as for estimating other KPIs in the TES system (such as confinement, land-area dimensions, and cost).
- Energy storage cost E^c (in $/MJ): Equation defines this as the direct cost of the energy stored (5.12).

$$E^m = \int_{T_{fus}}^{T_{dec}} C_p dT \quad \text{5.10}$$

$$E^v = \int_{T_{fus}}^{T_{dec}} \rho C_p dT \quad \text{5.11}$$

$$E^C = \frac{C}{E^m} \quad \text{5.12}$$

Where is the density (in kg/m^3), cp is the specific heat (in J/kg ^oC), and C is the cost (in $/kg) of the molten salts, T_{fus} and T_{dec} are the fusion and decomposition temperatures (in ^oC). Due to safety concerns, such as preventing solidification and decomposition, the temperature range considered in this analysis will always be higher than real ones and narrower. Table 5.4 lists the values for the TES materials that were chosen for this model. In this investigation, 700 ^oC was taken into consideration as the maximum temperature permissible and Solar Salt was employed as a benchmark for comparative purposes. It is obvious that only TES materials based on nitrate are appropriate for low temperature applications like PTC, where as the other materials are only appropriate for high temperature parabolic solar collector plants that operate up to 700 ^oC.

Table 5.4 Specific cost and energy of selected molten salt

Nitrate-based salts	Specific cost$/Kg	E^m MJ/Kg	E^v MJ/m^3	E^C $/MJ	Reference
Solar salt	1.3	0.491	901.1	2.65	[74]
Hitec	1.93	0.480	826.9	4.02	[74]
Hitec XL	1.66	0.464	928.1	3.58	[74]
$LiNaKNO_3$	1.1	0.683	1285.7	1.610	[75]
$LiNaKCaNO_3$	0.7	0.542	977.1	1.29	[75]

$LiNaKNO_3NO_2$	N/A	0.408	764.9	N/A	-
Chloride-based salts					
KMgCl	0.35	0.271	431.3	1.29	[76]
NaKMgCl	0.22	0.325	541.6	0.68	[76]
NaMgCaCl	0.17	0.289	739.7	0.57	[77]
NaKZnCl	0.8	0.447	986.6	1.79	[76]
KMgZnCl	1	0.298	553.4	3.36	[76]
Fluoride-based salts					
LiNaKF	2	0.391	824.1	5.11	[77]
NaBF	4.48	0.474	885.4	10.29	[78]
KBF	3.68	0.313	833.3	11.75	[78]
Carbonate-Based salts					
$LiNaKNO_3$	2.02	0.448	9912	4.15	[79]

5.8 Impacts of Salt HTF on Performance

The performance of the plant is primarily impacted by the following factors when molten salt is used as HTF in the solar field:

- Molten salt has a higher operating temperature range than synthetic oil.As a result, the Rankine cycle's efficiency can be increased by producing steam at greater temperatures.
- Molten salt significantly reduces the mass flow in the solar field, which lowers pressure loss in the piping. In comparison to a VP-1 solar field, both effects—low mass flow and low pressure loss—lead to a comparatively low pumping parasitic.
- The average temperature in the solar field likewise rises as a result of the higher output temperature. As a result, the solar field's heat losses are greater and its efficiency declines.
- HitecXL molten salt has a relatively high freezing point (around 120°C).

As a result, the functioning of freeze protection uses greater thermal energy. Throughout the night, the solar field temperature must be kept much above 120°C [99]. Additional heat losses result from that as well. A plant using Hitec solar salt as HTF performs well when all four effects are combined. The research was conducted for a maximum temperature of 450°C in the instance of the molten salt HTF. Due to the higher temperature and freezing point, performance gains are

noticeably greater than disadvantages. The effect that was not previously anticipated in this examination is the lower parasitic in the solar field, which results in the greatest improvement.

Chapter Six

Simulation of Parabolic Trough Solar Power Plant Using System Advisor Model (SAM)

6.1 Introduction

Under this chapter general over view of parabolic trough solar collector technology, solar resource evaluation and system description, mathematical modeling of parabolic trough solar collector, design parameters and system performance analysis will be centre of the topic. Simulations using Solar Advisor Modeling (SAM) based on satellite and Payranometer measurement driven data will be compared and validated against previous scientific works. Finally, simulation and optimization results proposed at Bole Lemi Industrial Park will be discussed.

6.2 Over View of Parabolic Trough Solar Collector Technology

The most established, successful and mature concentrating solar power technology for generating electricity is the parabolic trough solar power plant. Fig.6.2 shows a schematic representation of a parabolic trough solar power facility. These plants can be viewed to have three basic components: a solar field, a thermal energy storage system, and a power block. The solar field assemblies consist of many heat-transfer fluid-filled parabolic trough solar collectors (HTF). In order to monitor the sun from east to west, the solar collectors are organized in a series configuration known as loops and facing north-south. To maintain the generation of electricity, solar power facilities can use thermal energy storage (TES). Thermal energy storage typically has a capacity of several hours, and in order to ensure that electricity is still produced even after sunset, it is loaded with HTF during the day and emptied at sunset. The power block uses a heat exchanger to produce steam using the thermal energy that the solar field has captured. Regenerative Rankin cycles, which use steam turbine generators to produce electrical energy, are typically used in solar power plants [100]. Solar system energy technologies are compared using the electrical performance, solar to electric efficiency, land use factor, and capacity factor. Net capital cost, net present value, LCOE, and payback period are used in the economic comparison. The current and projected statuses of PTC plants, as well as technical advancements in several PTC-based commercial CSP plant components, were covered by Bilal Awan et al. [101]. A list

of 100 PTC plants that are open, under construction, or in the planning stages can be found throughout the world.

Eeddine Boukelia and Mecibah [102] conducted research in Algeria on the construction of parabolic trough solar thermal power plants, the operating principles of CSP plants, and an assessment of Algeria's capacity for concentrating solar power. The analysis proves the competitive viability of CSP facilities.

For solar parabolic trough power facilities in Algeria, Boukelia et al. [103] optimized, selected, and carried out a feasibility analysis. Two CSP facilities with thermal energy storage (TES) and fuel backup systems (FBS) have been optimized. Therminol VP-1 and molten salt were employed as the heat transfer fluids in the first and second plants, respectively.

Garca et al. [104] designed a simulation model that could estimate how well a 50 MWe CSP station would perform using energy storage and Therminol VP-1 as an HTF. Experimental data from a power plant in Spanish are used to verify the model's performance.

The effect of the solar multiple on energy expenditures, annual growth, and natural gas consumption for a 50 MW direct steam generation was examined by Montes et al. [105]. Both a thermal energy storage facility and an auxiliary boiler powered by natural gas are included at the plant.

Larran et al. [106] created a thermodynamic model to predict the efficiency of a hybrid solar thermal plant with a 100 MWe capacity as well as the quantity of fossil-fuel backup needed.

Kalogirou [107] looked at a solar thermal power plant in Cyprus with a 50 MW capacity and evaluated its technical performance, energy prices, and required land area. The optimal technology was suggested to be the parabolic trough system because of its advantages and industrial sophistication.

The energetic economics of a 100 MW solar parabolic trough power plant for four typical Algerian locations were examined by Abbas et al. [108]. The use of molten salt as the heat transfer fluid (HTF) in parabolic through solar power plants has the potential to cut the Levelized cost To enhance the performance of the plant, Reddy et al. [110] looked into energy and exegetics analyses under various operating situations. The aforementioned literature evaluation

indicates that no research has been done on the technological viability of PTSTPP in an area with a lot of DNI availability. Furthermore, there is no CSP technology that has been proven to work well in Ethiopia's climate. This study aims to fill a knowledge need in the area of solar thermal systems.

This study's primary goal is to suggest solar energy for the Bole Lemi Industrial Park using a PTC field, along with extra thermal energy storage tanks and molten salt as HTF through the main solar field of collecting.of energy (LCOE), according to Ruegamer et al[109] .'s discussion of the technology.

6.3 Introduction to System Advisor Model (SAM)

For the purpose of analyzing and evaluating various renewable energy projects, such as PV systems, solar water heating systems, thermal storage systems, parabolic trough technologies, central receiver systems, linear Fresnel technologies, Stirling dish technologies, wind power, biomass systems, geothermal energy systems, and hybrid/integrated power systems, NREL (sponsored by the U.S. Department of Energy) has developed the free software package SAM. Thus, Wagner et al. described the Linear Fresnel model's construction and operation [89,90]; in additional research, Wagner describes the Central Receiver Model [113]; Blair et al. also described the PV model [114]; and in a milestone report for the second quarter of 2015, Wagner describes the PV model. The hybrid/integrated power generating systems were covered by Turchi and Neises [115]. Turchi and Garvin talked about the molten salt power tower in another report [116]. Neises demonstrated how to implement user-defined bespoke power cycles in SAM[117]. The Generic Solar System (GSS), which Wagner and Zhu [118] introduced, is a CSP modeling suite that offers a more flexible way to model a generic power cycle and frees the user from being constrained to particular plant designs that are frequently found in other SAM models. In this instance, the user can easily construct different plant geometries and subsystem configurations by allowing the definition of optical and thermal properties. The SAM documentation page [119] contains information and updates on these models as well as numerous more SAM performance models. Some of SAM's various features are shown in the aforementioned instances. Transient System Simulation (TRNSYS), which was initially created at the University of Wisconsin for simulating various CSP plants, served as the foundation for the SAM code [120]. However, more fantastic features have been added to latest updates of

SAM. Sensitivity analyses are included in the most recent version (version 2020.11.29), and they can be used by executing parametric. SAM allows for the use of stochastic (probabilistic) models and P50/P90 analyses. Additionally, SAM has built-in macros for a number of particular studies, including combine cases, the tornado chart, sitting considerations, the solar resource file checker, converter, solar resource interpolation, and wind resource histogram.

If desired, one may also construct user-defined macros. While SAM allows integration with various programming languages like C, C++, C#, Java, Python, PHP, and Matlab[119][122], it also has its own scripting language called SAM lk script [121]. According to Dobos et al. [123], SAM uses the Transient Component Simulation (TCS) technique to increase performance, portability, and parallelism in CSP simulations. The fully dynamic type interface, multithreading, data types, and tolerance configurability are some of the TCS's standout characteristics. The physical trough and the empirical trough are the two choices offered by SAM for creating the CSP parabolic trough system. The physical trough is founded on the fundamentals of thermodynamic relations and energy balance, as stated by Wagner and Gilman [120]. When prior knowledge of system performance is unknown, the physical trough performs better than the empirical model because performance is generalized over the entire operational range of the power plant. The physical model is subject to various ambiguities and mistakes, though, because it is theoretically based and some assumptions must be made. With the usage of the empirical model, which is based on observable (previous) system performance, the situation is the opposite.

The output is more precise, but it is limited to parameters that fall inside a predetermined range, leaving no possibility for the system's performance to be flexible. A novel empirical model is presented in the current paper. The models for the solar field, power cycle, thermal storage, and parasitic losses were taken into consideration when modeling the parabolic trough system. The SAM window result summary is shown in Figure 6.1.

The performance model and the financial model are the two fundamental components of the SAM software. Calculating the electrical power (or energy) produced by the various renewable energy systems is the basis of the performance model.

In order to undertake some financial analysis and ascertain the project's economic viability, the output of the performance model is input into the financial model [92,94,102,103]. Mendelsohn et al. [124] list the Single Owner, All-Equity Partnership Flip (with and without debt), Leveraged Partnership Flip, and Sale Leaseback as the four primary financial structures (options) applicable in renewable energy projects, with the Single Owner structure being the simplest and most popular. The Commercial (distributed), LCOE Calculator (based on the Fixed Charge Rate technique), and No Financial Model options, among others, are nevertheless accessible as well (in case the user is not interested in any financial analysis). The current analysis, however, is based on the Levelized Cost of Energy (LCOE) Calculator option.

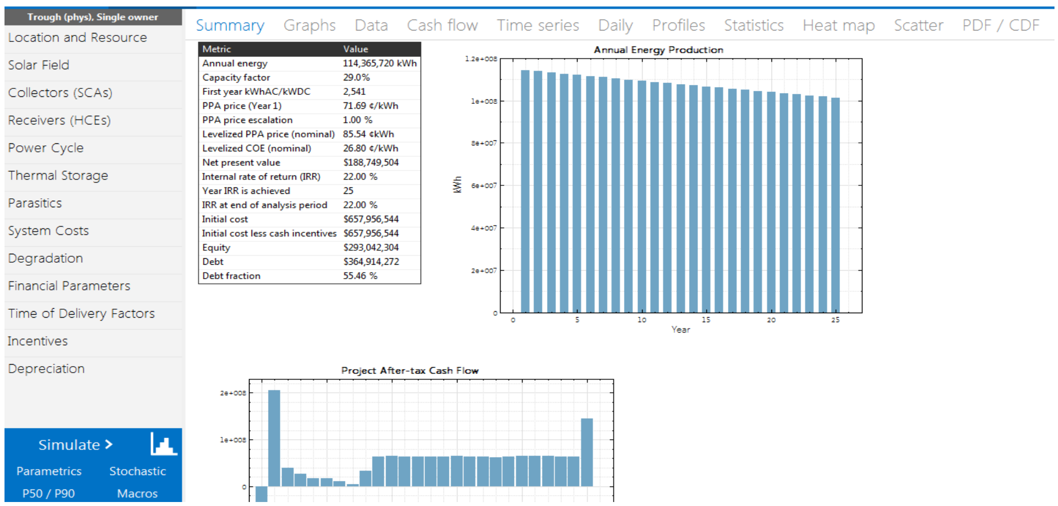

Figure 6.1 SAM main windows showing the results summary for a solar thermal power system

When evaluating the financial sustainability of a specific renewable energy system, one of the most important financial measures is the Levelized Cost of Energy (LCOE). The overall cost of producing energy (construction and operation) divided by the total amount of energy produced during a certain analysis period is known as the LCOE (cents/kWh). According to Short et al. [125], the LCOE can be represented numerically as follows:

$$\text{LCOE}=\frac{T_{LCC}}{\sum_{n=1}^{N}\left[{Q_n}/{(1+d)^n}\right]} \quad \ldots\ldots\ldots 6.1$$

Where T_{LCC}= Total Life Cycle Cost, Q_n – Energy output or saving in years

N- Analysis Period, n-years of analysis,d-discount rate

Since a lower LCOE implies that costs are lower and energy output is higher, it is likely that the project will be more lucrative. As a result, having a lower (minimum) LCOE is always preferred. Note that the LCOE is expressed mathematically in general terms in Equation 6.1.

A later section will provide the equation based on the specific LCOE approach employed in this analysis. In the event when the LCOE is lower than that of a traditional fossil fuel power station, renewable energy becomes cost-competitive. The internal rate of return (IRR), net present value (NPV), and power purchase agreement (PPA) cost are further financial indicators of importance. To assist the stakeholders in making decisions about the financial advantages of a certain renewable energy project, all these criteria are integrated into the SAM financial model.

6.4 System description

The CSP plant model is broken down into three subsystems, as shown in figure 6.2: (i) the solar field (see Appendix D), (ii) the thermal storage device (Appendix H), and (iii) the power block (See Appendix G). Cylindrical receivers receive sunlight from the sun using parabolic trough solar collectors that make up the solar field. The heat transfer fluid, which is moving through the receiver, transfers thermal energy from the solar field to the power block. After transferring the thermal power to a Rankin cycle power block, a turbine and a linked generator are employed to produce energy. The thermal energy storage system uses a two-tank design and molten salt as the storage medium.

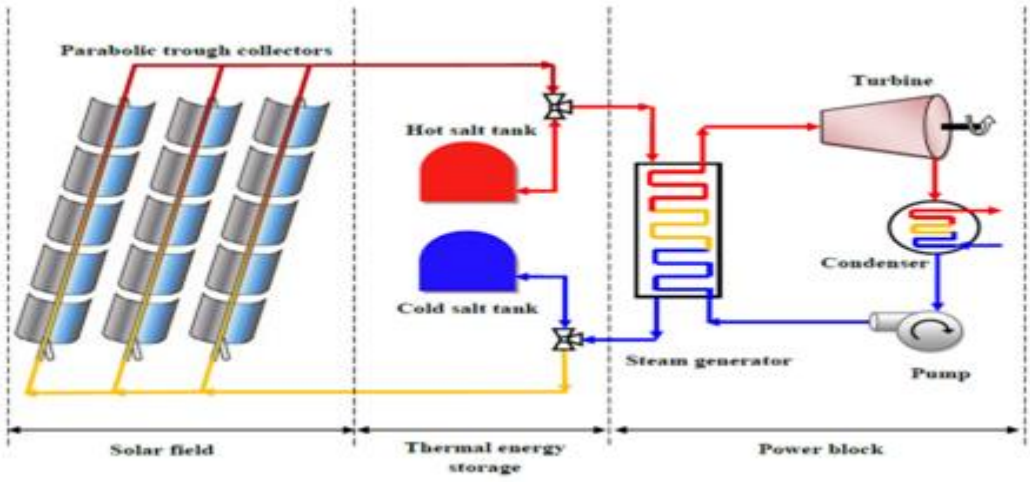

Figure 6.2 *Schematic diagram of parabolic solar trough solar collector power plant* [80]

Figure 6.3 shows a sectional view of a PTC receiver; a glass envelope is placed over a metal tube (absorber tube). For this particular design, the Schott PTR 7 receiver type is chosen. Appendix F contains the receiver parametric design specifications. To accommodate thermal expansion and reduce convective heat losses, the area between the glass envelope and absorber is either vacuumed or filled with air. To minimize radiative heat transfer loss, the absorber tube is coated with a selective surface that has a high solar absorption (>0.95 [126]) and a low thermal emittance. To reduce the impact of heat conduction, the receiver's length is increased to 4 meters or more.

Finally, to decrease the surface area for heat loss, the absorber's diameter is decreased (82 times smaller [127]) in comparison to the reflector's width. Direct solar radiation is concentrated on the focal line of the collector axis. The collector assembly has a single-axis monitoring mechanism built in to ensure that the collector's axis is aligned with the sun's beam.

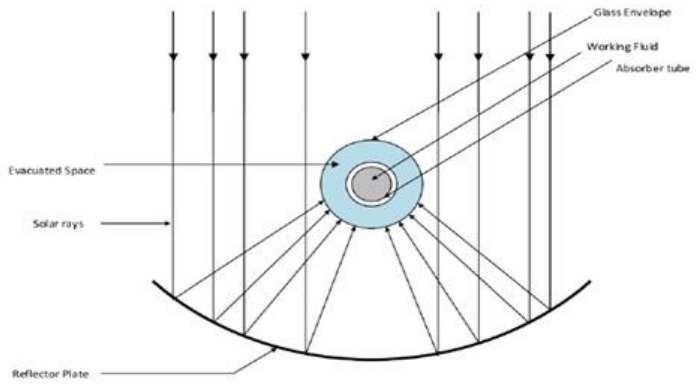

Figure 6.3 PTC Receiver sectional view [81]

Only the direct normal irradiance (DNI) part of solar energy is used by parabolic trough collectors. PTC solar power plants are the most developed commercially among the CSP power plants [128]. Parabolic trough collectors were chosen for the proposed plant layout investigated in this work because they absorb more heat than flat plate collectors.

6.5 Site Selection and Solar Resource Evaluation

For the engineers who develop and install projects, the location of the CSP plant is crucial. Many factors, including solar power supply, supporting services, soil, water, connectivity, community

considerations, environmental concerns, and the basic need for energy generation, have an impact on the choice of CSP sites.

There are two steps in the process for choosing a location for the PTC power station.

i) To get the best performance out of the design system, the DNI value must be more than 5KWh/m^2/day [129]. The yearly DNI for Bole Lemi Industrial Park is high (6.91 KWh/m^2/day), according to DNI criteria and the scant amount of data on solar radiation that is available.

ii) (ii) The provision of services like access to the grid, water, soil, and communications.

6.6 Technical Evaluation Methods

The strategy basically adheres to Wagner's [130] recommendations. Due to the numerous fields that must be given, Wagner suggested the following strategy:

- Set up the receiver and collector parts (See Appendix E)
- Determine transport operation limitations;
- Specify the loop's configuration;
- Specify the HTF and operating temperatures; and
- Specify the power cycle design point.

Update cost and finances and optimize unknown parameters. Specify thermal storage parameters and maximize solar multiple and TES capacity (See Appendix I)

6.7 Mathematical modeling and simulation

The CSP plant model taken into consideration for analysis in this study is shown in Figure 6.4. The solar field, thermal storage system, and power block are the three subsystems that make up the whole CSP plant model. Solar energy from the sun is directed to tubular receivers using parabolic trough solar collectors in the solar field. The heat energy from the solar field is absorbed by the heat transfer fluid (HTF) passing through the metal tubes of the receiver and transferred to the power block.

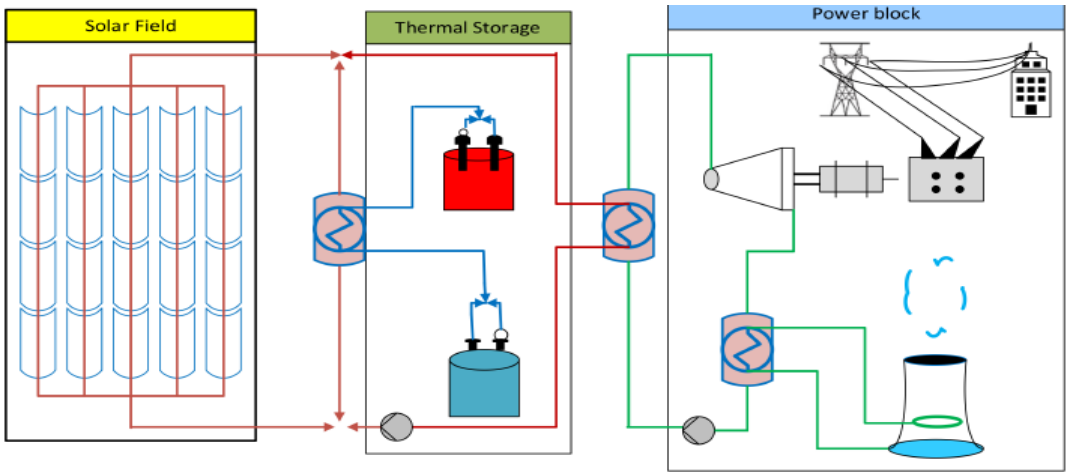

Figure 6.4 CSP plant model with thermal energy storage (TES) system[81]

The power block uses the Rankin cycle and comprises of a turbine connected to an alternator to produce electricity using thermal energy from the solar field. A two-tank system with Hitec solar salt as the storage substance is chosen for the TES system.

The following equations are used in this section to model the PTSC from a thermodynamic perspective. According to PTSC, the solar radiation absorption can be described as follows [131][132].

$$Sa = G_b * \eta_r \quad \ldots\ldots 6.2$$

Where the beam irradiance is Gb and the efficiency of the receiver is η_r and obtained with the following equation:

$$\eta_r = \varrho_c \,.\, \emptyset . \tau . \alpha_r . k_\theta \quad \ldots\ldots 6.3$$

Where ϱ_c is a mirror reflection coefficient, and the intercept factor is $\emptyset$, τ is the glass cover transmittance, α_r is the receiver's absorption, and k_θ is an incidence angle modifier of the Euro-Trough collector and can be found by [82]:

$$k_\theta = \cos(\theta i) - 5.2597 * 10^{-4} . \theta i - 2.85921 * 10^{-5} . \theta i^2 \quad \ldots\ldots 6.4$$

and the angle of incident θ_i is presented as follows :

$$\cos(\theta i) = \sqrt{\cos^2(\theta_z) + \cos^2(\delta) . \sin^2(\omega)} \quad \ldots\ldots 6.5$$

From the above equation θ_z, δ, and ω are zenith angle, declination angle, and hour angle, respectively. The thermal power generated from PTSC calculated from [4]

$$S_{\dot{u}} = A_{ap} . F_R \left[Sa - \frac{A_r}{A_{ap}} . U_L . (T_{r,i} - T_0) \right] \ldots \ldots 6.6$$

The areas can be calculated as follows using the information from the above equation: The collector aperture and receiver areas are A_{ap} and A_r, respectively; the factor of heat removal is F_R; the collector coefficient of overall heat loss is U_L; and $T_{(r,i)}$ the temperatures inlet to the receiver and ambient are and T_{amb}, respectively.

$$A_{ap} = [Wc - D_{c,O}] . L \ldots \ldots 6.7$$

$$A_r = \pi . D_{r,o} . L \ldots \ldots 6.8$$

Where the collector width and length respectively are Wc and Lc, and the outlet diameter of the cover and receiver are Dc, and D_r, respectively. Simply, we can calculate the heat removal factor by:

$$F_R = \frac{m_{\dot{r}} . C_{pr}}{A_r . U_L} . \left[1 - exp\left(\frac{A_r . U_L . F_1}{m_{\dot{r}} . C_{pr}} \right) \right] \ldots \ldots 6.9$$

Where $m_{\dot{r}}$ the receiver mass flow rate, C_{pr} is the molten salt specific heat and F_1 is the efficiency factor of the collector. The efficiency factor of the collector is defined as:

$$F_1 = \frac{U_o}{U_L} \ldots \ldots 6.10$$

Where the coefficient of collector overall heat transfer is U_O. Three different types of heat transfer coefficients are defined as the coefficient of heat loss from the receiver to the surroundings, which are then stated. The following formula can be used to calculate the heat transfer coefficient of convection between the cover and the surroundings, which is the first type of heat loss.

$$h_{c,ca} = \frac{Nu_a . K_a}{D_{c,o}} \ldots \ldots 6.11$$

Where the coefficient of the thermal air conductivity is K_a, and the Nusselt number is Nu_a and is presented as follows:

$$Nu_a = 0.193.Re^{0.618}.Pr^{0.33} \quad \ldots\ldots 6.12$$

Where Re is the Reynolds number, and Pr is the Prandtl number. And the second coefficient of heat transfer is the coefficient of radiation between the cover and surrounding and is presented as follows:

$$h_{c,ca} = \varepsilon_{cv.}\sigma.[T_C + T_{amb}].[{T_C}^2 + {T_{amb}}^2] \quad \ldots\ldots 6.13$$

Where, $\varepsilon_{cv.}$ is the cover emittance, σ is the constant of Stefan Boltzmann, and T_C is the average temperatures of cover.

6.8 Plant design parameters

The following collection of plant characteristics serves as input to SAM. To assess the plant's total thermal energy, efficiency, capacity factor, and net power generation [120] [75][134] [135][136][137]. These parameters are shown in Table 6.1.

Table 6.1 Design input parameters

<table>
<tr><th>Location</th><th>Latitude and Longitude</th></tr>
<tr><td>Bole Lemi Industrial Park, Ethiopia</td><td>8° 58' 17.2200" N 38° 51' 24.5088" E</td></tr>
<tr><td>Categories</td><td>
<table>
<tr><td colspan="2">Solar field parameters</td></tr>
<tr><td>Solar multiple</td><td>3</td></tr>
<tr><td>DNI at design</td><td>600 w/m^2</td></tr>
<tr><td>Ambient temperature</td><td>42 ºC</td></tr>
<tr><td>Wind velocity</td><td>5m/s</td></tr>
<tr><td>Field sub sections</td><td>2</td></tr>
<tr><td>Row spacing</td><td>15m</td></tr>
<tr><td>Stow angle</td><td>170º</td></tr>
<tr><td>Deploy angle</td><td>10º</td></tr>
<tr><td>HTF pump efficiency</td><td>0.85</td></tr>
<tr><td>Piping thermal loss coefficient</td><td>0.45 w/m^2-k</td></tr>
</table>
</td></tr>
</table>

	Freezing protection temperature	260 ºC
Collector Type	Euro Trough ET150	Collector parameters

Aperture area	817.5m^2
Aperture width	5.75m
Collector assembly length	150m
Modules per collector assembly	12
Average surface to focus path length	2.11
Length of single module	12.5
Water usage per wash	0.7L/ m^2
Wash per year	63

Receiver Type	HCEMS11

Inner diameter of absorber tube	0.067m
Outer diameter of absorber tube	0.07m
Inner diameter of glass envelope	0.122m
Outer diameter of glass envelope	0.125
Receiver thermal losses	166.25W/ m
Loop minimal flow rate	1kg/s
Loop maximal flow rate	12 kg/s
Loop minim flow velocity	0.1m/s
Field maximum flow velocity	2m/s
Field header minimum flow velocity	2m/s
Field header maximum flow velocity	3m/s

Molten Heat Transfer type	Hitec solar salt

	(molten)	Design point	
Cooling condenser type	Evaporative	Loops number	514
		Collector per loop	4
		Loop aperture area	3270m^2
		Field aperture area	1,680,780 m^2
		Total thermal output	1049.88M Wt
		Total land area	1517Acres
		Power Block	
		Design gross output	50MWe
		Estimated gross to net conversion	0.9
		Estimated net output at design	45MWe
		Rated cycle conversion efficiency	0.443
		Design inlet temperature	550 ºC
		Design outlet temperature	290 ºC
		Boiling operating pressure	150bar
Turbine	Steam Turbine		
Pump	Centrifugal	Storage hours	10hr
		Storage volume	30869.6m^3

6.9 Results and Discussions

6.9.1 Initial simulation of the 50 MWe CSP plant

The performance of the power plant for the Bole Lemi Industrial site in Addis Ababa is then simulated using the validated model. This is done to estimate how much energy the power plant could produce during the first year of operation in that area. To do this, the National Solar Radiation Database (NSRDB) website's Bole Lemi weather readings for a typical metrological year (TMY) were first downloaded (NREL Data Viewer n.d.). The TMY stands for the measures of weather information that would normally describe the yearly weather pattern at a particular place. A preliminary simulation of the model was run using the TMY file as input, with a solar multiple of 1.0 and 6 hours of thermal storage, to produce the result depicted in figure 6.5. The top chart in the illustration represents the resource beam normal irradiance, or DNI; the bottom chart represents the matching system thermal power generated.

The two charts' profiles show a strong correlation between the quantity of power generated and the DNI input. The output power is inversely proportional to the input DNI, meaning that the output power increases as the input DNI increases. Around the months of January through April and November through December, the average daily power output was at its highest, but around the months of June through September, when the DNI level is lowest, the average daily power output was at its lowest.

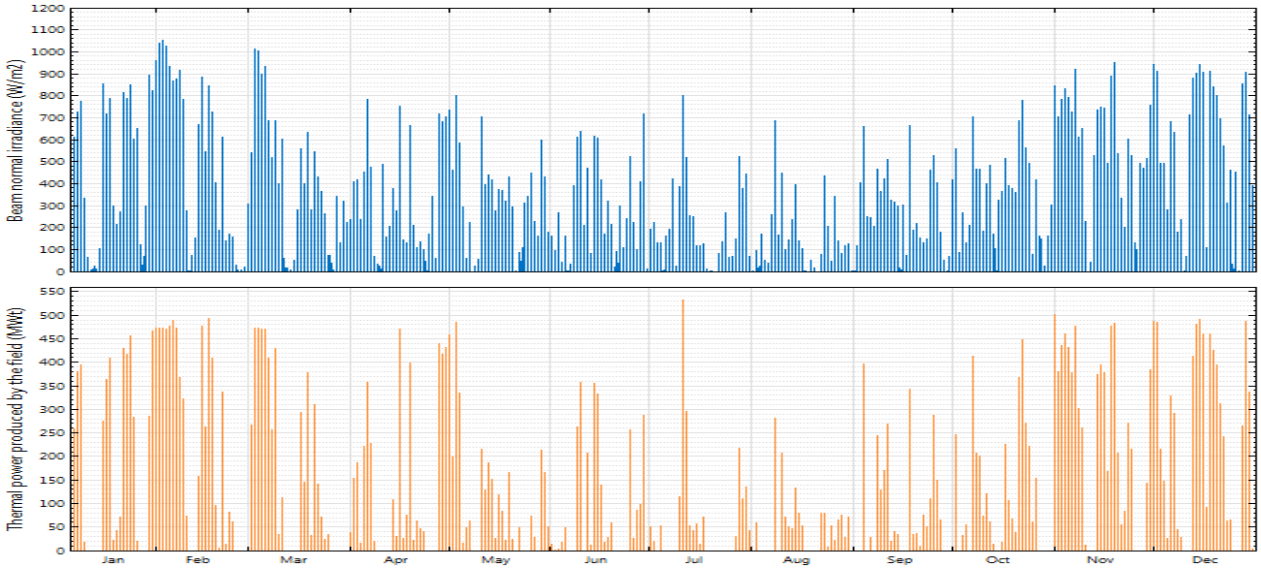

Figure 6.5 Proposed 50 Mwe CSP plant simulations (Bole Lemi, Addis Ababa)

The amount of electrical energy (kWh) produced by the system depends on its power output during a specific time frame. Figure 6.6 displays the monthly electrical energy production equivalent to the power output in Figure 6.5.

There are two humps in the energy profile. One took place in November and December, whereas the other (though less severe) took place in October and January. The areas with the highest energy production are shown by the humps. At these locations, the price of electricity is anticipated to be lower. According to the SAM, the power plant produced 114.36 GWh in total during the first year utilizing the specified input.

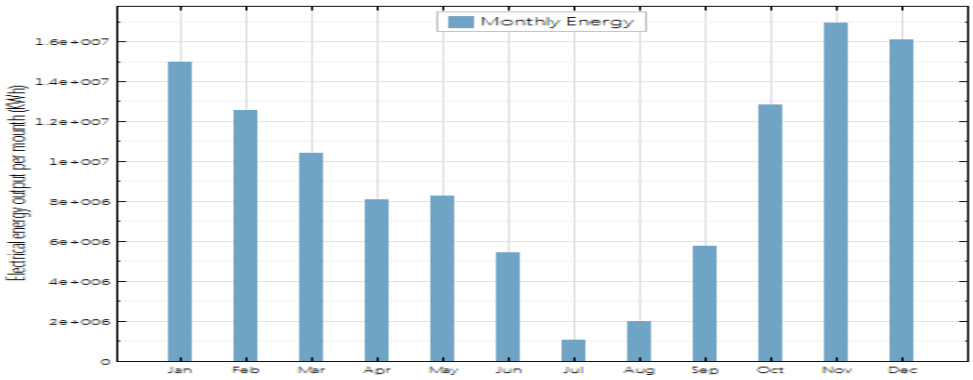

Figure 6.5Electrical energy output per month

From figure 6.7, the greatest power cycle efficiency results in an annual average of 0.25455, or almost 25.5 percent. From February through April and May through August, the mean thermal cycle efficiency dramatically decreases before beginning to rise from the end of August to November. This demonstrates unequivocally how weather influences the total effectiveness of solar energy installations.

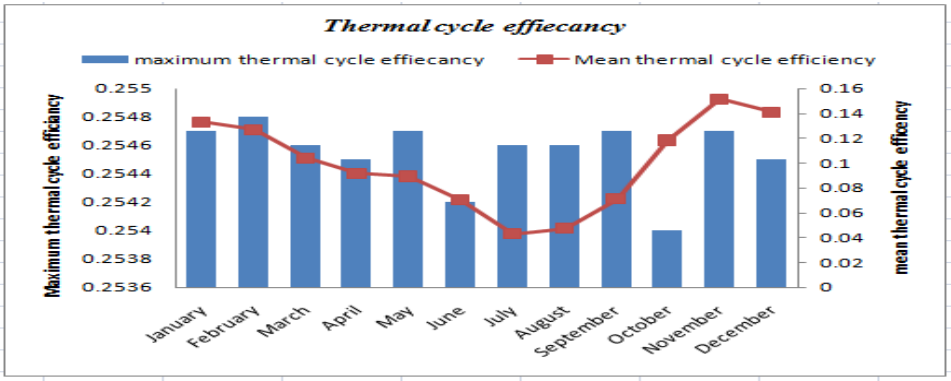

Figure 6.6 Overall power plant (cycle) efficiency

6.9.2 Parabolic trough concentrated power plant performance analysis

6.9.2.1 System performance

The projected PTC plant's monthly energy output is shown in Figure 6.8. November generated the greatest energy (42GWh), while August produced the least (11.6 GWh). The cold header inlet's minimum temperature increased as the HTF was circulated in a closed-loop, becoming close to 280 °C. Additionally, the maximum temperature of the hot header outlet is 499.2 °C. Throughout the year, the bulk of Bole Lemi Industrial Park receives sufficient sunlight for 11–12 hours per day.

In contrast to the sun rising on average at 6:16 a.m., power generation begins at 7.30 a.m. (see: https://www.timeanddate.com/sun/ethiopia/Addis Ababa?month=12&year=2020).

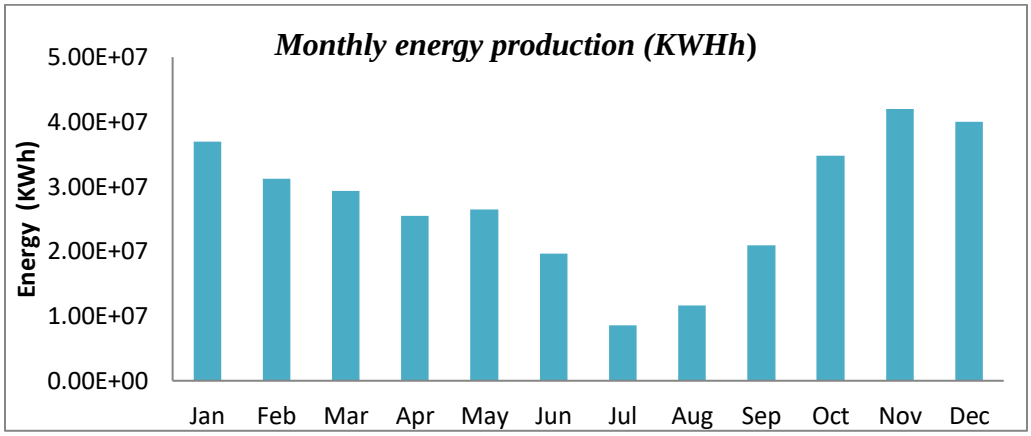

Figure 6.8 Monthly energy productions

The hot tank should be maintained at a temperature of at least 300°C to guarantee that the power plant starts up properly. The system performance parameter for each month of the year is shown in Figure 6.9a and 6.9b. The gross electric power output and total power incident on the field is highest in January, December and November. Greatest thermal power incident was 1156.442 MWt in January, while the power block's maximum power cycle gross and net electric power outputs were 52.5 and 50.8 MWe, respectively, in June. The maximum total energy absorbed by the solar field to the power block was 83071.9 MWt in November. Table 6.2 provides an overview of the PTCSP plant's net output energy, capacity factor, and overall plant efficiency. Compared to the other months, January, November, and December had greater system performance characteristics including cycle gross Power output, total power incident on the field,

and cycle power output on system. July and August are the months with the lowest power incident on the solar field and electrical power cycle gross output. Note that the term Megawatt electric (MWe) is the electricity output capability of a plant while Megawatt thermal (MWt) is input (solar source) energy required on the solar field.

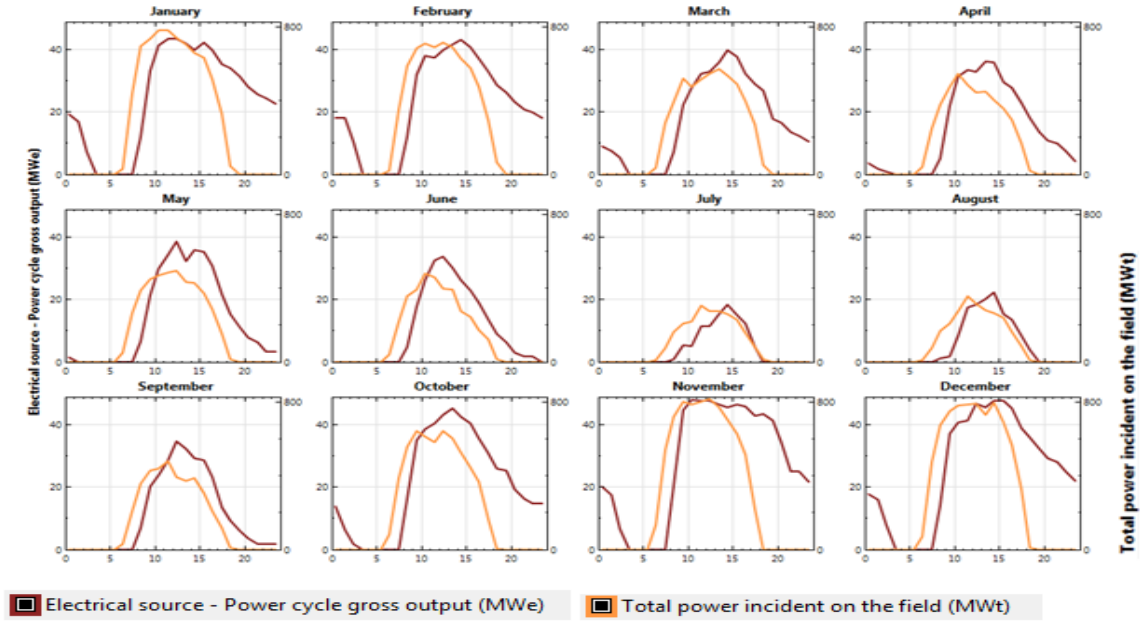

Figure 6.9 (a) Monthly system performance parameters

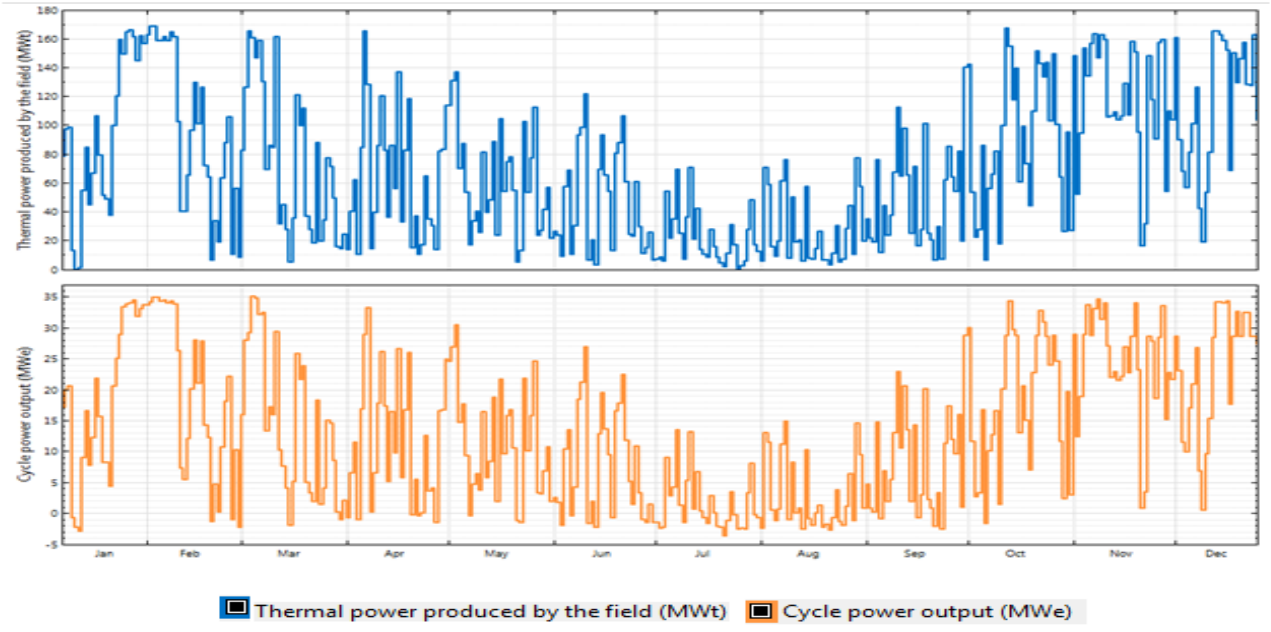

Figure 6.9 (b) Monthly system performance parameters

Table 6.2 Proposed Parabolic Trough Sola Collector Power plant Annual energy output

Metric	**Value**
Net Energy	114.36GWh
Estimated Gross to Net Conversion Factor	0.9
Plant Capacity Factor	29%
Plant Efficeincy	25%

6.9.4 Optimization of the CSP Plant

The optimization process aids in identifying the lowest LCOE value at the highest annual energy generation. By adjusting two key design factors, the solar multiple and full load hours of the TES, the proposed system is optimized.

One of the most crucial factors that significantly affect the Levlised Cost of Energy (LCOE) of the energy generated by the CSP system is the solar multiple. The ratio of the actual solar field size to the bare minimum size needed to operate the power block at maximum efficiency under typical irradiation conditions is known as the solar multiple. The usage of the power block may rise with an increase in the solar multiple and thermal energy storage, which lowers the plant's overall LCOE. However, raising the solar multiple also raises the system's capital expense. To find the solar multiple that provides the lowest LCOE within the design conditions of the proposed power plant, the contradictory effect of this parameter needs to be adjusted [141]. The proposed plant's performance under a range of solar multiples has been simulated. The thermal energy storage capacity is maintained along with the other design elements of the facility. Figure 6.10 displays the simulation results of the optimization process. When solar multiple is roughly 2.5, the LCOE drops from 1.19 $/kWh for solar multiple 1 to a minimal value of 0.452 cents/kWh. Following that, the LCOE starts to rise as a result of the plant's capital cost significantly rising. These results in the deduction that solar multiple 2.5 is the most cost-

effective value that provides the lowest LCOE of the electricity produced for these plant design parameters.

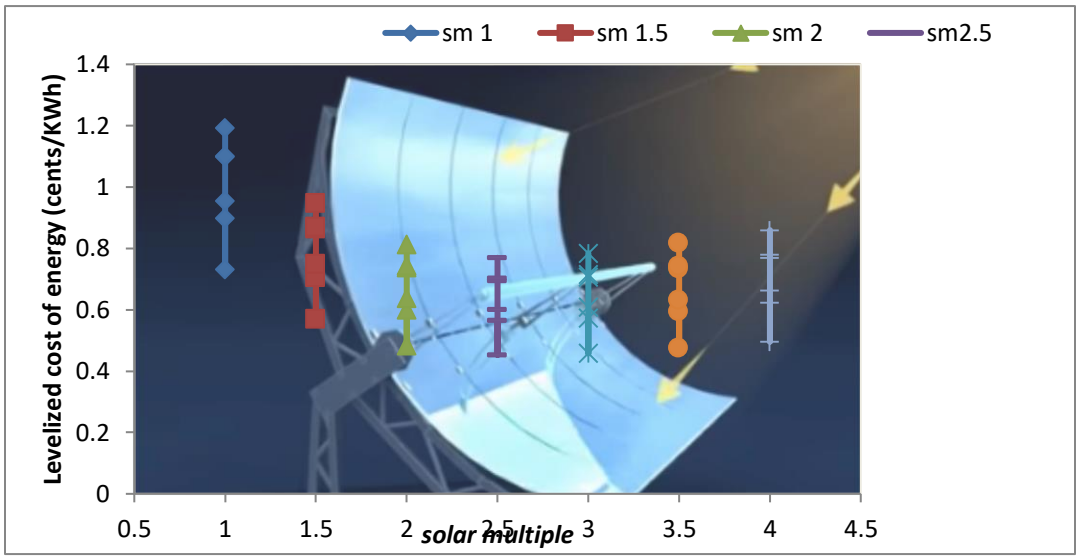

Figure 6.10 Levelized cost vs solar multiple

Figure 6.11 shows the difference in annual energy production and LCOE with maximum storage hours. Accordingly, before a specific value is achieved, the levelized cost of energy (LCOE) decreases with an increase in thermal energy storage (TES) full load hours before it starts to climb. The ideal number of storage hours is 10, which equates to an annual energy generation of 114.4 GWh and an LCOE of 0.32 cents/kWh.

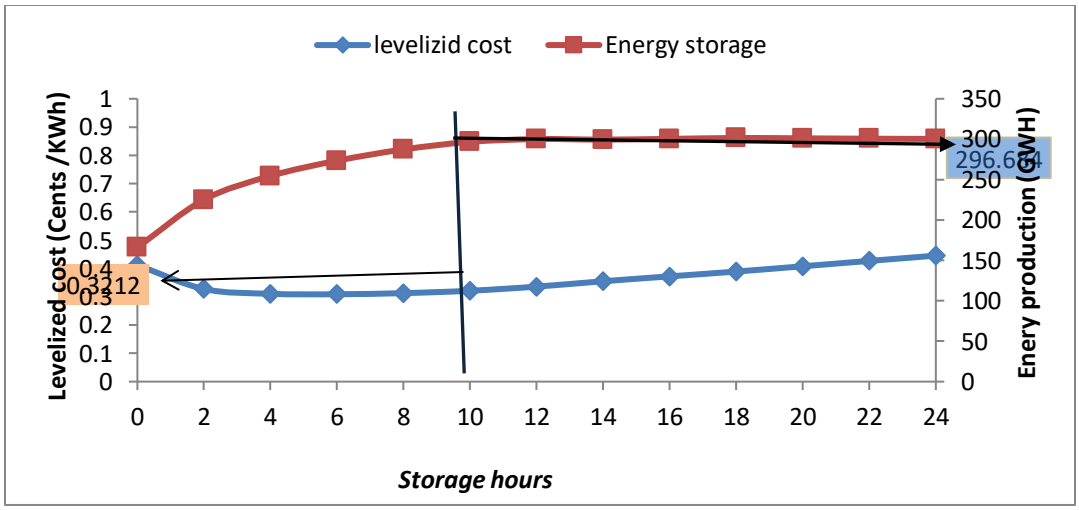

Figure 6.11 Annual Energy production Variation LCOE with Energy storage hours

Table 6.3 Annual energy yield comparison for the optimized CSP Plant

Metric	Initial	Optimized
Annual Net energy	64.9 GWh	114.4 GWh
Solar multiple	1.5	2.5
Full load hours of TES	6h	10h
Gross to net conversion	90%	90%
Capacity factor	16.5%	29%
Annual Water Usage	75,675.6m^3	123,480 m^3
LCOE (Nominal)	27.76 cents/KWh	26.8 cents/KWh
Total loop conversion efficiency	70%	70%

6.9.4 Comparison of performance of PTC solar thermal power plant

The parabolic trough concentrated solar thermal power plant is compared to earlier study literatures in Table 6.4. According to the comparison, the plant's capacity factor has increased, and its efficiency is within acceptable bounds. It is technically possible and has a strong potential for producing solar thermal energy, just like the PTCSP plant that was planned and built in Bole Lemi Industrial Park

Table 6.4 Comparison of PTCSP Plant output with other Literature

Author	Name Plate Plant Output (MWe)	Annual Energy Production(GWh)	Mean Plant efficiency (%)	Capacity Factor (%)
Present Work	50	114.4	9.93	29
R.Praveren et al.[81]	100	392.6	14.74	44.90
Boukelia [83]	50	118.45	17.25	27.30

6.10 Validation

Two validation benchmarks are used to compare the measured direct normal irradiance to the site's monthly sun irradiance. These two are typical model validation metrics that quantify both the long- and short-term performance of models. Figures 6.12 and 6.13 show how the system advisor model has been validated in comparison to model solar power plants from A. M. Taiea1 et. al [138] and Roberta C et. al [139].

1. The model's mean bias error (MBE)

MBE = $\{[\Sigma \text{model i-measure i})^2]/(n-1)$……...……..…..A

Where n is the number of data points I denotes a given event, and

2. The Model's Root mean square error is (RMSE)

RMSE = $\{[\Sigma \text{model i-measure i})^2]/(n-1)^{0.5}$…….…..…..…B

The percentage variances months are within a reasonable range of minimum which is 0.185% in November and maximum (3.3%) in February .and are to be expected given the weather fluctuations that would arise when comparing site data to a satellite-derived data set covering considerably wider areas.

Over the course of the rest of the year, there are no noticeable variations. We looked for potential relationships between monthly cloud cover, monthly cloud optical depth, and monthly clear-sky days using data that was acquired from satellites. No substantial dependencies were discovered, though. The difficulty of satellite-derived estimations to adequately depict the varied cloud patterns that occur during the day due to summertime heating at point locations may be one explanation for the breakdown in correlation over the summer months. Figure 6.12 compares the average hourly measured DNI with System Advisor Modeling predicted irradiance at Bole Lemi Industrial Park between 12:00 and 11:00 PM standard time. From the figure we can observe that the measured DNI and the SAM prediction are highest in February and lowest in August.

Table 6.5 ***Comparison of Measured & SAM modeled DNI at Bole Lemi Industrial Park***

Month	Average hourly Measured DNI	SAM hourly modeled DNI	Percentage difference
January	615.8	610.7	0.831635
February	647.2	625.97	3.33498
March	614.1	597.44	2.75022
April	596.2	599.48	0.548642

May	609.9	608.329	0.2579
June	436.4	440.86	1.0168
July	380.9	370	2.93012
August	365.4	356.78	2.3872
September	575.6	584.31	1.50184
October	607.45	618.44	1.79298
November	610.3	609.17	0.185326
December	564.2	560.86	0.593746

Mean Bias Error (MBE) and Root Mean Square Error (RMSE) is used to validate the observed and modeled solar irradiance to reduce modeling errors for the proposed power plant in Bole Lemi Industrial Park shown in Figures 6.12.

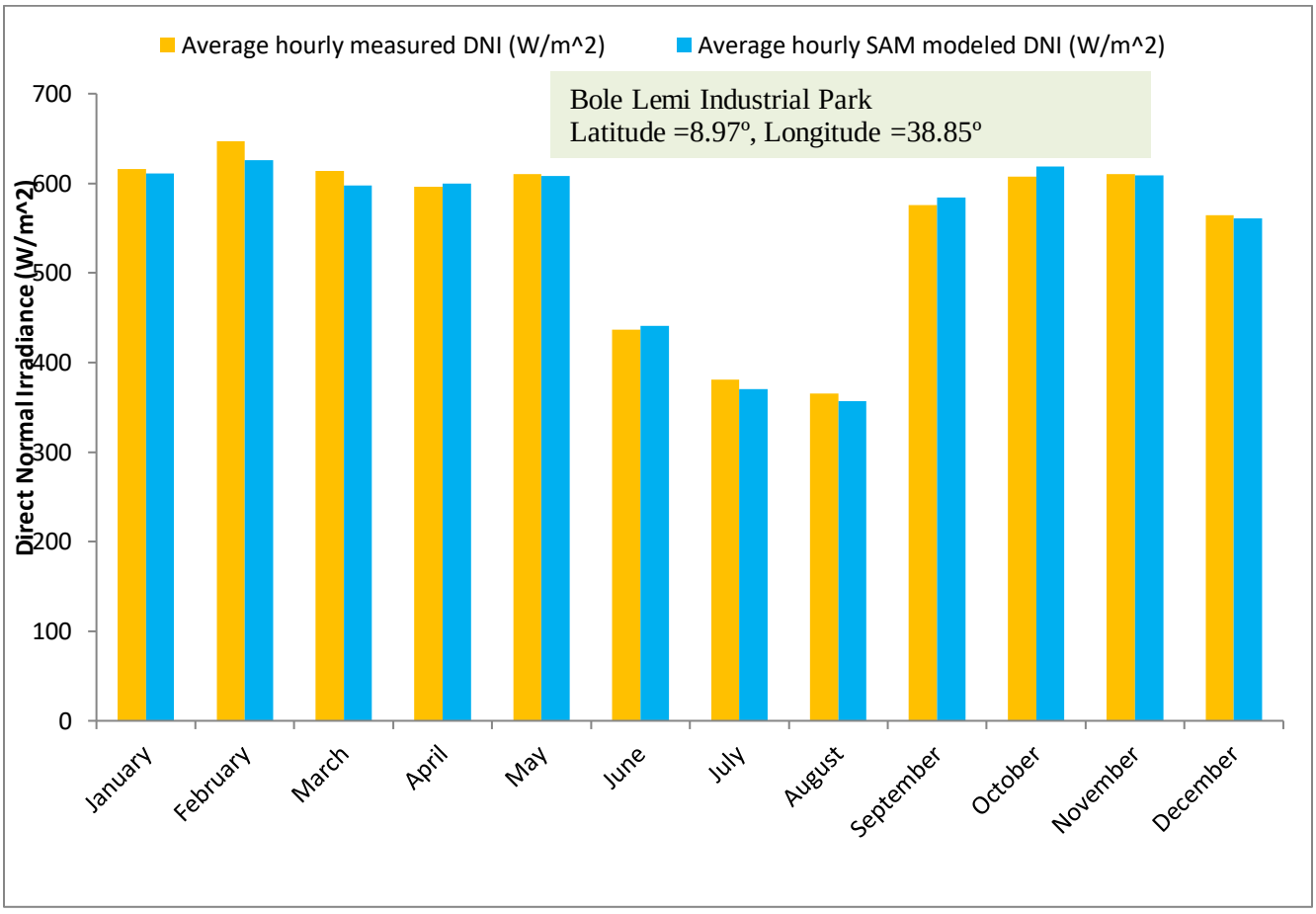

Figure 6.12 Hourly Measured vs SAM modeled predictions of Direct Normal Irradiance

The TMY data set was compared to 2020 for comparison's sake. With only a few minor weather variations, the meteorological outcomes agree with those in Table 6.5.

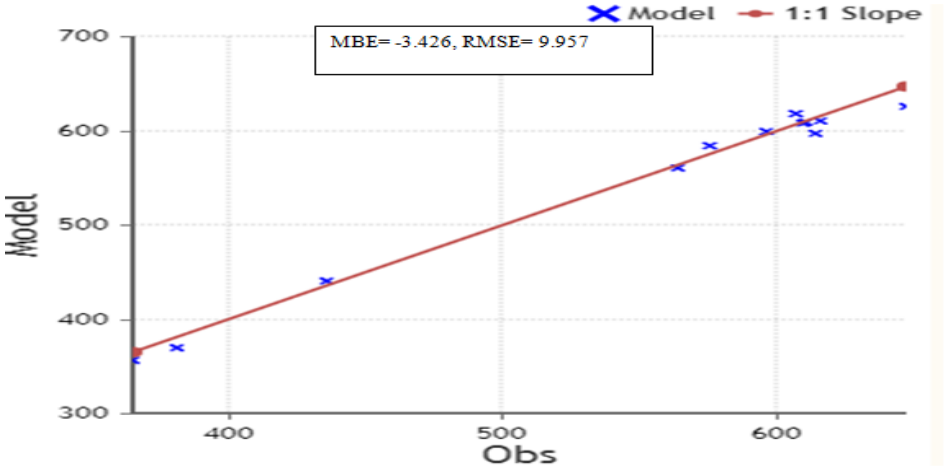

Figure 6.13 Comparison of hourly DNI site measurements observation with SAM estimates

6.11 Discussions

This thesis presented the design mathematical modeling system simulation and performance analysis of Parabolic Trough Collector technology for Bole Lemi Industrial Park Aplication. Each component's reliability is reviewed in detail, as well as the design considerations for collectors. The details of the collectors' use as well as common procedures and methods for energy conversion are provided, with a focus on industrial applications for the case of the clothing and textile industry. In addition to presenting and analyzing mathematical methods for testing thermal performance, an exposition of techniques for assessing PTC system performance is also provided. Finally, different research sources are employed to validate the main standards for measuring the effectiveness of thermal storage system hours, solar multiple, and levelized costs of energy.

In this analysis, five key concepts stand out. In our current examination, five key concepts stand out. First, it is crucial to lay out the geometric analysis of the solar components and assess the possibility for solar resource availability at the chosen site.

Second, it's critical to choose the right heat transfer fluids based on factors including operating temperature, thermal efficiency, viscosity, and overall cost.

Thirdly, the impact of materials on cost analysis should be mentioned. To make this technology competitively priced with traditional fossil fuel technologies, more research needs be conducted to discover materials that can be manufactured and installed with less expense.

Fourth, it's crucial to consider the effects of PTC system design and evaluation. The research's chronological list of papers demonstrates how computational methods, experimental validation, and mathematical modeling are used to enhance performance analysis of energy systems. The use of software tools like SAM enhances the design process by enabling faster and more accurate evaluation of a collector than is feasible with tests.

Finally, in order to evaluate various collector or system designs and standardize the energy conversion processes, it is crucial to create measurement and performance evaluation protocols for parabolic trough collector systems.

Chapter Seven

Conclusions and Recommendations

7.1 Introduction

This chapter being the last category of the thesis, the author will came across on conclusions and recommendations based on previously investigated chapters' results and scientific findings.

7.2 Conclusions

Concentrated solar energy facilities are within the category of completely clean renewable energy sources. Their growth thus coincides with Ethiopia's energy policy, which aims to enhance the penetration of renewable energy sources. Businesses and individuals are switching more frequently to renewable energy systems in order to maintain a clean environment as well as to deliver an adequate supply of energy at a reasonable cost. Therefore, compared to non-renewable energy occupations, there has been an increase in renewable energy jobs [142].

The Bole Lemi Industrial Park in Addis Ababa was identified based on the requirements of a CSP power plant, and simulation of parabolic trough collectors was carried out there. This was based on a 50 MW CSP plant, which can be utilized for a pilot scale study to comprehend and progress the development of solar power in Ethiopia and other countries. In order to aid in the analysis and comprehension of the behavior of the power plant, the thesis study focused on creating a predictive model. SAM, a free program developed by NREL to assist in the modeling and analysis of renewable energy systems, was used to generate the model. SAM is preferred over other renewable energy system modeling software because it is free and has the capacity to more precisely model and analyze various types (combinations) of renewable energy systems. The SAM prediction model was created and validated, as shown in the "Methodology" section. For Bole Lemi Industrial Park, the researcher used this model to perform several parametric analyses to find the ideal combinations of solar multiple, thermal storage hours, and levelized cost of energy (LCOE). For solar power plants, parametric sensitivity analysis ("What-If") can be used to identify the combinations that maximize the value of an output. The following inferences can be made from the analysis provided on this PTC thesis:

- From an industry perspective, the various facets of PTC technology's functioning, applicability, and development were explored.

- This model's inputs can be either measured data or satellite data, which offers places without access to measured radiation data some flexibility. At Bole Lemi Industrial Park, the yearly average DNI is 600 W/m^2, and the annual energy production yield is 114.4 GWh for the plant's optimal analysis.
- Molten salts can be employed at greater temperatures, have superior heat transmission capabilities, and are thermally stable, in contrast to synthetic oils or silicone solutions.
- The use of molten salt as a heat transmission fluid in the solar field would have a number of technical and practical benefits in addition to serving as a storage medium.
- Hitec The parabolic trough solar plant's efficiency may be improved by solar salt. To examine and improve variables such loop configuration and thermal capacity, however, more study and investigations are required.
- Over the past ten years, modeling and testing have undergone further progress. The quality and viability of the technology in industry have been greatly enhanced by the design of tools and standards suited to industrial systems.
- This study also demonstrated that a large reduction in levelized costs of energy can be achieved by running the power plant during the optimal solar multiple and thermal storage hours.

7.3 Recommendations

This thesis research is a foundation and ought to be used as a place to start for other studies. It is a fundamental advancement for the parabolic trough collector system, a very promising solar thermal technology. With the necessary advancements and study, these systems may become more commercialize in the future. The following are suggestions for how to improve this modeling and simulation project better:

- Sizing of storage is critical to increase the system's availability and move electricity output closer to times when demand is at its highest.
- Recent improvements in glass materials have decreased the rate of breaking, further lowering O&M expenses, but improvements in mirrors are also required. Costs associated with O&M can be significantly decreased with improvements in automation.
- The only heat transfer fluid used in this model was molten salt (Hitec salt). By using a direct steam generation (DSG) technology that produces water instead of molten salt, the models can be enhanced. As a result, several brand-new crucial elements, like collector efficiency can be introduced.
- Despite the fact that this technology is advanced, research is still needed to enhance its components. Mirrors and thermal improvement need to be the main study areas (with nano fluids or inserts). Changes to the receiver's design, such as the revolving receiver described by Norouzi et al. [143] or the V-shaped receiver presented by Rafiei et al. [144], may result in additional improvements.
- Projects involving parabolic troughs require a lot of capital, so cost reduction should be investigated at.
- Ethiopia should use more renewable energy, as there is a global worry that developing countries are experiencing an energy crisis and global warming. It is anticipated that the ecosystem will continue to suffer harm and contamination. One option for renewable energy is the parabolic trough solar collector, which should be used in enterprises that produce steam and heat water using fossil fuels.

APPENDIX A: Interview Guide

i) Objective of the Interview

The primary goal of the conducted interviews was to collect the necessary primary data since they provide in-depth information on the various factors that influence and pose obstacles to the adoption of solar thermal energy technology in Bole Lemi Industrial Park. Prior to conducting the interviews, an interview guide was developed.

The interview questions are based on the knowledge discovered in the literature review and theory chapters as well as prior interview knowledge. To provide the interviewee an overview, it opens with a brief explanation of the subject and the greater context of the thesis research. The actual interview then starts with a series of opening inquiries on the interviewee's background and knowledge of industrial solar thermal technology. The actual interview then starts with a series of opening questions on the interviewee's background, knowledge of solar energy systems, and potential difficulties for Bole Lemi Industrial Park.

ii) Introduction

- Could you please explain yourself and your job position in this industry?
- How long have you been working with this industry?
- What is thermal and electrical energy demand of Bole Lemi Industrial Park?
- How is Bole Lemi Industrial Park tackling climate change issues?

iii) General Understanding of Solar Energy

- What are the sources of renewable energy currently used to produce electricity and thermal energy demand in your industry? (Biomass, grid electricity, solar PV & Thermal)
- If you decide to install renewable energy to your industry, what knowledge/considerations are essential to you?

iv) **Driving factors**

- What would be the motivational factors for you to adopt solar thermal energy in your industry?
- How is the management's opinion on solar energy? Are they supportive or not?
- How are energy demand, operating cost, and CO_2 emission reductions motivating your industry to adopt Renewable energy systems such as solar energy?

v) Challenges

✓ What challenges have you confronted in embracing renewable energy practices in your industrial process?

✓ How are these obstructions perceived by the administration in your industry?

✓ What are some key reasons to keep you away from installing renewable energy for your industrial heat process?

✓ Do you think the price of fuel/gas/electricity, investment costs, and government policy could hinder your industry from adopting sustainability practices?

vi) **Conclusions**

☑ Do you have any points you believe to be necessary to the researcher's analysis that has not been addressed so far in the interview?

☑ Do you have any points you accept to be essential to our investigation that has not been addressed so far in the interview?

☑ If the researcher has any more questions, are you available any time?

☑ When the final research finding is released, do you wish to obtain a notification?

Appendix A' Electrical Rated power & rated current

NO	Machine name	Quantity	Rated power(kw,w)	Rated current(A)	Total power(KW,W)	Total current(A)
1	Big fusing machine	1	0.24KW	19A	240W	19A
2	Small fusing machine	3	0.06KW	17A	180W	51A
3	Thread sacking machine	3	6.7KW	12.7A	2011W	38A
4	small boiller	1	9KW	17.1A	9KW	17.1A
5	midum boiller	3	18KW	34A	54KW	102A

6	Big boiller shed 19	1	720KW	1369A	720KW	136A
7	Big boiller shed20	1	432KW	821.4A	432KW	821.4A
8	compressor shed 19	2	2.68KW	5.09A	5.36KW	10.2A
9	metal detector	2	0.154KW	0.7A	308W	1.4A
10	forklift	2	44.1KW	83.85A	88.2KW	167.8A
11	650 KVA generator	1	520KW	910A	1040KW	1820A
12	5550 KVA generator	1	440KW	836.6A	440KW	836.6A
13	small generator	1	8KW	15.2A	8KW	15.2A
14	embrodery	2	1KW	4.55A	2KW	9.09A
15	single phase iron	38	0.55kw	3.6A	20.9KW	136.8A
16	three phase I ron	20	1.65kw	10.8A	33KW	216A
17	Washing machine	6	7.6KW	17A	45.6KW	102A
18	fun motor drier machine	8	2.2KW	5A	11KW	40A
19	main motor drier machine	8	3KW	7.2A	24KW	21.6A
20	exetractor	2	7.5KW	15.4A	15KW	30.8A
21	sample washing machine	1	1.5KW	3.7A	1.5KW	3.7A
22	compressor shed 20	1	55KW	104.7A	55KW	104.7A
23	inspection machine	1	200W	0.6A	200W	0.6A
24	manual cutting layer machine	5	70W	0.58A	350W	2.9A
25	automatic cutting layer machine	5	190W	0.86A	950W	4.32A
26	cutting macine	7	924W	4.2A	6.5KW	29.4A
27	top light in shed 20	175	150W	0.68A	26.25W	119.32A
28	top light in shed 19	72	150W	0.68A	10.8KW	102A
29	LED lamp in shed 20	1296	20W	0.09A	25.92KW	117.82A
30	LED lamp in shed 19	448	20W	0.09A	8.9KW	40.32A
31	philipes lamp in shed 20	82	36W	0.164A	2.952KW	13.4A
32	philips lamp in shed 19	54	36W	0.164A	1944W	8.84A
33	desktop	61	396W	1.8A	24.2KW	109.8A

Appendix B: Power and Current Consumption of selected End Users at Bole Lemi Industrial Park

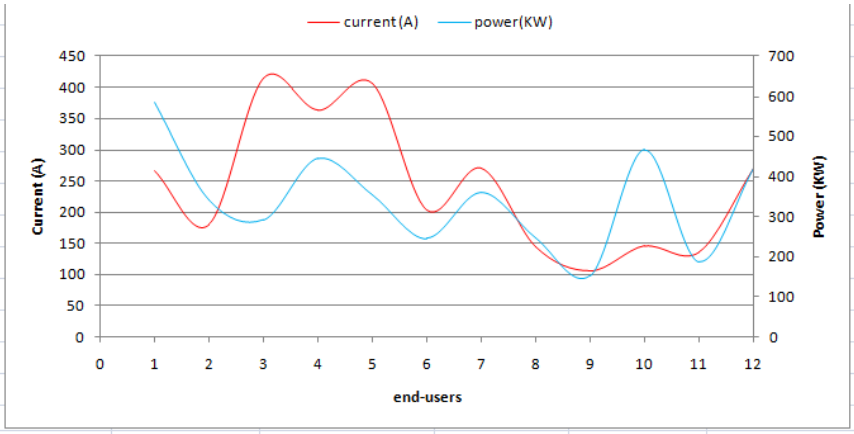

code	End- users
1	single needle
2	double needle chian stitch
3	double needle splite bartack
4	over lock four thread
5	over lock five thread
6	flat lock cylinder bed button hemming
7	cancy special machine
8	button holl
9	key holl
10	bartack stitch
11	bartack flat
12	button atach

Appendix C: Measured DNI (2020) at Bole Lemi Industrial Park

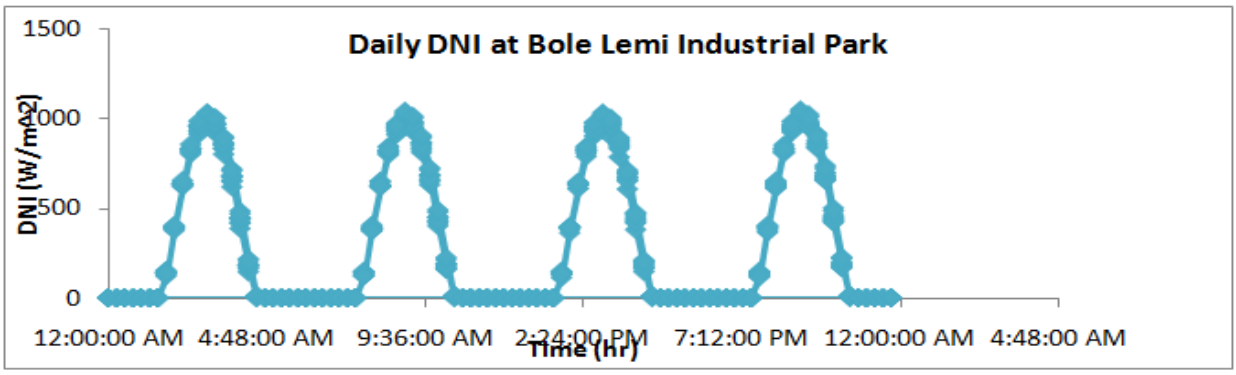

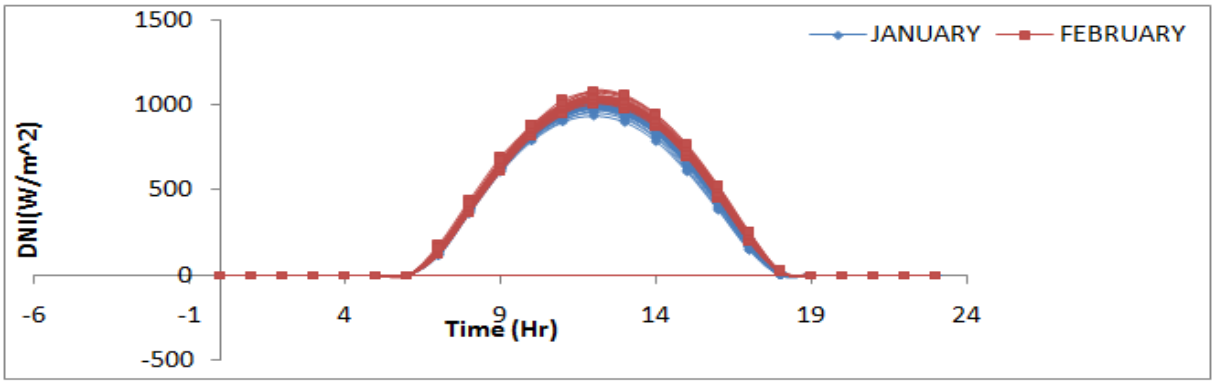

Appendix D: Solar field design points

Design Point

Single loop aperture	9810	m²	Actual number of loops	111	
Loop optical efficiency	0.741605		Total aperture reflective area	1.08891e+006	m²
Total loop conversion efficiency	0.699333		Actual solar multiple	2.5	
Total required aperture, SM=1	432004	m²	Field thermal output	500	MWt
Required number of loops, SM=1	44.0371				

Collector Orientation

Collector tilt	0	deg	Tilt: horizontal=0, vertical=90
Collector azimuth	0	deg	Azimuth: equator=0, west=90, east=-90

Mirror Washing

Water usage per wash	0.7	L/m²,aper.
Washes per year	63	

Plant Heat Capacity

Hot piping thermal inertia	0.2	kWht/K-MWt
Cold piping thermal inertia	0.2	kWht/K-MWt
Field loop piping thermal inertia	4.5	Wht/K-m

Land Area

Solar Field Area	702	acres	Non-Solar Field Land Area Multiplier	1.4	Total Land Area 983 acres

Single Loop Configuration

The specification below is only for one loop in the solar field.

Usage tip: To configure the loop, choose whether to edit SCAs, HCEs or defocus order. Select assemblies by clicking one or dragging the mouse over multiple items. Assign types to selected items by pressing keys 1-4.

Number of SCA/HCE assemblies per loop: 12 ◉ Edit SCAs ○ Edit HCEs ○ Edit Defocus Order [Reset Defocus]

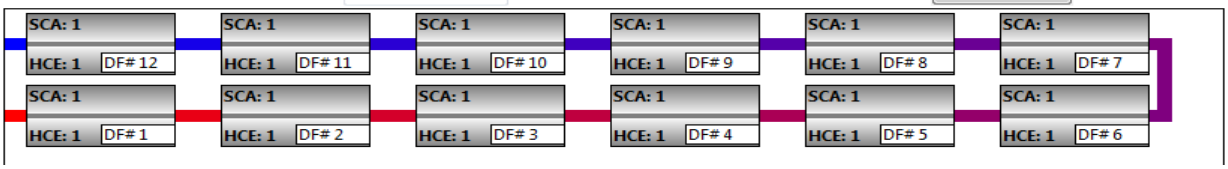

Appendix E: Collector geometry

Collector Geometry

Reflective aperture area	817.5	m²	Number of modules per assembly	12	m
Aperture width, total structure	5.75	m	Average surface-to-focus path length	1.8	m
Length of collector assembly	150	m	Piping distance between assemblies	1	m

Optical Parameters

Incidence angle modifier coef. F0	1	Geometry effects	0.98
Incidence angle modifier coef. F1	0.0506	Mirror reflectance	0.935
Incidence angle modifier coef. F2	-0.1763	Dirt on mirror	0.95
Tracking error	0.99	General optical error	0.99

Optical Calculations

Length of single module	12.5 m	End loss at summer solstice	0.999742
IAM at summer solstice	1.00158	Optical efficiency at design	0.853162

Collector Type 2

Collector name from library: Solargenix SGX-1 [Apply Values from Library]

Collector Geometry

Reflective aperture area	470.3	m²	Number of modules per assembly	12	
Aperture width, total structure	5	m	Average surface-to-focus path length	1.8	m
Length of collector assembly	100	m	Piping distance between assemblies	1	m

Optical Parameters

Incidence angle modifier coef. F0	1	Geometry effects	0.98
Incidence angle modifier coef. F1	0.0506	Mirror reflectance	0.935

Appendix F: Receiver Geometry

Receiver Geometry

Absorber tube inner diameter	0.066	m	Absorber flow plug diameter	0	m
Absorber tube outer diameter	0.07	m	Internal surface roughness	4.5e-005	
Glass envelope inner diameter	0.115	m	Absorber flow pattern	Tube flow	
Glass envelope outer diameter	0.12	m	Absorber material type	304L	

Parameters and Variations

	Variation 1	Variation 2	Variation 3	Variation 4*
Variant weighting fraction*	0.985	0.01	0.005	0
Absorber Parameters:				
Absorber absorptance	0.96	0.96	0.8	0
Absorber emittance	Table...	0.65	0.65	0
Envelope Parameters:				
Envelope absorptance	0.02	0.02	0	0
Envelope emittance	0.86	0.86	1	0
Envelope transmittance	0.963	0.963	1	0
	Broken Glass	Broken Glass	Broken Glass	Broken Glass
Gas Parameters:				
Annulus gas type	Hydrogen	Air	Air	Hydrogen
Annulus pressure (torr)	0.0001	750	750	0
Heat Loss at Design:				
Estimated avg. heat loss (W/m)	190	1100	1500	0
Optical Effects:				
Bellows shadowing	0.96	0.96	0.96	0.963
Dirt on receiver	0.98	0.98	1	0.98

Appendix G: Power Block design points

Power Block Design Point

Rated cycle conversion efficiency	0.25	
Design inlet temperature	545	°C
Design outlet temperature	280	°C
Boiler operating pressure	100	bar
Steam cycle blowdown fraction	0.02	
Fossil backup boiler LHV efficiency	0.9	
Aux heater outlet set temp	391	°C
Fossil dispatch mode	Minimum backup level	

Plant Control

Low resource standby period	2	hrs
Fraction of thermal power needed for standby	0.2	
Power block startup time	0.5	hr
Fraction of thermal power needed for startup	0.2	
Minimum required startup temp	250	'C
Max turbine over design operation	1.05	
Min turbine operation	0.25	

Appendix H: Storage System

Storage System

Full load hours of TES	10	hr	Tank heater capacity	25	MWht
Storage volume	9819.33	m^3	Tank heater efficiency	0.75	
TES Thermal capacity	2000	MWht	Hot side HX approach temp	5	°C
Parallel tank pairs	1		Cold side HX approach temp	7	°C
Tank height	20	m	Heat exchanger derate	1	
Tank fluid min height	1	m	Initial TES fluid temp	300	°C
Tank diameter	25.0024	m	Storage HTF fluid	Hitec Solar Salt	
Min fluid volume	490.967	m^3	User-defined HTF fluid	Edit...	
Tank loss coeff	0.4	W/m^2-K	Storage HTF min operating temp	238	°C
Estimated heat loss	0.32372	MWt	Storage HTF max operating temp	593	°C
Cold tank heater set point	250	°C	Fluid Temperature	412.5	°C
Hot tank heater set point	365	°C	TES fluid density	1827.65	kg/m^3
			TES specific heat	1.51395	kJ/kg-K

Appendix I: Financial and Cost Summary

Single Owner Inputs	
SYSTEM DESIGN	
Nameplate capacity (kW)	45,000.00
SYSTEM COSTS	
Total installed cost ($)	614,040,960
OPERATION AND MAINTENANCE COSTS	
Fixed annual cost ($/yr)	70.00
Escalation (% above inflation)	0.00
Fixed cost by capacity ($/yr)	65.00
Escalation (% above inflation)	0.00
Variable cost by generation ($/MWh)	4.00
Escalation (% above inflation)	0.00

KEY
Calculated
Input from SAM
SAM result

METRICS	
PPA price, year 1 (¢/kWh)	71.69
PPA price escalation (%/yr)	1.00
LPPA Price, nominal (¢/kWh)	76.83
LCOE, nominal (¢/kWh)	30.36
NPV ($)	130,302,585
IRR (%)	0.00
IRR Year	0
IRR at end of project (%)	18.18
Project Cost ($)	644,781,785
Debt ($)	325,041,213
Equity ($)	319,740,573
Debt Fraction (%)	50.4

FINANCIAL PARAMETERS	
Solution Mode	
IRR Target	22.00
Target year	25
PPA price ($/kWh)	Calculated
PPA price escalation (%/year)	1.00
Analysis Parameters	
Analysis period (years, 40 max)	25
Inflation rate (%/year)	3.00
Real discount rate (%/year)	8.20
Nominal discount rate (%/year)	11.45
Tax and Insurance Rates	
Federal income tax rate (%/year)	15.00
State income tax rate (%/year)	7.00
Sales tax (% of total direct cost)	5.00
Insurance rate (annual, % of installed cost)	0.50
Property Tax	
Assessed percentage (% of total installed cost)	0.20
Assesed value ($)	1,228,082
Annual decline (%/year)	0.00
Property tax rate (%/year)	0.00
Salvage Value	
Net salvage value (% of total installed cost)	15.00
End of analysis period value ($)	92,106,144

RESERVE ACCOUNTS			
Interest on reserves (%/year)	1.75		
Working capital reserve (months of operating costs)	6.00		
Debt service reserve account (months of P&I payments)	6.00		
Major equipment replacement reserve accounts	Replacement cost ($/W)	Year 1 dollars	Replacement frequency
Replacement reserve 1	0.25	11,250.00	5
Replacement reserve 2	0.20	9000	10
Replacement reserve 3	0.15	6750	5
Depreciation treatment for replacement reserves			
Federal	5-yr MACRS		
State	5-yr MACRS		

References

[1] S. A. Kalogirou, *Solar thermal collectors and applications*, vol. 30, no. 3. 2004.

[2] M. Wirz, M. Roesle, and A. Steinfeld, "Design point for predicting year-round performance of solar parabolic trough concentrator systems," *J. Sol. Energy Eng. Trans. ASME*, vol. 136, no. 2, pp. 1–7, 2014, doi: 10.1115/1.4025709.

[3] M. Jradi and S. Riffat, "Medium temperature concentrators for solar thermal applications," *Int. J. Low-Carbon Technol.*, vol. 9, no. 3, pp. 214–224, 2014, doi: 10.1093/ijlct/cts068.

[4] "Solar Engineering of Thermal Processes 3rd Edition by John A. Duffie, William A. Beckman (z-lib.org).pdf." .

[5] S. A. Kalogirou, "A detailed thermal model of a parabolic trough collector receiver," *Energy*, vol. 48, no. 1, pp. 298–306, 2012, doi: 10.1016/j.energy.2012.06.023.

[6] A. Fernández-García, E. Zarza, L. Valenzuela, and M. Pérez, "Parabolic-trough solar collectors and their applications," *Renew. Sustain. Energy Rev.*, vol. 14, no. 7, pp. 1695–1721, 2010, doi: 10.1016/j.rser.2010.03.012.

[7] E. Z. Moya, "Parabolic-trough concentrating solar power (CSP) systems," *Conc. Sol. Power Technol.*, pp. 197–239, 2012, doi: 10.1533/9780857096173.2.197.

[8] Y. Mulugetta and F. Drake, "Assessment of solar and wind energy resources in Ethiopia. II. Wind energy," *Sol. Energy*, vol. 57, no. 4, pp. 323–334, 1996, doi: 10.1016/S0038-092X(96)00074-6.

[9] H. Schnitzer, C. Brunner, and G. Gwehenberger, "Minimizing greenhouse gas emissions through the application of solar thermal energy in industrial processes," *J. Clean. Prod.*, vol. 15, no. 13–14, pp. 1271–1286, 2007, doi: 10.1016/j.jclepro.2006.07.023.

[10] W. Weiss, "Task 33: SOLAR HEAT FOR INDUSTRIAL PROCESSES Werner Weiss AEE - Institute for Sustainable Technologies Operating Agent for the Austrian Ministry of Transport, Innovation and Technology," 2004.

[11] S. Mekhilef, R. Saidur, and A. Safari, "A review on solar energy use in industries," *Renew. Sustain. Energy Rev.*, vol. 15, no. 4, pp. 1777–1790, 2011, doi: 10.1016/j.rser.2010.12.018.

[12] SolarPaces, "TASK IV: Solar Heat Integration in Industrial Processes," pp. 1–3, 2010, [Online]. Available: https://www.solarpaces.org/csp-research-tasks/task-annexes-iea/task-iv-solar-heat-integration-in-industrial-processes/.

[13] B. Norton, *Harnessing Solar Heat*, vol. 18, no. 1928. 2014.

[14] C. Lauterbach, B. Schmitt, and K. Vajen, "System analysis of a low-temperature solar process heat system," *Sol. Energy*, vol. 101, pp. 117–130, 2014, doi: 10.1016/j.solener.2013.12.014.

[15] E. Taibi, D. Gielen, and M. Bazilian, “The potential for renewable energy in industrial applications,” *Renew. Sustain. Energy Rev.*, vol. 16, no. 1, pp. 735–744, 2012, doi: 10.1016/j.rser.2011.08.039.

[16] B. Schmitt, “Classification of Industrial Heat Consumers for Integration of Solar Heat,” *Energy Procedia*, vol. 91, pp. 650–660, 2016, doi: 10.1016/j.egypro.2016.06.225.

[17] A. Modi, F. Bühler, J. G. Andreasen, and F. Haglind, “A review of solar energy based heat and power generation systems,” *Renew. Sustain. Energy Rev.*, vol. 67, pp. 1047–1064, 2017, doi: 10.1016/j.rser.2016.09.075.

[18] D. Pietruschka, R. Fedrizzi, F. Orioli, R. Söll, and R. Stauss, “Demonstration of three large scale solar process heat applications with different solar thermal collector technologies,” *Energy Procedia*, vol. 30, pp. 755–764, 2012, doi: 10.1016/j.egypro.2012.11.086.

[19] M. Calderoni, M. Aprile, S. Moretta, A. Aidonis, and M. Motta, “Solar thermal plants for industrial process heat in Tunisia: Economic feasibility analysis and ideas for a new policy,” *Energy Procedia*, vol. 30, pp. 1390–1400, 2012, doi: 10.1016/j.egypro.2012.11.153.

[20] I. E. P. Montesa, A. M. Beniteza, O. M. Chaveza, and A. E. L. Herrera, “Design and construction of a parabolic trough solar collector for process heat production,” *Energy Procedia*, vol. 57, pp. 2149–2158, 2014, doi: 10.1016/j.egypro.2014.10.181.

[21] A. Frein, M. Calderoni, and M. Motta, “Solar thermal plant integration into an industrial process,” *Energy Procedia*, vol. 48, pp. 1152–1163, 2014, doi: 10.1016/j.egypro.2014.02.130.

[22] S. Schramm and M. Adam, “Storage in solar process heat applications,” *Energy Procedia*, vol. 48, pp. 1202–1209, 2014, doi: 10.1016/j.egypro.2014.02.136.

[23] M. Larcher, M. Rommel, A. Bohren, E. Frank, and S. Minder, “Characterization of a parabolic trough collector for process heat applications,” *Energy Procedia*, vol. 57, pp. 2804–2811, 2014, doi: 10.1016/j.egypro.2014.10.313.

[24] S. H. Farjana, N. Huda, M. A. P. Mahmud, and R. Saidur, “Solar process heat in industrial systems – A global review,” *Renew. Sustain. Energy Rev.*, vol. 82, pp. 2270–2286, 2018, doi: 10.1016/j.rser.2017.08.065.

[25] M. Esen, “Thermal performance of a solar cooker integrated vacuum-tube collector with heat pipes containing different refrigerants,” *Sol. Energy*, vol. 76, no. 6, pp. 751–757, 2004, doi: 10.1016/j.solener.2003.12.009.

[26] R. Silva, M. Berenguel, M. Pérez, and A. Fernández-Garcia, “Thermo-economic design optimization of parabolic trough solar plants for industrial process heat applications with memetic algorithms,” *Appl. Energy*, vol. 113, pp. 603–614, 2014, doi: 10.1016/j.apenergy.2013.08.017.

[27] R. Silva, F. J. Cabrera, and M. Pérez-García, “Process heat generation with parabolic

trough collectors for a vegetables preservation industry in Southern Spain," *Energy Procedia*, vol. 48, pp. 1210–1216, 2014, doi: 10.1016/j.egypro.2014.02.137.

[28] G. Coccia, G. Di Nicola, and M. Sotte, "Design, manufacture, and test of a prototype for a parabolic trough collector for industrial process heat," *Renew. Energy*, vol. 74, pp. 727–736, 2015, doi: 10.1016/j.renene.2014.08.077.

[29] "SpringerBriefs in Applied Sciences and Technology," [Online]. Available: http://www.springer.com/series/8884.

[30] H. Esen, M. Esen, and O. Ozsolak, "Modelling and experimental performance analysis of solar-assisted ground source heat pump system," *J. Exp. Theor. Artif. Intell.*, vol. 29, no. 1, pp. 1–17, 2017, doi: 10.1080/0952813X.2015.1056242.

[31] M. Esen, "Thermal performance of a solar-aided latent heat store used for space heating by heat pump," *Fuel Energy Abstr.*, vol. 42, no. 1, p. 62, 2001, doi: 10.1016/s0140-6701(01)80659-7.

[32] A. E. Kabeel, M. H. Hamed, Z. M. Omara, and A. W. Kandeal, "Solar air heaters: Design configurations, improvement methods and applications – A detailed review," *Renew. Sustain. Energy Rev.*, vol. 70, no. November 2015, pp. 1189–1206, 2017, doi: 10.1016/j.rser.2016.12.021.

[33] T. Muneer, S. Maubleu, and M. Asif, "Prospects of solar water heating for textile industry in Pakistan," *Renew. Sustain. Energy Rev.*, vol. 10, no. 1, pp. 1–23, 2006, doi: 10.1016/j.rser.2004.07.003.

[34] T. Muneer, M. Asif, Z. Cizmecioglu, and H. K. Ozturk, "Prospects for solar water heating within Turkish textile industry," *Renew. Sustain. Energy Rev.*, vol. 12, no. 3, pp. 807–823, 2008, doi: 10.1016/j.rser.2006.10.024.

[35] C. Ramos, R. Ramirez, and J. Beltran, "Potential assessment in Mexico for solar process heat applications in food and textile industries," *Energy Procedia*, vol. 49, pp. 1879–1884, 2014, doi: 10.1016/j.egypro.2014.03.199.

[36] P. Frey, S. Fischer, H. Drück, and K. Jakob, "Monitoring Results of a Solar Process Heat System Installed at a Textile Company in Southern Germany," *Energy Procedia*, vol. 70, pp. 615–620, 2015, doi: 10.1016/j.egypro.2015.02.168.

[37] M. Horvat and M. C. Dubois, "Tools and methods for solar design - An overview of IEA SHC Task 41, Subtask B," *Energy Procedia*, vol. 30, pp. 1120–1130, 2012, doi: 10.1016/j.egypro.2012.11.125.

[38] "St. Mary's University," *Grants Regist. 2021*, pp. 815–815, 2020, doi: 10.1057/978-1-349-95988-4_843.

[39] EEPCo., "Ethiopian Power Sector Development, Powering Africa.," *https//pubs.naruc.org/pub.cfm?id=537C14D4-2354-D714-511E-CB19B0D7EBD9 (Accssesd 10 Sept. 2021)*, p. 117, 2014, [Online]. Available: https://pubs.naruc.org/pub.cfm?id=537C14D4-2354-D714-511E-CB19B0D7EBD9.

[40] L. Bickman and D. Rog, “Applied Research Design: A Practical Approach,” *SAGE Handb. Appl. Soc. Res. Methods*, pp. 3–43, 2014, doi: 10.4135/9781483348858.n1.

[41] C. Vignali, B. Hallier, and J. L. Stanton, “No Title.”

[42] K. Features, “Measurement of Solar Irradiance using the CMP 3 Pyranometer by,” pp. 4–7, 1990.

[43] C. A. Gueymard and D. R. Myers, “Solar Radiation Measurement : Progress in Radiometry for Improved Modeling,” pp. 1–2.

[44] G. C. Vliet, *Principles of Solar Engineering*, vol. 122, no. 2. 2000.

[45] كريستينا ،رود .كوكورس, “(مربيان راهنمايي) ورزشي هاي مهارت آموزش ."اقدسي محمدتقي ترجمة ،اول چاپ تبريز دانشگاهNo Title,” 1375.

[46] A. Ben Othman, K. Belkilani, and M. Besbes, “Global solar radiation on tilted surfaces in Tunisia: Measurement, estimation and gained energy assessments,” *Energy Reports*, vol. 4, pp. 101–109, 2018, doi: 10.1016/j.egyr.2017.10.003.

[47] S. A. M. Maleki, H. Hizam, and C. Gomes, “Estimation of hourly, daily and monthly global solar radiation on inclined surfaces: Models re-visited,” *Energies*, vol. 10, no. 1, 2017, doi: 10.3390/en10010134.

[48] C. Gueymard, “Prediction and performance assessment of mean hourly global radiation,” *Sol. Energy*, vol. 68, no. 3, pp. 285–303, 2000, doi: 10.1016/S0038-092X(99)00070-5.

[49] R. V. Padilla, G. Demirkaya, D. Y. Goswami, E. Stefanakos, and M. M. Rahman, “Heat transfer analysis of parabolic trough solar receiver,” *Appl. Energy*, vol. 88, no. 12, pp. 5097–5110, 2011, doi: 10.1016/j.apenergy.2011.07.012.

[50] “azimut.” .

[51] M. M. Rolim, N. Fraidenraich, and C. Tiba, “Analytic modeling of a solar power plant with parabolic linear collectors,” *Sol. Energy*, vol. 83, no. 1, pp. 126–133, 2009, doi: 10.1016/j.solener.2008.07.018.

[52] V. Quaschning, R. Kistner, and W. Ortmanns, “Influence of direct normal irradiance variation on the optimal parabolic trough field size: A problem solved with technical and economical simulations,” *J. Sol. Energy Eng. Trans. ASME*, vol. 124, no. 2, pp. 160–164, 2002, doi: 10.1115/1.1465432.

[53] M. Iqbal, “the Solar Constant and Its Spectral Distribution,” *An Introd. to Sol. Radiat.*, pp. 43–58, 1983, doi: 10.1016/b978-0-12-373750-2.50008-2.

[54] T. Stuetzle, N. Blair, J. W. Mitchell, and W. A. Beckman, “Automatic control of a 30 MWe SEGS VI parabolic trough plant,” *Sol. Energy*, vol. 76, no. 1–3, pp. 187–193, 2004, doi: 10.1016/j.solener.2003.01.002.

[55] M. Collares-Pereira and A. Rabl, “The average distribution of solar radiation-correlations between diffuse and hemispherical and between daily and hourly insolation values,” *Sol.*

Energy, vol. 22, no. 2, pp. 155–164, 1979, doi: 10.1016/0038-092X(79)90100-2.

[56] L. T. Wong and W. K. Chow, "Solar radiation model," *Appl. Energy*, vol. 69, no. 3, pp. 191–224, 2001, doi: 10.1016/S0306-2619(01)00012-5.

[57] C. Gueymard, "Critical analysis and performance assessment of clear sky solar irradiance models using theoretical and measured data," *Sol. Energy*, vol. 51, no. 2, pp. 121–138, 1993, doi: 10.1016/0038-092X(93)90074-X.

[58] I. Edition, *2011 ASHRAE HANDBOOK Heating , Ventilating , and*. 2011.

[59] J. Mikulović and Ž. Đurišić, "Models for the Calculation of Diffuse Radiation on Solar Collectors," *Ijeec - Int. J. Electr. Eng. Comput.*, vol. 4, no. 1, pp. 10–17, 2020, doi: 10.7251/ijeec2001010m.

[60] G. V. Parishwad, R. K. Bhardwaj, and V. K. Nema, "Data bank: Estimation of hourly solar radiation for India," *Renew. Energy*, vol. 12, no. 3, pp. 303–313, 1997, doi: 10.1016/s0960-1481(97)00039-6.

[61] N. Nijegorodov, "Improved ashrae model to predict hourly and daily solar radiation components in Botswana, Namibia, and Zimbabwe," *Renew. Energy*, vol. 9, no. 1-4 SPEC. ISS., pp. 1270–1273, 1996, doi: 10.1016/0960-1481(96)88508-9.

[62] P. D. Tagle-Salazar, K. D. P. Nigam, and C. I. Rivera-Solorio, "Parabolic trough solar collectors: A general overview of technology, industrial applications, energy market, modeling, and standards," *Green Process. Synth.*, vol. 9, no. 1, pp. 595–649, 2020, doi: 10.1515/gps-2020-0059.

[63] G. L. Harding and B. Window, "Free molecule thermal conduction in concentric tubular solar collectors," *Sol. Energy Mater.*, vol. 4, no. 3, pp. 265–278, 1981, doi: 10.1016/0165-1633(81)90065-4.

[64] R. W. Bradshaw and N. P. Siegel, "ES2008-54174," pp. 1–7, 2016.

[65] T. Bauer, W.-D. Steinmann, D. Laing, and R. Tamme, "Thermal Energy Storage Materials and Systems," *Annu. Rev. Heat Transf.*, vol. 15, no. 15, pp. 131–177, 2012, doi: 10.1615/annualrevheattransfer.2012004651.

[66] R. Ferri, A. Cammi, and D. Mazzei, "Molten salt mixture properties in RELAP5 code for thermodynamic solar applications," *Int. J. Therm. Sci.*, vol. 47, no. 12, pp. 1676–1687, 2008, doi: 10.1016/j.ijthermalsci.2008.01.007.

[67] Coastal, "HITEC ® Heat Transfer Salt," *Coast. Chem. Co.*, 2009.

[68] F. Boss, T. Fluri, R. Branke, and W. Platzer, "Simulation of Parabolic Trough Power Plants With Molten Salt As Heat Transfer Fluid," *SolarPaces Conf.*, no. SEPTEMBER, 2012.

[69] U. Herrmann and D. W. Kearney, "Survey of thermal energy storage for parabolic trough power plants," *J. Sol. Energy Eng. Trans. ASME*, vol. 124, no. 2, pp. 145–152, 2002, doi:

10.1115/1.1467601.

[70] A. Gil *et al.*, “State of the art on high temperature thermal energy storage for power generation. Part 1-Concepts, materials and modellization,” *Renew. Sustain. Energy Rev.*, vol. 14, no. 1, pp. 31–55, 2010, doi: 10.1016/j.rser.2009.07.035.

[71] R. W. Bradshaw and D. A. Brosseau, “Improved Molten Salt Heat Transfer Fluid Development.,” *DOE Sol. Energy Techology Progr. Rev.*, 2007, [Online]. Available: https://www.osti.gov/servlets/purl/1267150.

[72] K. M. Powell, A. Sriprasad, W. J. Cole, and T. F. Edgar, “Heating, cooling, and electrical load forecasting for a large-scale district energy system,” *Energy*, vol. 74, no. C, pp. 877–885, 2014, doi: 10.1016/j.energy.2014.07.064.

[73] J. Birnbaum, M. Eck, M. Fichtner, T. Hirsch, D. Lehmann, and G. Zimmermann, “A direct steam generation solar power plant with integrated thermal storage,” *J. Sol. Energy Eng. Trans. ASME*, vol. 132, no. 3, pp. 0310141–0310145, 2010, doi: 10.1115/1.4001563.

[74] E. González-Roubaud, D. Pérez-Osorio, and C. Prieto, “Review of commercial thermal energy storage in concentrated solar power plants: Steam vs. molten salts,” *Renew. Sustain. Energy Rev.*, vol. 80, no. March 2016, pp. 133–148, 2017, doi: 10.1016/j.rser.2017.05.084.

[75] K. Vignarooban, X. Xu, A. Arvay, K. Hsu, and A. M. Kannan, “Heat transfer fluids for concentrating solar power systems - A review,” *Appl. Energy*, vol. 146, pp. 383–396, 2015, doi: 10.1016/j.apenergy.2015.01.125.

[76] M. Mehos *et al.*, “Concentrating Solar Power Gen3 Demonstration Roadmap,” *Nrel/Tp-5500-67464*, no. January, pp. 1–140, 2017, doi: 10.2172/1338899.

[77] W. Ding, A. Bonk, and T. Bauer, “Molten chloride salts for next generation CSP plants: Selection of promising chloride salts & study on corrosion of alloys in molten chloride salts,” *AIP Conf. Proc.*, vol. 2126, 2019, doi: 10.1063/1.5117729.

[78] D. F. Williams and K. T. Clarno, “Evaluation of salt coolants for reactor applications,” *Nucl. Technol.*, vol. 163, no. 3, pp. 330–343, 2008, doi: 10.13182/NT08-A3992.

[79] T. Wang, D. Mantha, and R. G. Reddy, “Novel high thermal stability LiF–Na2CO3–K2CO3 eutectic ternary system for thermal energy storage applications,” *Sol. Energy Mater. Sol. Cells*, vol. 140, pp. 366–375, 2015, doi: 10.1016/j.solmat.2015.04.033.

[80] E. Bellos and C. Tzivanidis, “A detailed exergetic analysis of parabolic trough collectors,” *Energy Convers. Manag.*, vol. 149, pp. 275–292, 2017, doi: 10.1016/j.enconman.2017.07.035.

[81] R. P. Praveen, M. A. Baseer, A. B. Awan, and M. Zubair, “Performance analysis and optimization of a parabolic trough solar power plant in the middle east region,” *Energies*, vol. 11, no. 4, pp. 1–18, 2018, doi: 10.3390/en11040741.

[82] M. J. Montes, A. Abánades, J. M. Martínez-Val, and M. Valdés, “Solar multiple

optimization for a solar-only thermal power plant, using oil as heat transfer fluid in the parabolic trough collectors," *Sol. Energy*, vol. 83, no. 12, pp. 2165–2176, 2009, doi: 10.1016/j.solener.2009.08.010.

[83] T. E. Boukelia, M. S. Mecibah, B. N. Kumar, and K. S. Reddy, "Investigation of solar parabolic trough power plants with and without integrated TES (thermal energy storage) and FBS (fuel backup system) using thermic oil and solar salt," *Energy*, vol. 88, pp. 292–303, 2015, doi: 10.1016/j.energy.2015.05.038.